



***TERMINALIA PHANEROPHLEBIA CRUDE AQUEOUS LEAF
EXTRACT ACTIVATES THE NRF2-MEDIATED ANTIOXIDANT
DEFENCE TO PREVENT OXIDATIVE STRESS IN HUMAN
HEPATOCELLULAR CARCINOMA CELLS***

Marcilyn R. Nyahada

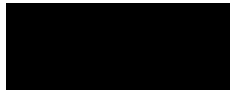
BMedSci Honors (UKZN)

Submitted in fulfillment of the requirements for the degree of
Master of Medical Science in the
Discipline of Medical Biochemistry and Chemical Pathology
School of Laboratory Medicine and Medical Sciences
College of Health Sciences
University of KwaZulu-Natal
Durban

2021

DECLARATION

This dissertation contains the original work by the author and has not been submitted in any form to another university. The use of work by others has been duly acknowledged in the text. The research described in this study was carried out in the Department of Medical Biochemistry and Chemical Pathology, School of Laboratory Medicine and Medical Science, Faculty of Health Sciences, University of KwaZulu-Natal, Durban, under the supervision of Dr RB Khan.



Marcilyn R Nyahada

26 November 2021

Date

DEDICATION

I thank the Almighty God for the opportunity, strength, will power and healthy life.

This thesis is dedicated to my mother and the memory of my beloved father who both not only raised and nurtured me but also taxed themselves dearly over the years for my education and intellectual development.

To my family and friends for the constant source of moral, emotional and spiritual support. I am truly thankful to everyone who contributed towards the completion of this thesis.

ACKNOWLEDGEMENTS

The author would like to acknowledge the department of Medical Biochemistry and the School of Laboratory Medicine and Medical Sciences for all reagents and consumables provided, the supervisors, colleagues and family for all the support.

TABLE OF CONTENTS

DECLARATION	i
DEDICATION	ii
ACKNOWLEDGEMENTS	iii
TABLE OF CONTENTS.....	iv
LIST OF ABBREVIATIONS.....	viii
LIST OF FIGURES	xii
ABSTRACT.....	xvii
CHAPTER 1: INTRODUCTION	1
1.1 Background	1
1.2 Problem statement.....	4
1.3 Rationale.....	4
1.4 Research questions	5
1.5 Null hypothesis.....	5
1.6 Hypothesis.....	5
1.7 Aim.....	5
1.8 Objectives.....	5
CHAPTER 2: LITERATURE REVIEW	7
2.1 Cancer.....	7
2.2 The liver	8
2.3 Hepatocellular carcinoma (HCC).....	10
2.3.1 Incidence	10
2.3.2 Risk factors in the pathogenesis of liver cancer.....	11
2.3.3 Current treatments.....	12
2.3.4 HepG2 cells as a model of HCC.....	13
2.4 Medicinal Plants.....	13

2.5 <i>Terminalia phanerophlebia</i>	15
2.4.2 Phytochemistry of Terminalia species	16
2.6 Oxidative stress	19
2.6.1 Free radical production	19
2.6.2 Antioxidant defence	20
2.6.3 ROS-mediated cellular effects	21
2.7 Apoptosis.....	24
2.7.1 The intrinsic pathway.....	24
2.7.2 The extrinsic pathway.....	25
2.7.3 End-stage cell death	27
CHAPTER 3: MATERIALS AND METHODS	29
3.2 Tissue culture	29
3.2.1 Trypsinisation	30
3.2.2 Cell counting.....	30
3.3 Preparation of plant extracts.....	30
3.4 3-(4, 5-dimethylthiazol-2-yl)-2, 5-diphenyltetrazolium bromide (MTT) assay.....	30
3.4.1 Principle	30
3.4.2 Protocol.....	31
3.5 Thiobarbituric acid reactive substances (TBARS) assay	32
3.5.1 Principle	32
3.5.2 Protocol	33
3.6 Nitric oxide synthase (NO) activity assay.....	34
3.6.1 Principle	34
3.6.2 Protocol.....	35
3.7 The lactic acid dehydrogenase (LDH) assay.....	35
3.7.1 Principle	35
3.7.2 Protocol.....	36

3.8 Luminometry	36
3.8.1 ATP assay	37
3.8.2 GSH assay	38
3.8.3 Caspase assay	39
3.8.4 Annexin V and Necrosis assay	40
3.8.5 Cytochrome P ₄₅₀ 3A4, CYP3A4.....	41
3.8.6 Mitochondrial membrane potential ($\Delta\Psi_M$) - JC-10 Assay.....	43
3.9 Western Blot.....	44
3.9.1 Principle	44
3.9.2 Protocol	45
3.10 Quantitative polymerase chain reaction (qPCR).....	47
3.10.1 Principle	47
3.10.2 Protocol	48
3.11 Statistical analysis	49
CHAPTER 4: RESULTS	50
4.1 MTT Assay.....	50
4.2 ATP Assay.....	52
4.3 JC-10 Assay.....	53
4.4 TBARS Assay	54
4.5 NO Assay	55
4.6 GSH assay	55
4.7 LDH Assay	56
4.8 qPCR	57
4.9 Western blotting	58
4.10 Caspase activity.....	60
4.11 Markers of apoptosis and necrosis	62
4.12 Cytochrome P ₄₅₀ 3A4 activity	63

CHAPTER 5: DISCUSSION.....	64
CHAPTER 6: CONCLUSION	70
REFERENCES	71
APPENDIX.....	82
1. Nrf2 gene amplification	82
2. GPx-1 and NF-κB gene amplification	82
3. SOD2 gene amplification.....	83
4. Nitrates standard curve	83
5. Protein standardisation.....	84
6. Turnitin plagiarism report	84

LIST OF ABBREVIATIONS AND SYMBOLS

$\Delta\Psi M$	Mitochondrial membrane potential
%	Percentage
μg	Microgram
μm	Micrometre
mM	Millimolar
ADP	Adenosine diphosphate
AIF	Apoptosis inducing factor
AP-1	Activator protein-1
Apaf-1	Apoptotic protease activating factor-1
ATM	Ataxia telangiectasia mutated
ATP	Adenosine triphosphate
dATP	Deoxy adenosine triphosphate
Bax	Bcl-2 associated X protein
BCA	Bicinchoninic acid assay
Bcl-2	B-cell lymphoma 2
BCLC	Barcelona clinic liver cancer
Bid	BH3-interacting domain death agonist
BSA	Bovine serum albumin
CARD	Caspase recruitment domain
CCM	Complete culture medium
CDKs	Cyclin dependent kinases
CKs	Checkpoint kinases
CLRs	C-type lectin receptors
c-Myc	Cellular myelocytomatosis
CNS	Central nervous system
COX-2	Cyclooxygenase
CST	Cell signalling technology
Cu^{2+}	Cupric ion
CVS	Cardiovascular system
CYP3A4	Cytochrome P ₄₅₀ 3A4

DAMPs	Damage associated molecular patterns
DISC	Death induced signal cascade
DMSO	Dimethyl sulfoxide
DNA	Deoxyribonucleic acid
EDTA	Ethylenediaminetetraacetic acid
ELISA	Enzyme linked immune-sorbent assay
EMEM	Eagle's minimum essential medium
ER	Endoplasmic reticulum
FADD	Fas associated protein with death domain
FCS	Foetal calf serum
GAPDH	Glyceraldehyde 3-phosphate dehydrogenase
GR	Glutathione reductase
GSSG	Glutathione disulfide
GSH	Glutathione
Gpx	Glutathione peroxidase
H ₂ O ₂	Hydrogen peroxide
H ₃ PO ₄	Phosphoric acid
HBsAg	Hepatitis B surface antigen
HBV	Hepatitis B virus
HBx	Hepatitis B viral proteins
HCC	Hepatocellular carcinoma
HCl	Hydrochloric acid
HCV	Hepatitis C virus
HIV	Human immunodeficiency virus
HEK293	Human embryonic kidney cells
HepG2	Hepatocellular carcinoma cell
HGF	Hepatocyte growth factor
HNE	Hydroxynonenal
HO-1	Heme oxygenase
HSP90	Heat shock protein 90
IAP	Inhibitor of apoptosis protein
IC ₅₀	Half-maximal inhibitory concentration
IL	Interleukin

IRF-3	Interferon regulatory factor-3
JNK	Jun N-terminal kinase
K ⁺	Potassium ion
LDH	Lactate dehydrogenase
LMPA	Low melting point agarose
MAPK	Mitogen-activated protein kinase
MCF-7	Michigan cancer foundation 7
MDA	Malondialdehyde
MOMP	Mitochondrial outer membrane permeabilization
MTT	3-(4, 5-Dimethyl-2-thiazolyl)-2, 5-diphenyl-2H-tetrazolium bromide
MyD88	Myeloid differentiation factor-88
NAD ⁺	Nicotinamide adenine dinucleotide
NADH	Nicotinamide adenine dinucleotide hydrogen
NADPH	Nicotinamide adenine dinucleotide phosphate hydrogen
NAFLD	Non-alcoholic fatty liver disease
NCDs	Non-communicable diseases
NEDD	N-(1-naphthyl)ethylenediamine
NF-κB	Nuclear factor kappa-light-chain-enhancer of activated B-cells
NLRs	NOD-like receptors
NO	Nitric oxide
NOS	Nitric oxide synthase
Nrf2	Nuclear factor erythroid 2–related factor 2
O ₂ ^{•-}	Superoxide
·OH	Hydroxyl
ONOO ⁻	Peroxynitrite
OSCs	Oxidosqualene cyclases
P2X7	Purinoceptor 7
PAMPs	Pathogen associated molecular patterns
PARP	Poly (ADP-ribose) polymerase
PBS	Phosphate buffer saline
PI	Propidium iodide
PRRs	Pattern recognition receptors
PS	Phosphatidylserine

PGE2	Prostaglandin E2
qPCR	Quantitative polymerase chain reaction
RFU	Relative fluorescent units
RIG	Retinoic acid inducible gene
RLU	Relative light units
RNA	Ribonucleic acid
rRNA	Ribosomal RNA
RNS	Reactive nitrogen species
ROOH	Hydroperoxides
ROS	Reactive oxygen species
RT	Room temperature
Smac/DIABLO	Second mitochondria-derived activator of caspases/DIABLO
SCGE	Single cell gel electrophoresis
SDS	Sodium dodecyl sulfate
SOD	Superoxide dismutase
STAT3	Signal transducer and activator of transcription 3
tBID	Truncated p15 BID
TBARS	Thiobarbituric acid reactive substances
TBA/BHT	Thiobarbituric acid/ butylated hydroxytoluene
TBE	Tris/Borate/EDTA
tBid	Truncated Bcl-2 homology domain-3 interacting death domain agonist
TGF- β	Transforming growth factor beta
TNF	Tumour necrosis factor
TLRs	Toll-like receptors
<i>T. phanerophlebia</i>	<i>Terminalia phanerophlebia</i>
TBS	Tris buffered saline
TTBS	Tris buffered saline with 0.1% Tween 20
UGTs	UDP-glycosyltransferases
UI	Uncertainty interval
USA	United States of America

LIST OF FIGURES

Figure 2.1: Global cancer statistics 2020. Liver cancer in both males and females ranks 6th in incidence (4.7%), but is ranked 3rd in mortality (8.3%) (Sung et al., 2021).....	8
Figure 2.2: Cross-sectional view of the liver lobule (Khonsary, 2017).....	9
Figure 2.3: Incidence and mortality age-standardised rates for liver cancer in both sexes (Aslantürk, 2018).....	11
Figure 2.4: Pathogenesis of HCC associated with HBV. Viral integration into the hepatocyte genome initiates molecular events that causes cell death and/or inflammation and culminates in the development of fibrosis, cirrhosis and HCC [Adapted from (Arzumanyan <i>et al.</i> , 2013)].	12
Figure 2.5: (A) Clustered leaves at the end of the branch of <i>T. phanerophlebia</i> . (B) The leaves with distinct veins and seeds of <i>T. phanerophlebia</i> , (C) The bark of <i>T. phanerophlebia</i> . (Adapted from candidegardening.com)	15
Figure 2.6: Some of the phytochemicals possessed by <i>Terminalia</i> species. The medicinal properties are credited to the phytochemical secondary metabolites present in <i>Terminalia</i> plants namely triterpenoids (A,B,C,D), tannins (F), flavonoids (G), alkaloids, anthocyanins (H), gallic acid, chlorophyll a and b, vitamin E, glycosides, saponins (E) and calcium oxalate crystals (Kaur <i>et al.</i> , 2009, Liao <i>et al.</i> , 2019).....	18
Figure 2.7: Oxidative stress. A state of imbalance between oxidants and antioxidants results in the pathogenesis of cancer, cardiovascular diseases, chronic kidney diseases as well as other neurodegenerative diseases like Alzheimer's disease. (<i>Prepared by author</i>).	19
Figure 2.8: Antioxidant reactions showing the catalytic transformation of ROS/RNS by SOD, catalase and Gpx to nontoxic stable molecules. The Haber-Weiss- or Fenton-type reactions lead to the formation of the highly reactive oxygen species ·OH. Superoxide may react with NO to produce the cytotoxic substrate ONOO ⁻ . The antioxidants protect cells against an excessive generation of reactive oxygen and nitrogen species and secondary oxidative stress while maintaining the physiological concentrations and vasodilating action of NO (Sáez and Están-Capell, 2014).....	21
Figure 2.9: A summary of ROS damage on macromolecules. Damage in nucleic acids results in base oxidation, damage in lipids results in aldehydes and secondary by-products of lipid peroxidation such as malondialdehyde (MDA) and damage to proteins causes carbonylation (Juan <i>et al.</i> , 2021).....	22

Figure 2.10: Activation of MAPKs through ROS. MAPKs play a pivotal role in signal transduction from the onset of stimuli such as an oxidative stress environment on the cell surface through activation of NF-κB to activation of target genes [Adapted from (Ijomone et al., 2021)].	23
Figure 2.11: The intrinsic apoptotic pathway (Adapted from the Easy Biology Class).	25
Figure 2.12: The extrinsic apoptotic pathway. Caspases are activated through the death receptor ligand. Binding of the Fas-ligand recruits the initiator caspases in their inactive forms, procaspase-8 and procaspase-10 which are activated into their active forms. The DISC is formed which activates the downstream signal cascade (Glowacki <i>et al.</i> , 2013).	26
Figure 2.13: Characteristics of apoptosis (Adapted from Winoto lab). Apoptosis is chiefly regulated by caspases and the target cell shrinks forming blebs that later bud off as apoptotic bodies that are engulfed by phagocytes.	28
Figure 3.1: The MTT assay principle. The MTT salt (yellow) is reduced by the enzyme mitochondrial dehydrogenase to formazan (purple) in the mitochondria of active cells [Adapted from (Ali-Boucetta <i>et al.</i> , 2011)] .	31
Figure 3.2: TBARS assay principle. The reactive substances which are by-products of lipid peroxidation e.g. MDA react with TBA/BHT producing a coloured compound [Adapted from R & D Systems].	33
Figure 3.3: NO assay principle. Reactive nitrogen species (RNS) which lead to oxidative stress are tested using the azodye. A red coloured product indicates the presence of RNS [Adapted from (Lopes, 2014)].	34
Figure 3.4: LDH assay principle. The LDH protein is rapidly released into the cell culture supernatant when the plasma membrane is damaged. The yellow tetrazolium salt, INT, is reduced by NADH into a red, water-soluble formazan-class dye detected by a spectrophotometer at an absorbance of 450 nm [Adapted from (Forest <i>et al.</i> , 2015)].	36
Figure 3.5: Luciferin reagent permeates the membranes of viable cells to interact with intracellular ATP. Intracellular ATPases are inactivated and the reaction produces bioluminescent light that is measured via luminometry to determine the intracellular ATP levels [Adapted from (Niles <i>et al.</i> , 2007)].	37
Figure 3.6: Cells are lysed in the presence of the luciferin substrate and glutathione S-transferase. Glutathione in the cells contributes to the formation of luciferin. Luciferin Detection Reagent is then added to produce light that is directly proportional to the amount of GSH in the reaction [Adapted from (Lou <i>et al.</i> , 2014)].	38

Figure 3.7: After the cleavage of Z-DEVD substrate, aminoluciferin is released, resulting in luciferase activity and generation of light by luciferase [Adapted from (Khalilzadeh <i>et al.</i> , 2018)].....	40
Figure 3.8: In a healthy viable cell, PS is confined in the inner phospholipid bilayer but translocates to be exposed externally in apoptotic cells. Propidium iodide (PI) permeates the membrane of necrotic cells to bind with DNA producing a fluorescent DNA dye and aids in distinguishing between apoptotic and necrotic cells [Adapted from SinoBiological].....	41
Figure 3.9: CYP enzymes selectively act on a luminogenic substrate depending on the structure of the proluciferin substrate resulting in a luminometric luciferin product. The Luciferin Detection Reagent is added after the CYP reaction has been completed [Adapted from Biovision].....	42
Figure 3.10: The JC-10 dye forms polymer aggregates exhibiting red fluorescence in an intact, polarised membrane and monomer aggregates exhibiting green fluorescence in an unpolarised membrane resulting from apoptosis [Adapted from G-Biosciences]	43
Figure 3.11: Western Blot assay principle. A sample containing proteins is loaded onto an SDS-PAGE gel and electrophoresis is used to separate the proteins depending on their molecular weight. The exact replica of SDS-PAGE gel is transferred to a membrane that is further suspended in a primary antibody which binds to a specific band on the blot. The secondary antibody conjugated to an enzyme (alkaline phosphatase or horseradish peroxidase) is then allowed to bind to the primary antibody. Chemiluminescence reagent is added to the membrane for color development of specific bands before viewing [Adapted from Labmanager].	45
Figure 3.12: qPCR workflow. Custom primers and PCR reagents are used for amplification reactions. Reactions are run in pre-set real-time PCR instruments and the data collected is analysed using specialized software (Adapted from Bio-Rad).....	48
Figure 4.1: (A) Cell viability of HepG2 cells following 48 hours treatment with <i>T. phanerophlebia</i> . A dose-dependent decline was observed relative to the untreated control therefore <i>T. phanerophlebia</i> has anti-proliferative effects on the HCC cell line. (B) Cell viability of Hek293 cells remained the same for both the treated cells and the untreated control. (C) A dose-dependent decrease in cell viability observed post a 48 hours exposure of HepG2 cells to <i>T. phanerophlebia</i>	52
Figure 4.2: ATP concentration. There was significant decrease in the IC ₅₀ (* <i>p</i> = 0.0104) [* Unpaired <i>t</i> -test with Welch's correction].	53

Figure 4.3: A significant 2-fold decrease in membrane potential ($p = 0.0024$) was displayed relative to the control. [** Unpaired t – test with Welch`s correction]	54
Figure 4.4: An 8-fold decrease in MDA concentration was noted in the IC ₅₀ -treated HepG2 cells compared to the control (** $p = 0.0030$; Unpaired t -test with Welch's correction).	54
Figure 4.5: Nitrates and nitrites concentration for the IC ₅₀ displayed a slight decrease of 1.039-fold relative to the control.....	55
Figure 4.6: A decrease in the GSH concentration was observed for IC ₅₀ ($p = 0.0430$) treatments [*Unpaired t -test with Welch`s correction].	56
Figure 4.7: The extracellular LDH released from IC ₅₀ -treated cells was similar to the control.	56
Figure 4.8: Gene expression following treatment with <i>T. phanerophlebia</i> . (A) <i>Nrf2</i> gene expression had a 1.152-fold increase. (B) The mRNA for <i>GPx-1</i> in the IC ₅₀ -treated HepG2 cells had 1.755-fold decrease compared to the control (* $p = 0.0151$). (C) <i>T. phanerophlebia</i> increased <i>SOD2</i> gene expression for the IC ₅₀ treatment by 1.279-fold. (D) A significant decrease (1.654-fold) in <i>NFKB</i> mRNA expression was observed for the <i>T. phanerophlebia</i> treated cells (** $p = 0.0078$).	57
Figure 4.9: Protein expression following treatment with TP. (A) Fas protein expression was significantly decreased following TP treatment of HepG2 cells (***($p < 0.0001$)). (B) The IC ₅₀ remained similar to the control for STAT3 protein expression. (C) TP decreased HSP90 protein expression for the IC ₅₀ treatment (***($p < 0.0001$)). (D) Significant increase in SOD2 protein expression was observed for the TP treated cells (***($p < 0.0001$)). (E) The protein expression of p38 was increased by the IC ₅₀ treatment (* $p = 0.0114$). [*Unpaired t -test with Welch`s correction].....	59
Figure 4.10: Significant decrease in initiator caspase 8 (***($p = 0.0004$)) and caspase 9 (***($p = 0.0004$)), as well as effector caspase 3/7 (***($p = 0.0003$)) luminescence was observed in <i>T. phanerophlebia</i> treated HepG2 cells. [*Unpaired t-test with Welch`s correction].....	61
Figure 4.11: There was significant decrease in apoptotic and necrotic cells ($p = 0.0263$). [*Unpaired t -test with Welch`s correction]	62
Figure 4.12: A non-significant 0.28-fold decrease in CYP3A4 activity was observed for the IC ₅₀ treatment.....	63
Figure 5.1: The collective biochemical effects of <i>T. phanerophlebia</i> crude aqueous leaf extracts on HepG2 cells. There was a decrease in both $\Delta\Psi_M$ and ATP resulting in HSP90 activity which increased O ₂ ^{•-} and H ₂ O ₂ . The increase in O ₂ ^{•-} triggered the upregulation of Nrf2	

and SOD2 which neutralised the free radicals to H₂O by GSH. Even though p38 was upregulated, apoptotic cell death was prevented through downregulation of NF-κB and STAT3
(prepared by author).....69

ABSTRACT

Cancer is the second leading cause of death throughout the world, contributing 23% of deaths attributed to non-communicable diseases (NCDs). Hepatocellular carcinoma (HCC) is the most common type of liver cancer. Incidence and mortality rates of HCC are higher in Africa due to prevalent risk factors. The prognosis is poor and thousands of lives are claimed yearly despite treatments like chemotherapy. Treatments are expensive and inaccessible to all cancer patients. Additionally, drug metabolism has limitations of solubility, toxicity, inefficacy and bio-distribution. Ayurvedic medicines are pivotal in the stability of several proteins that are essential for malignant transformation. Anti-inflammatory, antimicrobial and antioxidant properties expressed by a variety of *Terminalia* species can be alluded to the phytochemicals such as flavonoids, tannins, coumarins and terpenoids they possess. *Terminalia phanerophlebia* (*T. phanerophlebia*) could therefore be an interesting therapeutic alternative for cancer therapy. This study investigated the antioxidant potential and antiproliferative activity of *T. phanerophlebia* crude aqueous leaf extract in HepG2 cells. The HepG2 cells were exposed to *T. phanerophlebia* for 48 hours. The MTT assay was used to determine the IC₅₀, which was then used for all subsequent assays. Metabolic effects were ascertained by quantifying cytochrome P₄₅₀ 3A4 activity, mitochondrial membrane potential (ΔΨ_M) and ATP concentration. The cells were assayed for lipid peroxidation and nitrates/nitrites as markers of oxidative and nitrosative stress respectively, and membrane integrity was evaluated by quantifying extracellular LDH. Caspases 8, 9 and 3/7 activity, phosphatidylserine externalization and necrosis were luminometrically detected as an indication of cell death. Protein expression of Fas, STAT3, HSP90, SOD2 and p38 were evaluated by western blotting, while gene expression of *NF-κB*, *Nrf2* and *SOD2* were assessed by qPCR. A dose-dependent decrease in cell viability (IC₅₀ = 1396 μg/mL) was attributed to increased bioavailability of *T. phanerophlebia* (CYP3A4 was decreased 0.28 fold). Intracellular ATP decreased (*p* = 0.0104) concurrently with ΔΨ_M (*p* = 0.0024), and was consistent with superoxide production. However, the decreased lipid peroxidation (*p* = 0.0030) and nitrates/nitrites concentration (1.039-fold) associated with reduced extracellular LDH (1.086-fold) suggested avoidance of oxidative damage. Indeed, increased superoxide prompted the upregulation of *Nrf2*, and *SOD2* gene and protein (*p* < 0.0001) expression. The hydrogen peroxide produced was detoxified by GSH (*p* = 0.0430) and GPx-1 (*p* = 0.0151), which were decreased in the process. Increased ROS produced by *T. phanerophlebia* also upregulated p38 (*p* = 0.0114), p38, but *NF-κB* (*p* = 0.0078)

and HSP90 ($p < 0.0001$) were decreased, and STAT3 was similar to the control. Apoptosis was not induced as indicated by the decreased protein expression for Fas ($p < 0.0001$), as well as the decline in caspase 8 ($p = 0.0004$), caspase 9 ($p = 0.0004$) and caspase 3/7 ($p = 0.0003$) activity. *T. phanerophlebia* also caused significant decrease in necrotic cells ($p = 0.0263$) and phosphatidylserine externalisation. Taken together the results indicate that although *T. phanerophlebia* resulted in mitochondrial superoxide production, oxidative damage was prevented by the upregulation of Nrf2 that recruited antioxidants to combat the oxidative stress environment. In addition, the upregulation of p38 was minimal and NF- κ B was not activated resulting in non-progression of apoptosis.

Key words: *Terminalia phanerophlebia*, hepatocellular carcinoma, apoptosis, oxidative stress, HepG2 cells, *Nrf2*, p38

CHAPTER 1: INTRODUCTION

1.1 Background

Cancer is a life-threatening disease that results from irregular cell proliferation and is one of the leading causes of death in both developed and developing countries. Liver cancer has moved from the fourth to the third leading cause of cancer deaths globally between 2018 and 2020 (Sung *et al.*, 2021, Bray *et al.*, 2018). Hepatocellular carcinoma (HCC) is the most common type of liver cancer; its development is associated with the hepatitis virus, aflatoxin-contaminated foods, heavy alcohol consumption, smoking, obesity and type 2 diabetes (El-Serag, 2020). Non-alcoholic fatty liver disease (NAFLD) and non-alcoholic steatohepatitis is increasingly contributing to the development of HCC (Singal *et al.*, 2020). Current liver cancer treatments include surgery, radiotherapy, chemotherapy drugs such as doxorubicin, biological therapy and immune mediated therapies (Meli *et al.*, 2019). However, neurological, cardiac, renal and pulmonary toxicity are some of the side effects associated with these treatments. In addition, some cancer drugs display non-selective toxicity by affecting normal cells, and cancer cells can also develop resistance making drug development a complicated task (Jain *et al.*, 2016).

Over the years, researchers have become increasingly interested in the investigation of natural compounds, both in their natural forms and as templates for synthetic modification because they have been used expansively in traditional medicine as treatment for many diseases (Yadav *et al.*, 2010, Salmon, 2015, Porras *et al.*, 2020). Over 4000 phenolic compounds isolated from vascular plants have been identified to have multiple therapeutic applications and the best-known resources of natural medicine (Hebbani *et al.*, 2021). Approximately 60% of the current anticancer agents are derived from natural sources and medicinal plants are now being used as alternative anticancer drugs (Dinesh *et al.*, 2014, Ashraf, 2020). Medicinal plants contain a vast number of secondary metabolites, which include anthocyanins, lignans, flavonoids, coumarins, isocatechins, flavones and catechins. These phytochemicals have been identified to produce physiological effects in the human body, including mechanisms involved in the inhibition of genotoxic effects, increase in anti-inflammatory and antioxidant activities, anti-haemolytic, anti-hyperlipidemic, antimicrobial, anticarcinogenic, cell proliferation, regulation of signal transduction pathways and apoptosis (Dinesh *et al.*, 2014, Akhtar *et al.*, 2020).

Terminalia is the second largest genus of the family *Combretaceae* and has 200-250 species of which 14 arise from African as well as Asian, American and Oceania (Australian) origin (Beigi *et al.*, 2018, Fahmy *et al.*, 2015). The *Terminalia* species such as *Terminalia bellerica* and *Terminalia arjuna* are widely used to treat an array of diseases due to their antimicrobial, antibacterial, antimalarial, antihypertensive, antithrombotic, antiulcer, antimutagenic, antiprotozoal and hepatoprotective properties (Gupta, 2012). These effects were caused by multiple mechanisms of the plant phytocompounds, which involve antioxidant, anti-inflammation, inhibition of lipid synthesis and increased fatty acid oxidation (Hebbani *et al.*, 2021). In 2020, Patra and colleagues (2020) established a link between reactive oxygen species (ROS) and apoptosis following exposure of oral squamous cell carcinoma (Cal33) cells to *T. bellerica* extract. The extract significantly facilitated the accumulation of ROS that resulted in mitochondrial apoptosis through DNA damage, indicating ROS as the pivotal constituent in the regulation of apoptosis. The study also revealed that there was selective anti-proliferative activity alluded to the gallic acid in the *T. bellerica* extract known for strong free radical scavenging capacity (Patra *et al.*, 2020). A study conducted by Hebbani and co-researchers (2021) on rat erythrocyte membranes revealed that the bark extract of *Terminalia arjuna* had gastroprotective, cardioprotective, hepatoprotective and renal protective effects that may have been attributed to the high phytochemical composition in the bark extract (Hebbani *et al.*, 2021). In 2012, Nair and co-investigators elucidated three triterpenoids namely β -sitosterol, β -sitostenone and stigmast-4-ene3, 6-dione derived from the ethanolic extract of the stems of *Terminalia phanerophlebia* (*T. phanerophlebia*) (Nair *et al.*, 2012). The study showed that the anti-inflammatory activity of *T. phanerophlebia* was due to the crude extract and β -sitosterol, which were discovered to be selective inhibitors of cyclooxygenase-2 (COX-2), an enzyme that promotes cell proliferation and produces prostaglandins to promote inflammation, pain and fever (Nair *et al.*, 2012, Yadav *et al.*, 2010). Another recent study in adenocarcinomic human alveolar basal epithelial cells (A549) lung cancer cells showed that *T. phanerophlebia* modulated oxidative stress by increasing antioxidant protein expression and was associated with caspase-dependent apoptosis (Benede, 2020).

Oxidative stress results from the imbalance of oxidants and antioxidants and has been implicated in the pathogenesis of diseases such as cancer, cardiovascular diseases and chronic kidney diseases (Nyahada *et al.*, 2021). The mitochondria is the main source of endogenous ROS production and exogenous sources include radiation, smoke, heavy metals and xenobiotics (Banerjee and Roychoudhury, 2018). Incomplete reduction of O_2 results in free

radicals such as the superoxide anion ($O_2^{\cdot-}$), hydrogen peroxide (H_2O_2) and hydroxyl ion ($\cdot OH$) (Zweier and Talukder, 2006). Peroxynitrite ($ONOO^-$) is another free radical resulting from the reaction of $O_2^{\cdot-}$ and nitric oxide (NO). Antioxidants such as superoxide dismutase (Budhu *et al.*), glutathione (GSH), glutathione peroxidase (Gpx) and catalase are regulated by the modulator of oxidative stress, nuclear factor erythroid 2-related factor 2 (Nrf-2) and are employed to combat oxidants (Costilla *et al.*, 2019). Prolonged oxidative stress conditions lead to lipid peroxidation, DNA damage and protein carbonylation which may lead to cell death (Rodríguez-García *et al.*, 2020).

Apoptosis is programmed cell death that can be triggered by cellular stress or DNA damage and it is dominantly regulated by caspases (Carneiro and El-Deiry, 2020). Caspase-8, caspase-9 and caspase-10 are initiator caspases and caspase-3, caspase-6 and caspase-7 are executioner caspases (Pfeffer and Singh, 2018a). Binding of the Fas ligand to its cognate transmembrane receptor (Bedekar *et al.*) to form the Fas/Fas complex is key to inducing the extrinsic apoptotic pathway, as it initiates formation of the death inducing complex (DISC) and caspase-8 activation (Alkhouri *et al.*, 2015). Alternatively, extrinsic apoptosis may be mediated by TNF α . This inflammatory cytokine activates NF- κ B or triggers RIP1 kinase-induced cell death (Cockram *et al.*, 2021). The intrinsic apoptotic pathway is triggered by mitochondrial outer membrane permeabilization (MOMP). The MOMP results in the release of cell death modulators such as cytochrome c from the intermembrane space leading to a cascade of reactions including the formation of the apoptosome and caspase-9 activation (Tait and Green, 2010). Pro-apoptotic proteins (Bax, Bak, Bad, Puma, Bcl-x and Bid) and anti-apoptotic proteins (Bcl-2, Bcl-xL, Bcl-w, Brag-1) regulate intrinsic apoptosis. In turn, the Bcl-2 family is regulated by tumour suppressors (p53) and mitogen-activated protein kinases (MAPKs) such as p38; p53 is ultimately responsible for activating Bax, while p38 suppresses apoptosis by activating Bcl-2 (Arumugam *et al.*, 2017). Overexpression of anti-apoptotic proteins or under-expression of pro-apoptotic proteins causes inhibition of apoptosis leading to cancer (Pfeffer and Singh, 2018b).

The discovery of effective medicinal plants and explication of the mechanisms of their phytochemicals could lead to the development of chemo-preventive drugs that are not only specific to cancerous cells, but also protect normal cells. There is a gap in the literature regarding the mechanisms underlying the effects of *T. phanerophlebia*; more specifically, the

hepatoprotective effects (Meli et al., 2019). The hepatocellular carcinoma (HepG2) cell line is comprised of immortal cancerous hepatic cells that are commonly used in drug metabolism and hepatotoxicity studies because of retained differentiated hepatic functions, making them a good *in vitro* model for cytotoxicity studies (Donato et al., 2015). The purpose of this study is to determine the biomolecular mechanism underlying the effects of *T. phanerophlebia* on human HepG2 cells.

1.2 Problem statement

Liver cancer is the 6th most frequent malignancy and the 3rd leading cause of cancer deaths worldwide (Cao et al., 2021). Hepatocellular carcinoma is the most common type of liver cancer globally and it is expected to claim about 64 525 lives annually in sub-Saharan Africa by 2030 (Xie et al., 2021). Excessive alcohol consumption, diabetes, obesity, hepatitis viral infections and corollary effects of medications are some contributing factors that may induce the onset of liver diseases such as liver cancer (Boyle et al., 2018). Despite the current treatments available on the market, the estimated five-year survival span following treatment is usually not reached and often involves poor prognosis (Shunmugam, 2016). Cancer-related death rates are exceptionally high as most cases are difficult to diagnose through routine examinations leading to late diagnosis as well as limited access to timely and effective treatment (Rabbani et al., 2018).

1.3 Rationale

Hepatocellular carcinoma is amongst the leading causes of mortality in the world and chemotherapy is the most used treatment for cancer. Not only is chemotherapy expensive, but it is also not specific to cancerous cells and can be invasive. Some anti-cancer drugs have limited bio-distribution, poor solubility, stability and their metabolism have various challenges of toxicity and inefficacy. It is therefore important to find an affordable yet potently effective alternate treatment that is naturally sourced. Various *Terminalia* species (*T. catappa*, *T. arjuna*, *T. bellerica*, *T. ferdinandiana*, *T. irvorensis* and *T. superba*) and their decoctions have been used in previous studies to treat breast, skin and prostate cancer respectively. Widely distributed throughout KwaZulu-Natal and Mpumalanga regions of South Africa, *T. phanerophlebia* has been used to treat a range of ailments. There is evidence of the anti-inflammatory properties of *T. phanerophlebia*, but the hepatoprotective properties are yet to be investigated. This study will utilise human liver cancer cell line, HepG2 that was initially derived from a well-differentiated hepatocellular carcinoma of a 15-year-old Caucasian male

in 1975. An aqueous leaf extract of *T. phanerophlebia* will be used in order to mimic the concoctions used by traditional herbalists.

1.4 Research questions

Does *T. phanerophlebia* induce hepatoprotective properties in HepG2 cells?

Does *T. phanerophlebia* induce apoptosis in HepG2 cells?

Does *T. phanerophlebia* possess antioxidant potential in HepG2 cells?

1.5 Null hypothesis

T. phanerophlebia does not have anti-proliferative or antioxidant effects in HepG2 cells.

1.6 Hypothesis

T. phanerophlebia will exert anti-proliferative and antioxidant effects in HepG2 cells.

1.7 Aim

The aim of this study is to investigate the anti-proliferative effects and antioxidant potential of *T. phanerophlebia* crude aqueous leaf extract on human hepatocellular carcinoma (HepG2) cells.

1.8 Objectives

A crude aqueous leaf extract of *T. phanerophlebia* will be used to

- assess cell viability of HepG2 cells treated with *T. phanerophlebia* by
 - using the 3-(4,5-dimethylthiazol-2-yl)-2,5-diphenyl tetrazolium bromide (MTT) assay to obtain an IC₅₀ to be used in subsequent assays.
 - quantifying ATP using luminometry.
- evaluate possible cell death induced in HepG2 cells by *T. phanerophlebia* by
 - using luminometry to detect phosphatidylserine using the annexin V assay as an early marker of apoptosis to quantify apoptotic cells.
 - determining the possible activity of different caspases to elaborate pathways of apoptosis using luminometry.
 - verifying the possible presence of proliferative proteins (HSP90 and Stat3) and anti-proliferative proteins (Fas, p38, NF- κ B) using the western blot and qPCR assays.

- determine the possible amelioration of oxidative stress by *T. phanerophlebia* in HepG2 cells by
 - using the TBARS and NO assays to detect possible oxidant (ROS and RNS respectively) production.
 - quantifying GSH using luminometry.
 - using qPCR to detect possible antioxidant enzyme gene expression (*Nrf2*, *SOD2*, *GPx-1*).

CHAPTER 2: LITERATURE REVIEW

2.1 Cancer

Cell division and proliferation is a tightly regulated process under normal circumstances, but when cells by-pass these regulations, it results in cancer. Cancer cells accumulate a series of biochemical changes that makes them resistant to signalling pathways such as apoptosis resulting in unregulated cell cycle, cell division and tumour formation. However, the process does not occur overnight and can take 5-20 years for specific signs and symptoms to be detected (Jemal *et al.*, 2011). The lack of distinct symptoms causes a serious worldwide health burden and it is the main reason for high mortality rates and short survival time of cancer patients (Ozakyol, 2017). According to Ferlay *et al.* (2021), in 2020 there were an estimated 19.3 million new cases of cancer (18.1 million excluding non-melanoma skin cancer) and almost 10.0 million deaths from cancer (9.9 million excluding non-melanoma skin cancer) worldwide (Figure 2.1) (Ferlay *et al.*, 2021). The most commonly diagnosed cancers worldwide were female breast cancer, lung and prostate cancers; liver cancer was the 6th most diagnosed cancer (Figure 2.1) with an estimated 906,000 new liver cancer cases in 2020 (Sung *et al.*, 2021). However, liver cancer is the 3rd leading cause of death worldwide (830000 deaths in 2020) exceeded only by lung cancer (1.79 million deaths) and colorectal cancer (935000) (Sung *et al.*, 2021). Incidence to mortality rate is 0.95 for hepatocellular carcinoma (HCC), the dominant type of liver cancer, and 5-year survival is only 6.9% (Ozakyol, 2017). The majority of patients are usually diagnosed in the later stages of cancer and overall median survival time is as short as 11 months (Ozakyol, 2017).

The prevalence of liver cancer in Africa and Asia is higher than in Western countries and more common in middle- and low-income countries than in developed nations. This is due to the prevalence of risk factors such as hepatitis B virus (HBV) and hepatitis C virus (HCV) in the population; poor medical expertise and facilities for early diagnosis, lack of effective treatment after diagnosis, late presentation of patients with large tumours, low awareness of the benefits of HCC treatment and ways of preventing underlying liver disease are also contributing factors (Ferenci *et al.*, 2010). Exposure to radiation as well as certain lifestyles such as sedentary living and smoking also contribute to the prevalence of liver cancer in Africa and Asia (Bray *et al.*, 2018).

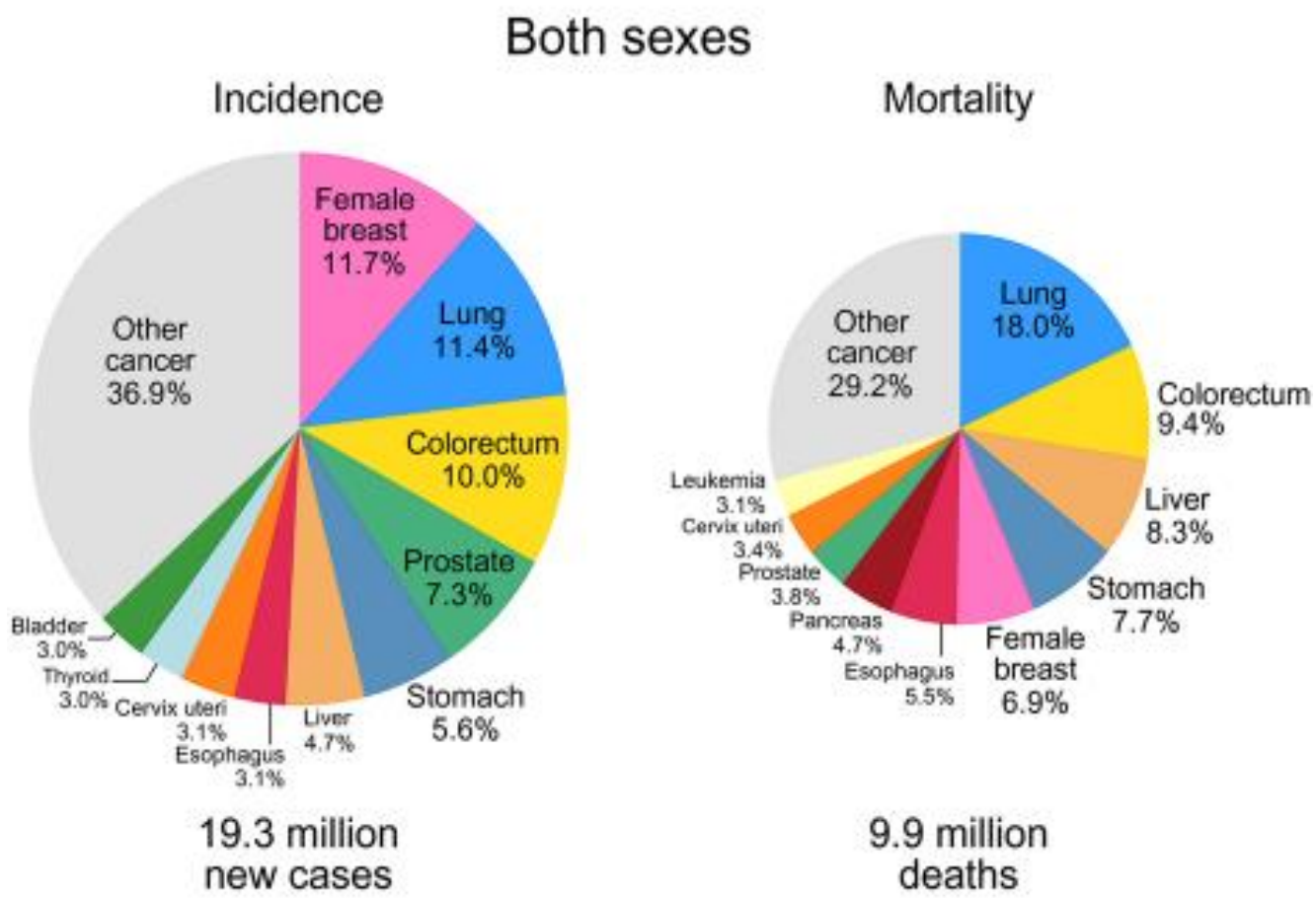


Figure 2.1: Global cancer statistics 2020. Liver cancer in both males and females ranks 6th in incidence (4.7%), but is ranked 3rd in mortality (8.3%) (Sung et al., 2021).

2.2 The liver

The liver is located in the abdominal cavity and not only is it the largest organ in the body, but it is also multifunctional (Khonsary, 2017). The liver lobule (Figure 2.2), a cylindrical structure 0.8-2mm in diameter and a few millimeters long, is the pivotal functional unit of the liver (Khonsary, 2017). There are 50000-100000 individual lobules in the human liver. The liver receives blood supply from the gastrointestinal tract through the portal vein and it flows into the sinusoids before collecting in the central vein (Ozougwu, 2017). Hepatocytes are cells of the main parenchymal tissue of the liver and are used as an *in vitro* model because they have the closest resemblance to the human liver and produce a metabolic profile of a given drug that is very similar to that found *in vivo* (Gomez-Lechon *et al.*, 2003). Venous sinusoids are covered by hepatic cells, endothelial cells and kupffer/reticuloendothelial cells. Kupffer cells are resident macrophages that engulf bacteria and foreign matter through phagocytosis in the hepatic blood. The Space of Disse/perisinusidal spaces is highly permeable to allow free

plasma delivery and they empty excess fluid through the lymphatic vessels. The liver has high blood flow and low vascular resistance under normal circumstances. In the event of liver cirrhosis, the parenchymal cells are replaced with fibrous tissue which contracts around the blood vessels resulting in increased blood flow resistance.

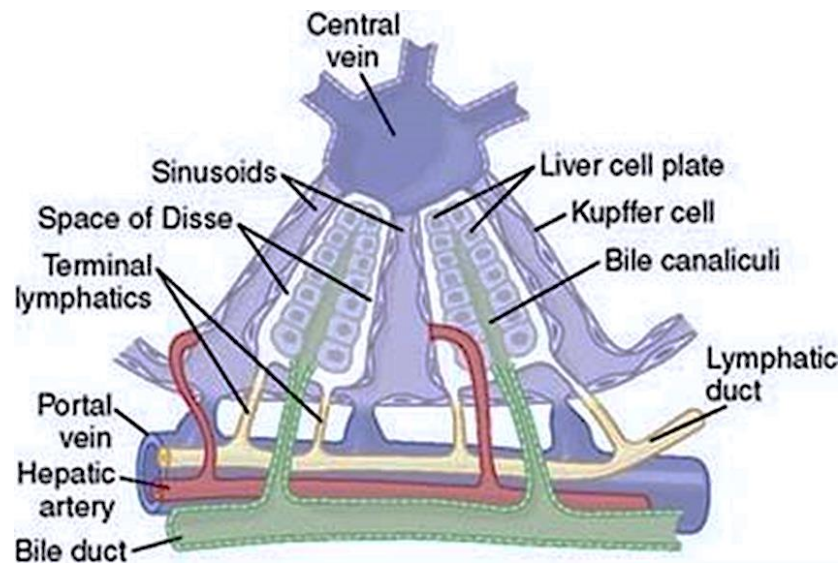


Figure 2.2: Cross-sectional view of the liver lobule (Khonsary, 2017).

Regeneration is one of the liver's most profound properties. Partial hepatectomy triggers the release of hepatocyte growth factor (HGF) from the mesenchymal cells which causes cell division and growth (Stöß *et al.*, 2020). Tumour necrosis factor (TNF) and interleukin-6 (IL-6) may also be involved in triggering liver regeneration. The remaining lobes enlarge and restore the liver to its original size. Hepatocytes replicate once or twice before returning to their quiescent state. This process takes only 5-7 days in rats. Transforming growth factor- β (TGF- β) and cytokines secreted by hepatic cells are inhibitors of cell proliferation and thus terminate regeneration (Khonsary, 2017).

The liver has a vast array of functions in the body. Amino acid deamination, carbohydrate metabolism such as glycogen storage, gluconeogenesis, oxidation of fatty acids, synthesis of cholesterol, lipoproteins and plasma proteins, phospholipids, fat from proteins and carbohydrates occur in the liver (Mitra and Metcalf, 2012). The liver also cleanses the blood through Kupffer cells, has blood reservoir properties attributed to its large surface area for blood veins, increases lymphatic flow due to permeability of the hepatic sinusoids, stores iron

as ferritin and excess vitamins for up to 5-10 months. Proteins involved in blood coagulation such as prothrombin, fibrinogen, accelerator globulin and factor VII are all formed in the liver. Another major function of the liver is xenobiotic metabolism, which utilises the cytochrome P450 enzymes, CYPs (Ozougwu, 2017).

The liver is ideally located in the abdominal cavity to receive absorbed nutrients and to detoxify absorbed xenobiotics such as drugs and toxins that may be harmful. Liver enzymes transform endogenous and exogenous toxins and drugs such as sulphonamides, penicillin and erythromycin enabling them to be water-soluble and excreted in bile or urine (Guengerich *et al.*, 2016). Hormones produced by endocrine glands such as thyroxine and steroids such as estrogen, cortisol and aldosterone are also solubilised and excreted in bile and urine. Phase I reactions are catalysed by CYPs, followed by phase II reactions that conjugate the substances with glucuronide, sulfate, amino acids or glutathione (Girvan and Munro, 2016, Ozougwu, 2017).

2.3 Hepatocellular carcinoma (HCC)

Derived from hepatocytes and accounting for 85-90% of all primary liver cancers, HCC is the dominant form of liver cancers globally (Altekruse *et al.*, 2014, Chen and Wong, 2020).

2.3.1 Incidence

According to previous studies, HCC occurs more in men than women (Figure 2.3A) and has geographical distribution with more cases recorded in developing countries (Figure 2.3B) (El-Serag, 2020). Global cancer statistics for 2020 has reported liver cancer in males to be ranked as second position in mortality rates (Sung *et al.*, 2021). The disparity could be due to differences in behaviours, epigenetics, endogenous sex hormones, alcohol consumption patterns and immune responses. High mortality rates are recorded in Asia Pacific, East Asia, and central Sub-Saharan Africa and lowest in southern Latin America and tropical Latin America. HCC incidence has been marginally reduced by aggressive hepatitis B virus vaccination, aflatoxin-reduction programs and the use of antivirals to treat HBV and HCV infections. Coffee consumption, aspirin and metformin have in recent epidemiological studies shown to significantly decrease the incidence of HCC in diabetic patients (Singal *et al.*, 2020).

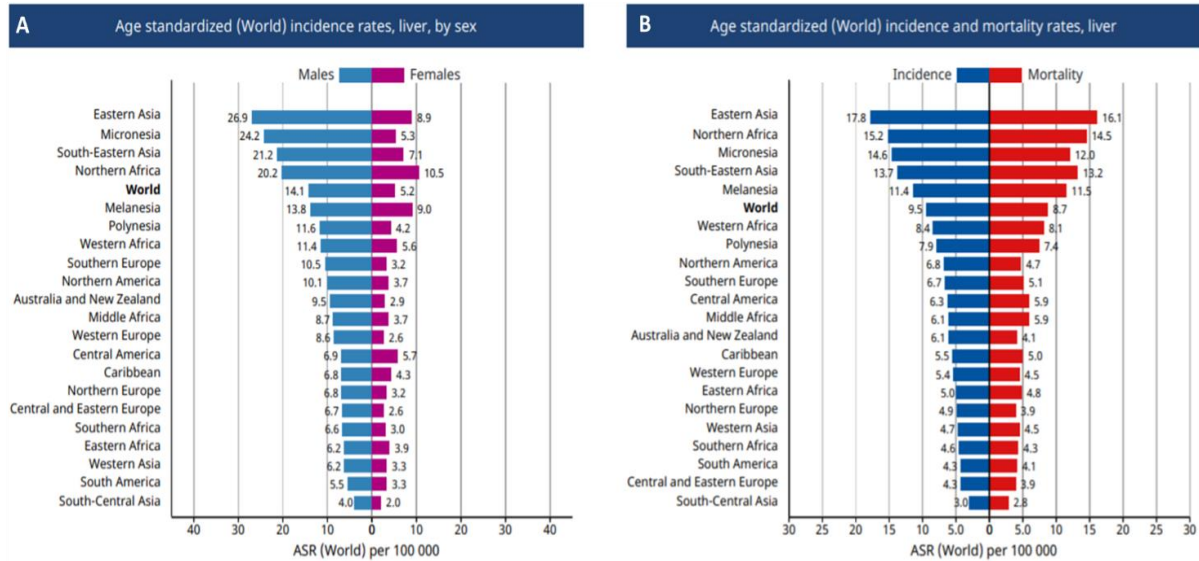


Figure 2.3: Incidence and mortality age-standardised rates for liver cancer in both sexes (Aslantürk, 2018).

2.3.2 Risk factors in the pathogenesis of liver cancer

There are major and minor risk factors of HCC. Chronic HBV, HCV, aflatoxin B₁, chronic alcohol consumption, cirrhosis, obesity, non-alcoholic fatty liver disease (NAFLD) and diabetes are considered to be the major causes of HCC (Liver, 2018). Wilson's disease, hemochromatosis and alpha-1-antitrypsin deficiency are minor risk factors associated with the development of HCC (Tanash and Piiulainen, 2019, Nowak *et al.*, 2018, Jayachandran *et al.*, 2020).

Hepatitis B virus exerts hepatocarcinogenic effects through the process of the inflammation, regeneration and fibrosis associated with cirrhosis (Figure 2.4) (Bréchot, 2004). The pathogenesis of HBV to HCC can either be direct or indirect. The direct mechanism involves the integration of the HBV DNA within or near functional cellular genes into chromosomes of hepatocytes (Figure 2.4). The HBx protein is a transcriptional activator that activates the Raf-Ras-MAPK pathway and inhibits the tumour suppressor protein, p53. The indirect mechanism (Figure 2.4) involves inflammation and regeneration, followed by cirrhosis associated with chronic HBV infection (Di Bisceglie, 2009). Cirrhosis is severe damage emanating from fibrosis and is a risk factor of HCC (Niu and Hann, 2017). Recent studies have suggested that 25% of people with HCV develop cirrhosis, especially if they are infected by another virus such as HBV or HIV and are chronic alcohol consumers. Stimulation of signal transduction

pathways within cells by HBx leads to the activation of interleukins and inflammasomes. In addition to activation of NF- κ B by acting on two distinct NF- κ B inhibitors, I κ B α and p105, HBx also induces the proliferation of HCC cells through AP1 overexpression as a result of ER stress (Lim *et al.*, 2013, Cho *et al.*, 2015).

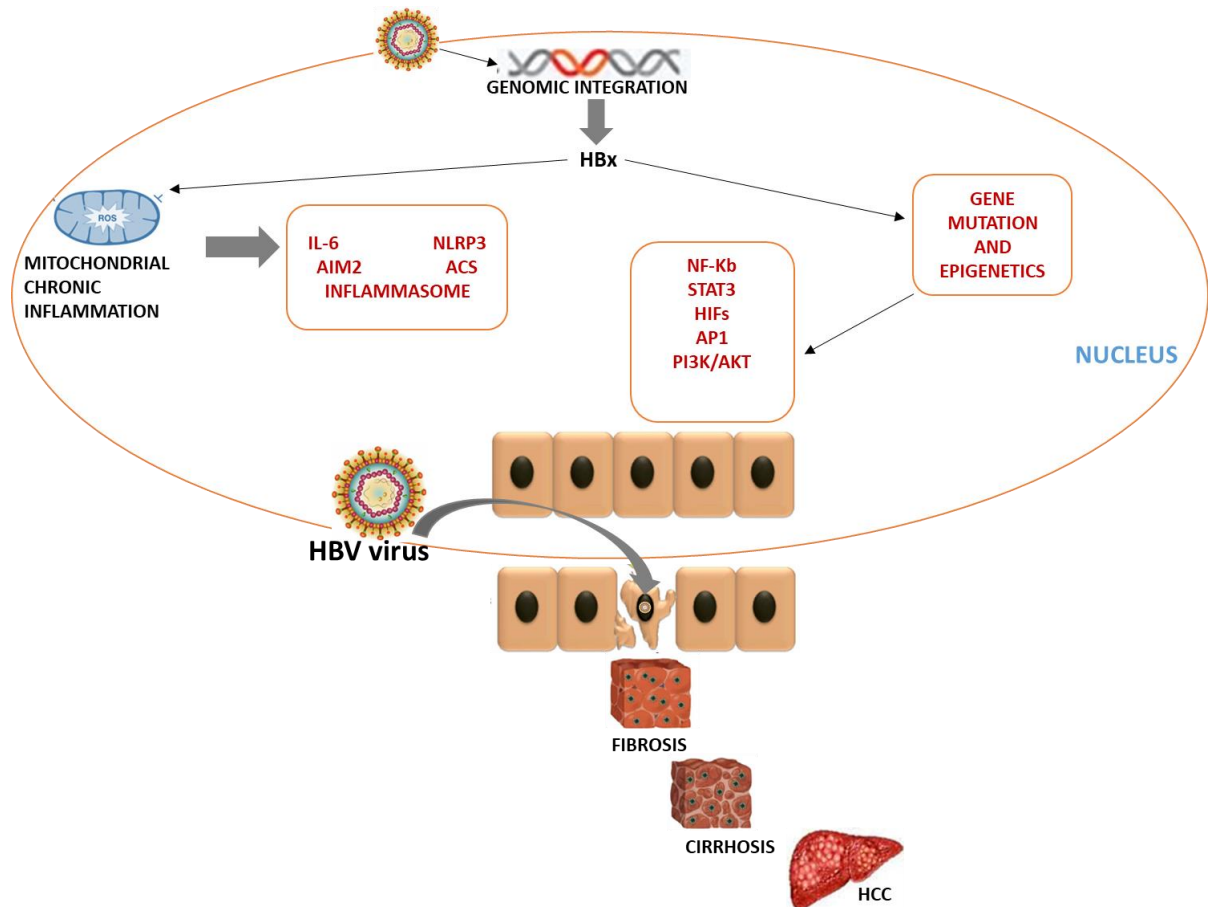


Figure 2.4: Pathogenesis of HCC associated with HBV. Viral integration into the hepatocyte genome initiates molecular events that causes cell death and/or inflammation and culminates in the development of fibrosis, cirrhosis and HCC [Adapted from (Arzumanyan *et al.*, 2013)].

2.3.3 Current treatments

The HBV vaccine is the primary preventative measure being implemented to reduce the risk of contracting the virus, which is a risk factor of HCC (Singal *et al.*, 2020). In severe cases surgical resection, radiotherapy, percutaneous ethanol injection, trans-arterial chemoembolization, chemotherapy and liver transplantation are the current treatments used for HCC. The treatment undertaken by each patient may differ and is highly dependent on the stage of tumour progression. Unfortunately, the available treatments are expensive, require well equipped medical facilities, and exert debilitating side effects such as toxicity and unfavorable bio-distribution that render the cancer patients incapacitated during the treatment window.

Additionally, these therapeutic options are not specific to cancer cells therefore may also affect and destroy healthy non-cancer cells (Liver, 2018, Raavé *et al.*, 2018).

The greatest challenge with the current available treatments is the poor prognosis due to late stage diagnosis due to the lack of presentable symptoms during earlier stages (Young *et al.*, 2019). Another challenge is the recurrence of the HCC even after liver transplants thus the estimated 5-year survival span is usually not achieved. Therefore, it is important that scientists continue to conduct research in order to identify the potential of naturally sourced compounds as a potent therapeutic agent against HCC as well as other forms of cancers (Pinna *et al.*, 2018). Over the years, medicinal plants have gained a lot of interest due to their easy accessibility and affordability, as well as their rich composition of phytochemicals that can be used in drug development and treating various ailments.

2.3.4 HepG2 cells as a model of HCC

The human liver cancer cell line, HepG2, was established in 1975 from the tumour tissue of a 15–year old Caucasian male who had hepatocellular carcinoma (Neumann *et al.*, 2007). The HepG2 cell line is commonly used in drug metabolism and hepatotoxicity studies because of its high proliferation rates, the epithelial-like morphology that executes distinguished hepatic functions reminiscent of the bile canaliculi and sinusoidal domains (Donato *et al.*, 2015). It has retained differentiated hepatic functions including macronutrient metabolism, blood volume regulation, immune system support, endocrine control of growth signaling pathways, lipid and cholesterol homeostasis and xenobiotic metabolism, thus making them a good *in vitro* model for cytotoxicity studies (Donato *et al.*, 2015). Furthermore, its non-tumourigenic properties make it an ideal model for *in vitro* hepatotoxicity studies (Donato *et al.*, 2015).

2.4 Medicinal Plants

Primary health care in developing countries is derived from ethnobotany with 60% of the worlds' population using traditional medicines extracted from one or more medicinal plants (Beigi *et al.*, 2018). In developed countries like the United States of America, 25% of the synthetic drugs are of herbal origins. There are no or minimal side effects from treatments prepared using medicinal plants; it is thus considered to be very safe, affordable and easily accessible alternative therapeutic option that can also be included in an individual's daily diet (Pushpangadan *et al.*, 2018).

In 2017, Sheikh and co-researchers used *Capparis spinosa* crude ethanolic extract on HepG2 cells. This medicinal plant inhibited cell proliferation in a dose dependent manner, increased expression of the Cdk inhibitory protein (Cip1/p21) and enhanced apoptosis of HepG2 cells by activation of caspase-8 and caspase-9, and down regulation of Bcl-2 (Sheikh *et al.*, 2017). In another study, the hepatoprotective activities of 64 crude ethanol extracts of Cambodian medicinal plants were investigated against tBHP-induced cytotoxicity in HepG2 cells. The study also assessed the cytoprotective mechanism pertaining to the expression of heme oxygenase (HO-1) and nuclear factor erythroid 2–related factor 2 (Nrf2). Of the 64 Cambodian plants, *Peliosanthes weberi* and *Tinospora crispa* exhibited hepatoprotective effects on tBHP-induced cytotoxicity in HepG2 cells. This could be alluded to the induction of Nrf2-mediated expression of HO-1 suggesting that *Tinospora crispa* or *Peliosanthes weberi* may be used therapeutically against liver disease that is characterized by oxidative stress (Lee *et al.*, 2017).

The *Terminalia* genus is amongst the most widely used medicinal plants to preserve human health and longevity. *Terminalia citrina* (*T. citrina*) for example is used for stomach aches and to relieve diarrhoea as well as haemorrhoids, whilst *T. ferdinandiana* possesses potent inhibitory properties against gastrointestinal protozoan parasite *Giardia duodenalis*. The leaf and fruit extracts of *T. ferdinandiana* also inhibited cellular proliferation against colorectal (Caco2) cells (Shalom and Cock, 2018). Some species have been found to treat hypertension, hyperglycaemia, constipation, malaria, tuberculosis, sexually transmitted infections and possess antioxidant properties which result in reduction of degenerative diseases. Shalom and co-researchers (2018) reported anti-cancer properties displayed by *T. ferdinandiana* leaf and fruit extracts (Shalom and Cock, 2018). The extracts inhibited cellular proliferation and also induced cellular metabolic rates lower than those at the commencement of the experiment. It is possible that the antiproliferative mechanism of these extracts involve induction of apoptosis through multiple pathways because caspase 3 activity was significantly increased, but caspase levels differentiating the apoptotic pathways were not tested (Shalom and Cock, 2018). In the same study, *T. ferdinandiana* ethyl acetate, methanolic and aqueous fruit and leaf extracts induced an increase in caspase 3 protein expression in Caco2 cells thus suggesting contribution to cell death by both the extrinsic and intrinsic apoptotic pathways. *Terminalia* species have been identified as central nervous system (CNS) and cardiovascular system (CVS) stimulants and induce the same effects as those of digoxin. *T. catappa*, *T. irvorensis* and *T. superba* decoctions have been used to treat breast, skin and prostate cancer respectively (Cock, 2015). One of the species, *T. arjuna* displayed potent anti-inflammatory properties in experimental

rodent models (Biswas *et al.*, 2011). The therapeutic properties of *Terminalia* species may be attributed to the phytochemicals possessed by the species like flavonoids, triterpenoids, saponins, tannins and β -sitosterol, which has an effect on inflammation by increasing prostaglandin E2 (PGE2), a coronary vasodilator (Beigi *et al.*, 2018).

2.5 *Terminalia phanerophlebia*

Terminalia is Latin for terminus referring to the clustered leaves at the end and *phanerophlebia* is Greek referring to the distinct veins under the leaves (Palmer and Pitman, 1972). *Terminalia phanerophlebia* (Figure 2.5) from the Combretaceae family is generally known as Lebombo cluster leaf. In South Africa, the tree number for *T. phanerophlebia* is 549 and is widely distributed in northern KwaZulu-Natal, Mpumalanga, Swaziland and marginally distributed in Mozambique (Nonyane, 2014). These trees are found in sandy, loam soils in valley bushveld, along streams and on stony hillsides. *T. phanerophlebia* is characterised by terminal leaf clusters (Figure 2.5A) and leaves with distinct veins (Figure 2.5B). The bark (Figure 2.5C) and roots of the plant are used to make concoctions used to treat a wide range of ailments. Flowering time is from October to February and flowers are white (Figure 2.5A, B) with a strong, unpleasant scent (Maurin, 2009).



Figure 2.5: (A) Clustered leaves at the end of the branch of *T. phanerophlebia*. (B) The leaves with distinct veins and seeds of *T. phanerophlebia*, (C) The bark of *T. phanerophlebia*. (Adapted from candidegardening.com)

2.5.1 Uses of *Terminalia phanerophlebia*

Terminalia species have been used to treat backaches, bilharzias, pneumonia, syphilis, earache, hookworm and dysmenorrhoea (Shai *et al.*, 2008). In their study, Shai *et al.* (2008) found *T. sambesiaca* and *T. phanerophlebia* to have the highest antifungal and antibacterial activity than the other species tested (Shai *et al.*, 2008). The triterpenoids found in the crude extract and ethanol extract of the stems of *T. phanerophlebia* have the ability to inhibit the cyclooxygenase enzyme COX-2 and therefore the plant is said to possess anti-inflammatory effects (Nair *et al.*, 2012). In 2014, Madikizela and other investigators discovered two compounds reported for the first time from *T. phanerophlebia*, methyl gallate (methyl-3,4,5-trihydroxybenzoate) and a phenylpropanoid glucoside, 1,6-di-O-coumaroyl glucopyranoside (Madikizela, 2014). Both compounds exuded antimicrobial properties and thus substantiated the use of *T. phanerophlebia* to treat tuberculosis and related symptoms in traditional medicine (Madikizela, 2014). Sibandze and van Zyl (2009) found *T. phanerophlebia* leaves to display *in vitro* antimalarial activity in their study on Swazi medicinal plants (Sibandze and Van Zyl, 2009). Root decoctions are used in various parts of Africa as an eyewash agent and to treat diarrhea, colic and schistosomiasis. Hot infusions of outer layers of roots are used to treat pneumonia (Maurin, 2009).

2.4.2 Phytochemistry of *Terminalia* species

A variety of *Terminalia* species have been found to possess secondary metabolites such as triterpenoids, tannins, flavonoids, alkaloids, anthocyanin, gallic acid, chlorophyll a and b, vitamin E, glycosides, saponins and calcium oxalate crystals (Figure 2.6) (Zhang *et al.*, 2019). Bioflavonoids such as quercetin have antitumour activities and also block the activity of HNE-induced JNK from lipid peroxidation through inhibition of glycolysis, cell cycle and enzymes (Uchida, 2008). Flavonoids also alter signal transduction in pro-tumour pathways and trigger apoptosis in tumour cell lines as well as cause T- cell proliferation (Jain *et al.*, 2016).

There are two types of saponins, steroidal aglycone and triterpenoid aglycone. Seeds, tubers, roots and leaves contain the highest concentration of saponins in a plant. Saponins are known for their antitumour properties through cell cycle arrest and apoptosis with the half-maximal inhibitory concentration (IC_{50}) values of 0.2 mM. Man and coinvestigators (2010) found that the cycloartane saponins induced apoptosis and modulated an ERK-independent NF- κ B signaling pathway resulting in a down-regulation of the expression of the HCC tumour marker α -fetoprotein and suppression of HepG2 cell growth (Man *et al.*, 2010).

Triterpenoids are metabolites of isopentenyl pyrophosphate oligomers that can alter multiple dysregulated cellular pathways (Bishayee *et al.*, 2011). They exhibit cytotoxicity against tumour cells and have been used for chemoprevention and therapy of mammary carcinoma because of their potent anti-inflammatory and anticarcinogenic properties. Most Asian countries employ triterpenoids for their sedative, cardiotoxic, antipyretic, hepatoprotective, anti-inflammatory and analgesic properties (Sen and Samanta, 2014). Several studies identified other biological activities of triterpenoids including antiviral, antipruritic antimicrobial, antiangiogenic and spasmolytic activities. Triterpenoids have also been found to preserve the integrity of normal cells, whilst being cytotoxic to cancer cells (Bishayee *et al.*, 2011). They were found to act through the intrinsic apoptosis pathway to prevent tumour progression (Yadav *et al.*, 2010). The main compounds found in triterpenoids are cucurbitanes; cucurbitacin I suppressed proliferation of MDA-MB-468 cells by increasing apoptosis and decreasing phosphor-STAT3, while cucurbitacin displayed inhibitory effects on the growth of MCF-7 cells by decreasing COX-2 (Jayaprakasam *et al.*, 2003, Blaskovich *et al.*, 2003). They also inhibited the G₂-M phase of the cell cycle as well as increase in cytochrome c and apoptosis (Yang *et al.*, 2007).

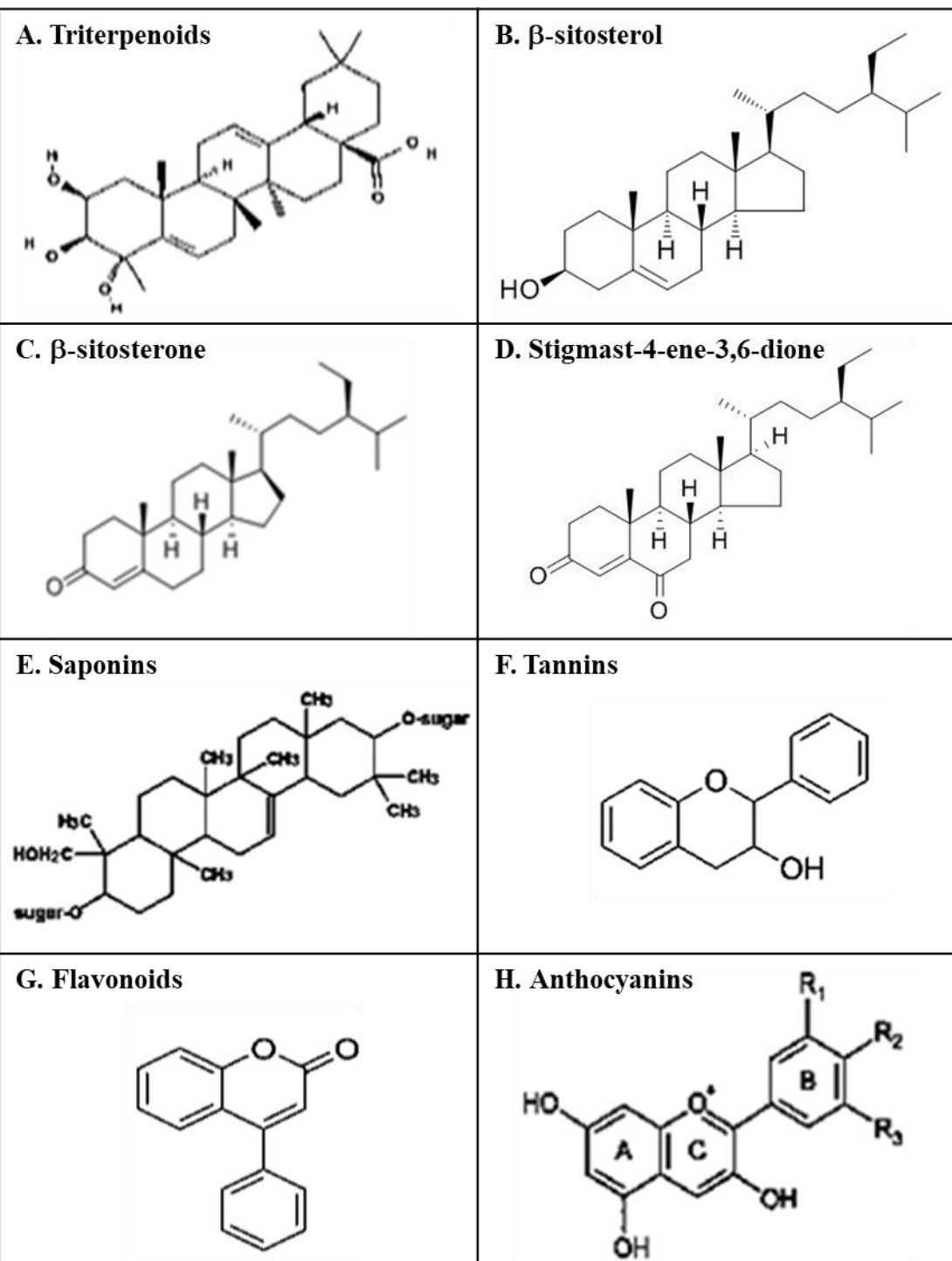


Figure 2.6: Some of the phytochemicals possessed by *Terminalia* species. The medicinal properties are credited to the phytochemical secondary metabolites present in *Terminalia* plants namely triterpenoids (A,B,C,D), tannins (F), flavonoids (G), alkaloids, anthocyanins (H), gallic acid, chlorophyll a and b, vitamin E, glycosides, saponins (E) and calcium oxalate crystals (Kaur *et al.*, 2009, Liao *et al.*, 2019).

2.6 Oxidative stress

Oxidative stress is the state of imbalance between reactive oxygen species (ROS)/reactive nitrogen species (RNS) and antioxidants (Figure 2.7). Within intact mitochondrion, ROS are produced but is balanced by the antioxidants such as superoxide dismutase (SOD2) and glutathione peroxidase (Gpx) (Lenaz, 2001, Siti *et al.*, 2015). Excess cellular levels of ROS may have detrimental effects to proteins, nucleic acids, lipids, membranes and organelles leading to the activation of cell death processes such as apoptosis (Redza-Dutordoir and Averill-Bates, 2016b).

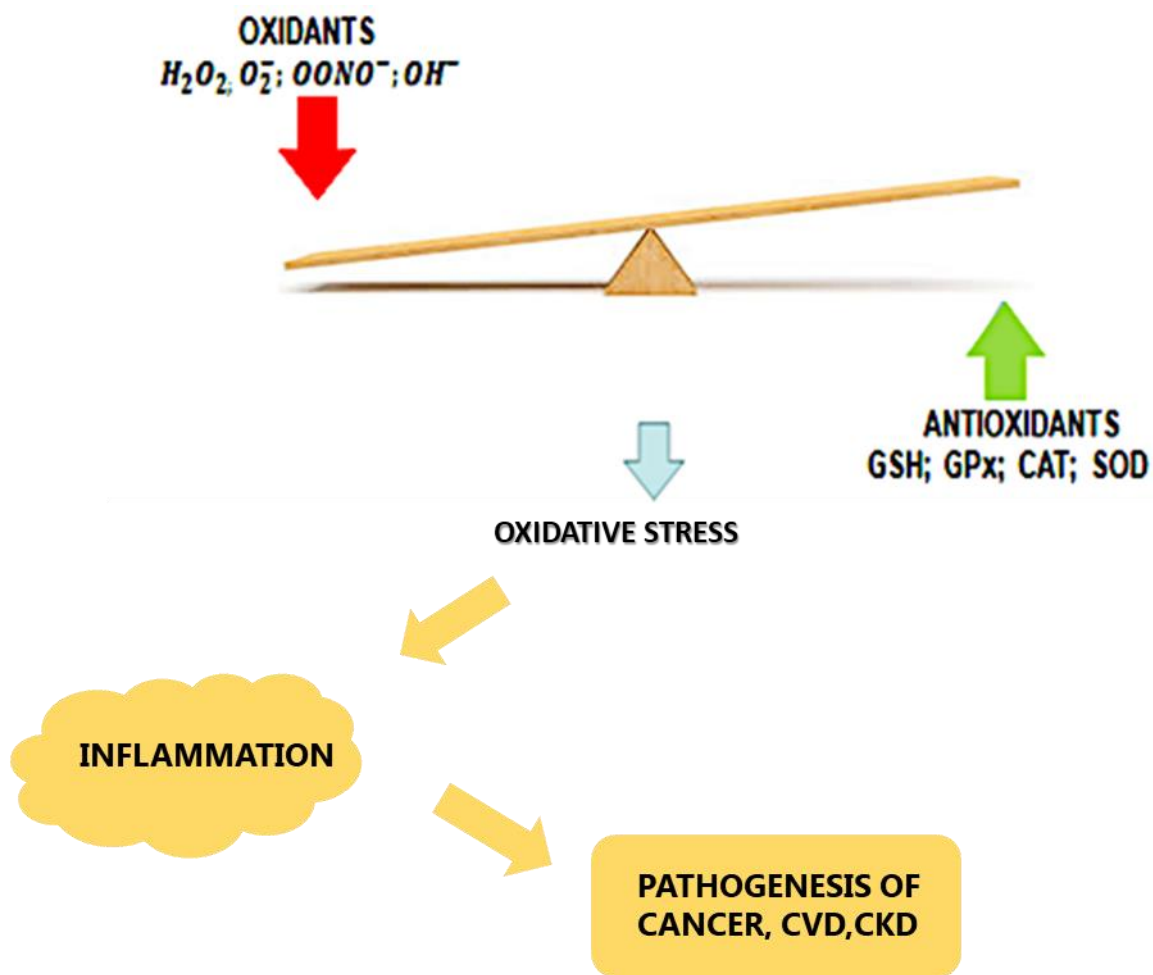


Figure 2.7: Oxidative stress. A state of imbalance between oxidants and antioxidants results in the pathogenesis of cancer, cardiovascular diseases, chronic kidney diseases as well as other neurodegenerative diseases like Alzheimer's disease. (*Prepared by author*).

2.6.1 Free radical production

In aerobic metabolism, partial reduction of molecular oxygen gives rise to a series of free radicals, termed ROS/RNS, which are highly unstable and very reactive oxidants. Examples of oxidants are the superoxide radical (O_2^-), hydrogen peroxide (H_2O_2) and highly reactive

hydroxyl radical ($\cdot\text{OH}$) (Figure 2.7). On the other hand, antioxidant enzymes are the proteins involved in the catalytic transformation of reactive oxygen species and their by-products into stable nontoxic molecules (Figure 2.8) (Sáez and Están-Capell, 2014). Under normal circumstances, the generation of ROS in cells exists in equilibrium with a variety of antioxidant defenses and may trigger the signal transduction pathways leading to the activation of different transcription factors and gene expression. However, an increase of ROS above a critical threshold may induce oxidative stress (Polster, 2013).

2.6.2 Antioxidant defence

Antioxidant enzymes catalyze mainly three different reaction mechanisms: dismutation, peroxidase reactions, and thiol reductions. Superoxide dismutases (SODs) are antioxidants which have copper/zinc/manganese isoforms and dismutate $\text{O}_2^{\cdot-}$ as well as modulate nitric oxide (NO) levels (Figure 2.8). Catalase is a heme homotetrameric enzyme that catalyses the decomposition of H_2O_2 to water and oxygen (Figure 2.8), detoxifies phenols, formic acid, methanol and ethanol, and may carry out peroxidation reactions in mammals. Glutathione (GSH) together with α -tocopherol has antioxidative properties (Hausladen and Alscher, 2017). Glutathione peroxidases (Gpxs) are a superfamily of eight isoenzymes (GPx-1-Gpx8); the most ubiquitous and abundant isoenzyme is GPx-1 and carries one selenocysteine, whilst Gpx2 is the enzyme of the gastrointestinal tract (Sáez and Están-Capell, 2014). Gpx catalyzes the reduction of hydroperoxides (-ROOH) to alcoholic groups and water by oxidising GSH to glutathione disulfide (GSSG), which can be reduced back to GSH by the enzyme GSH reductase (GR), using NADPH as a reducing substrate (Figure 2.8) (Sáez and Están-Capell, 2014). The capacity to recycle GSH makes the GSH cycle able to prevent the depletion of cellular thiols and play a pivotal role as an antioxidant mechanism for aerobic cells. The coordination and synchronized activities of SOD, catalase, GSH and Gpx complete and ensure the antioxidant strategy to avoid the production of the highly reactive $\cdot\text{OH}$ via the Fenton reaction and peroxynitrite (ONOO^-), formed by the reaction of $\text{O}_2^{\cdot-}$ with the vasoactive intermediate NO (Khalaf, 2019). The Nrf-2 protein is a transcription factor that is ubiquitously and constitutively expressed by cells, thus ensuring their prompt protective response to oxidative, inflammatory and metabolic stresses (Robledinos-Antón *et al.*, 2019). The transcription of components of the glutathione and thioredoxin antioxidant systems, enzymes involved in phase I and phase II detoxification of xenobiotics, NADPH regeneration, and heme metabolism are regulated by Nrf2. In addition to antioxidant responses, Nrf2 is also involved

in autophagy, intermediary metabolism, stem cell quiescence, and unfolded protein response (Tonelli *et al.*, 2018).

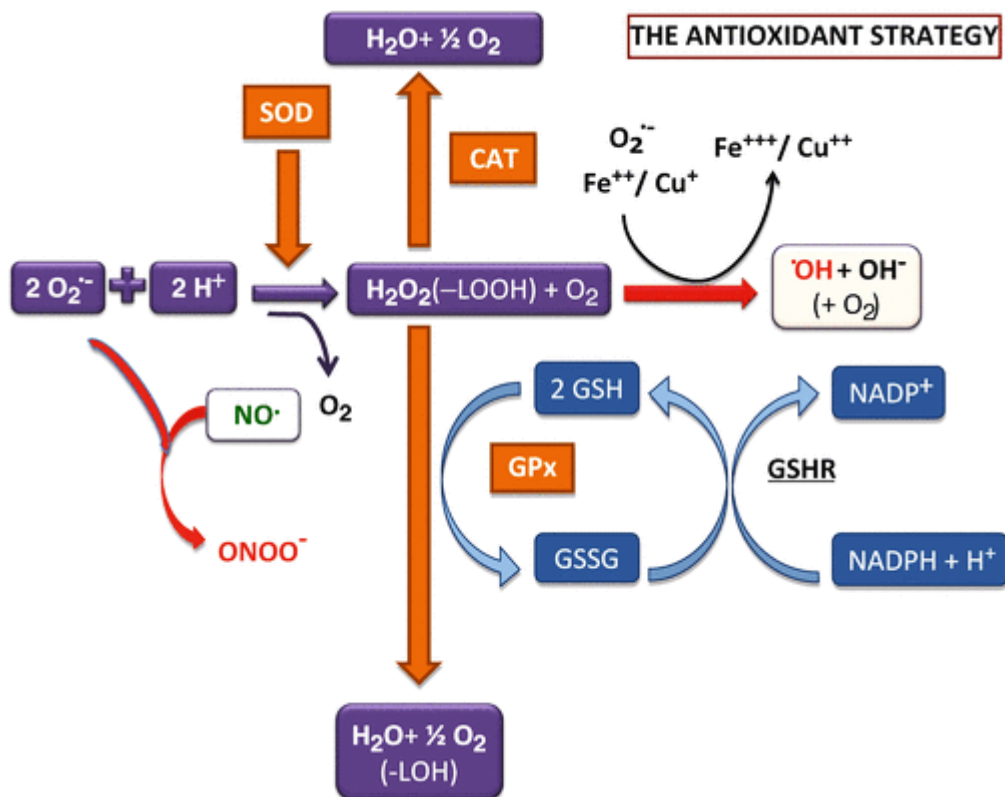


Figure 2.8: Antioxidant reactions showing the catalytic transformation of ROS/RNS by SOD, catalase and Gpx to nontoxic stable molecules. The Haber-Weiss- or Fenton-type reactions lead to the formation of the highly reactive oxygen species ·OH. Superoxide may react with NO to produce the cytotoxic substrate ONOO⁻. The antioxidants protect cells against an excessive generation of reactive oxygen and nitrogen species and secondary oxidative stress while maintaining the physiological concentrations and vasodilating action of NO (Sáez and Están-Capell, 2014).

2.6.3 ROS-mediated cellular effects

Highly reactive ROS/RNS are capable of damaging membrane phospholipids, proteins, carbohydrates and nucleic acids through an oxidative modification process giving rise to a number of different oxidative stress by-products (Figure 2.9) (Sáez and Están-Capell, 2014). During lipid peroxidation, a free radical oxidizes an unsaturated lipid chain forming a lipid hydroperoxide and an alkyl radical. This alters the membrane structure, affecting its fluidity thus damaging its integrity. This process is initiated by the attack of a ·OH at one of the bis-allelic positions in the fatty acid side chains. The association of oxygen-derived free radical with polyunsaturated fatty acids results in a number of extremely reactive electrophilic

aldehydes during the process of lipid peroxidation due to continuing free radical chain reactions before they are terminated (Juan *et al.*, 2021, Srinivas *et al.*, 2019). Quantification of primary products of lipid peroxidation is difficult due to their high instability and reactivity. Thus, the concentration of secondary oxidation products, which are mostly aldehydes derived from these initial hydroperoxides such as malondialdehyde (MDA) are measured (Hebbani *et al.*, 2021). The effects of ROS on proteins include oxidation of amino acid residues, cleavage of peptide bonds and aggregation between proteins. A wide range of diseases have been linked to the presence of oxidised proteins, such as Alzheimer's disease, rheumatoid arthritis and others (Juan *et al.*, 2021). The DNA damage caused by ROS from endogenous or exogenous sources has been a significant breakthrough in carcinogenesis research. The ROS react with nitrogenous bases and deoxyribose, causing significant oxidative reactions which lead to mutations, carcinogenesis, apoptosis, necrosis and hereditary diseases (Juan *et al.*, 2021).

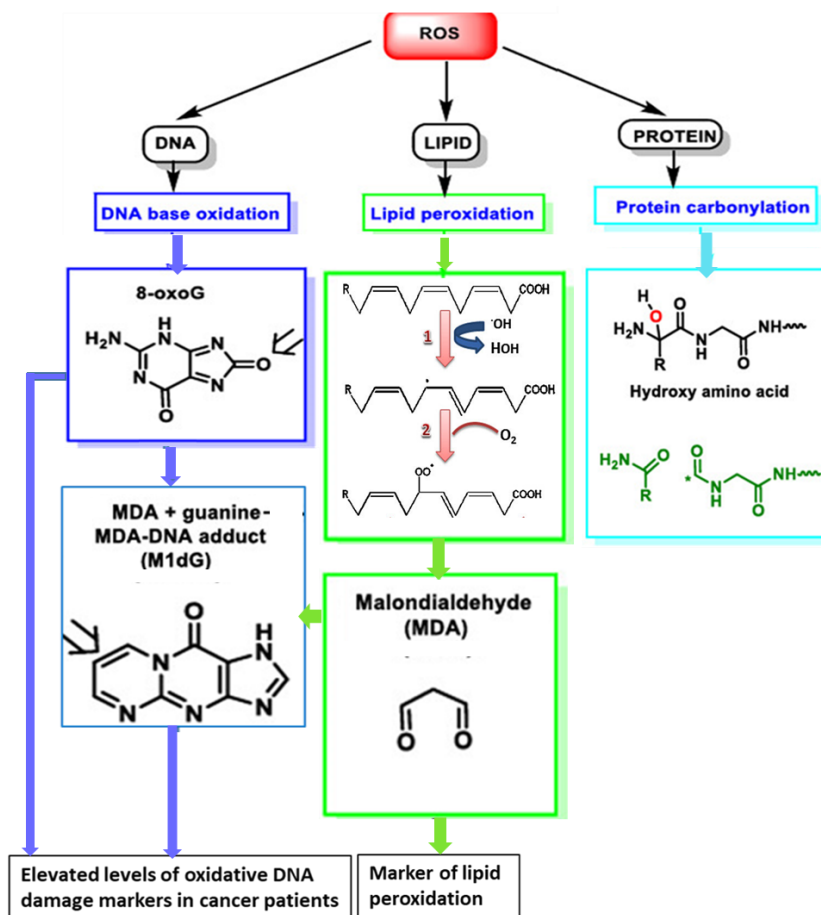


Figure 2.9: A summary of ROS damage on macromolecules. Damage in nucleic acids results in base oxidation, damage in lipids results in aldehydes and secondary by-products of lipid peroxidation such as malondialdehyde (MDA) and damage to proteins causes carbonylation (Juan *et al.*, 2021).

Increase in ROS production in a cell also leads to the activation of mitogen-activated protein kinases (MAPKs) such as p38, ERK and JNK. The MAPKs play a crucial role in signal transduction from the cell surface to the nucleus (Son *et al.*, 2011, Jalmi and Sinha, 2015). Initially I κ B inhibits the action of NF- κ B, but after the MAPKs are activated NF- κ B is activated through phosphorylation and dimerization of I κ B (Figure 2.10) (Ijomone *et al.*, 2021). Activated NF- κ B is translocated from the cytoplasm to the nucleus where it triggers transcription of target genes (An *et al.*, 2019, Bagaev *et al.*, 2019). Activation of these anti-proliferative proteins such as p38, NF- κ B and Fas by an oxidative stress environment is pivotal in the cascade of events leading to apoptosis (Gào and Schöttker, 2017).

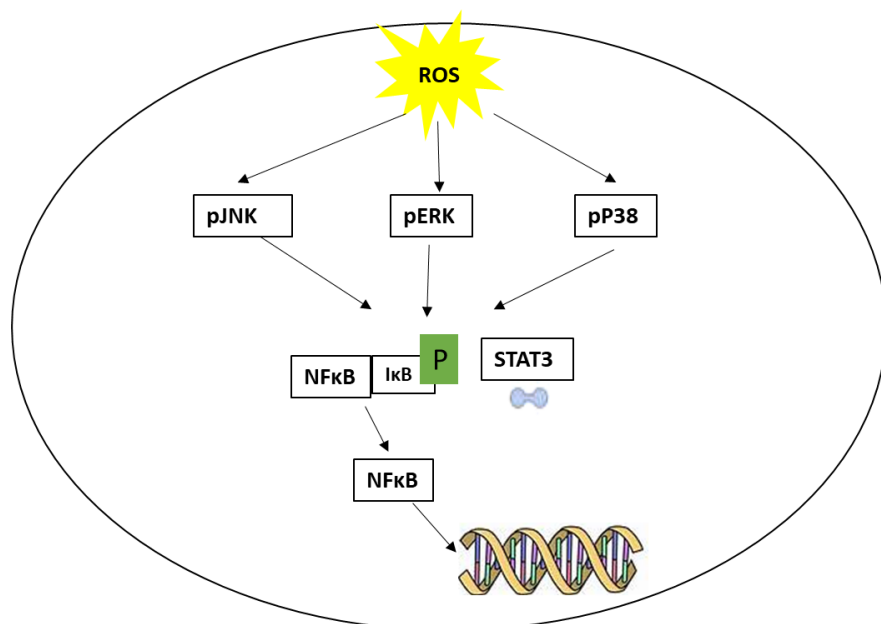


Figure 2.10: Activation of MAPKs through ROS. MAPKs play a pivotal role in signal transduction from the onset of stimuli such as an oxidative stress environment on the cell surface through activation of NF- κ B to activation of target genes [Adapted from (Ijomone *et al.*, 2021)].

The oxidative stress environment also triggers the activation of proliferative proteins such as HSP90 and STAT3. The activity of STAT3 has a critical role in the induction of survival factors such as the activation of Bcl-2 family, increased transcription of the survivin gene and prevention of apoptosis (Fathi *et al.*, 2018, Gritsko *et al.*, 2006, Levy and Lee, 2002). In a study by Xu and co-researchers (2017), HSP90 was found to increase the phosphorylation of PKM2 at Thr-328. The Thr-328 phosphorylation was critical for maintaining PKM2 stability and its biological functions in regulating glycolysis, mitochondria respiration, proliferation and inhibition of apoptosis in HCC cells thus enhancing the cells' survival (Xu *et al.*, 2017). In a

different study, HSP90 was found to increase transcription of the surviving gene (Fortugno *et al.*, 2003).

2.7 Apoptosis

Apoptosis features a characteristic set of morphological and biochemical features, whereby cells undergo a cascade of self-destruction (Shakeri *et al.*, 2017). Apoptosis is a highly regulated process that is essential for the development and survival of multicellular organisms (Nikoletopoulou *et al.*, 2013). It is governed chiefly by caspases (cysteine-aspartic proteases), which are always present as procaspases, an inactive form containing a pro-domain that contains a caspase recruitment domain and can be activated by cleavage (Redza-Dutordoir and Averill-Bates, 2016a). Inhibitor of apoptosis proteins (IAPs) have a zinc binding domain that binds directly to caspases and inhibits their activity, but mitochondrial proteins called second mitochondria-derived activator of caspases (SMAC) and direct inhibitor-of-apoptosis protein-binding protein with low PI (DIABLO) in-turn inhibit the inhibitors in case of cell injury and need for apoptosis (Martinez-Ruiz *et al.*, 2008). There are also mitochondrial proteins, Htra2/Omi, apoptosis-inducing factor and endonuclease G, that can also inhibit IAPs. The tumour suppressor protein p53 is a key regulator of DNA damage response and can promote DNA repair, apoptosis or cell cycle arrest (Nayak *et al.*, 2018).

The extrinsic/death-receptor-mediated and intrinsic/mitochondrial mediated are the two mechanisms that also regulate apoptosis. Regulation of apoptosis is crucial for preserving normal cellular homeostasis and the B-cell lymphoma 2 (Bcl-2) family of pro-apoptotic proteins such as Bcl-2-associated death promoter, Bcl-2 associated X protein (Bax) and anti-apoptotic proteins such as Bcl-2 and Bcl-x contribute extensively to the regulation of apoptosis (Peña-Blanco and García-Sáez, 2018, Liu *et al.*, 2002). Unregulated apoptosis contributes to tumour development, neurodegenerative disorders and autoimmune diseases (Peña-Blanco and García-Sáez, 2018). Some oncogenic mutations disrupt apoptosis, leading to tumour initiation, progression or metastasis and thus affecting the malignant phenotype. Most cytotoxic anticancer agents induce apoptosis and medicinal plants are considered rich sources for chemotherapeutic agents (Nayak *et al.*, 2018).

2.7.1 *The intrinsic pathway*

The intrinsic pathway (Figure 2.11) is initiated by signals from the cytosol and is also referred to as the mitochondrial pathway. Signaling is due to cell stress such as endoplasmic reticulum stress or DNA damage. Sensory proteins such as ataxia telangiectasia mutated (ATM) and checkpoint kinases (CHKs) activate p53, which is also involved in cell cycle regulation. The tumour suppressor protein p53 recruits other regulatory proteins such as p21, a cyclin dependent kinase (CDK) inhibitor. It also inhibits Bcl-2 and activates Bax which alters the mitochondrial outer membrane permeability (MOMP) by perforating the mitochondrial membrane (Peña-Blanco and García-Sáez, 2018). The pores in the mitochondria result in the release of cytochrome c into the cytosol and this is considered as a death signal. Cytochrome c facilitates the formation of an apoptosome with apoptosis protease activating factor 1 (APAF-1), ATP and procaspase-9 that activates the initiator caspase, caspase-9 (Shakeri et al., 2017). Caspase-9 triggers the cleaving of procaspase-3 into its active form, caspase-3, which further activates the nuclease enzymes by degrading the nuclease inhibitors. The nucleases will degrade nucleic acids in the nucleus.

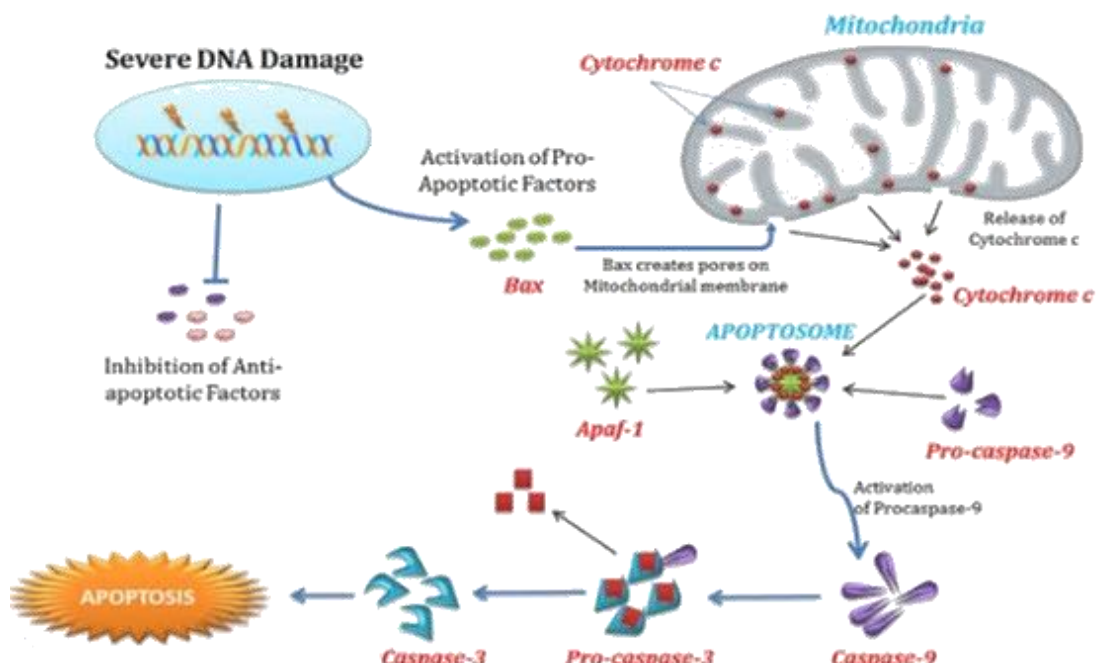


Figure 2.11: The intrinsic apoptotic pathway (Adapted from the Easy Biology Class).

2.7.2 *The extrinsic pathway*

Signaling originating from outside the cell initiates the extrinsic apoptotic pathway (Figure 2.12). Cellular stress such as DNA damage triggers extracellular response by the Fas-ligand, a transmembrane protein expressed on cytotoxic T-lymphocytes, which migrates towards the cell

membrane and binds to the FAS-ligand associated death domain containing receptors (FADD/FasR) (Figure 2.12). The Fas ligand signals through the trimerisation of the FasR resulting in death induced signaling cascade (DISC). The DISC activates the initiator caspase-8 from its inactive form, procaspase-8. Caspase-8 activates the executioner caspase, caspase-3, and can also activate BH3-interacting domain death agonist (Bid) into the active form truncated p15 Bid (tBid), which simultaneously activates the Bax/Bak pro-apoptotic proteins responsible for perforating the mitochondrial membrane and initiating the intrinsic pathway of apoptosis (Peña-Blanco and García-Sáez, 2018).

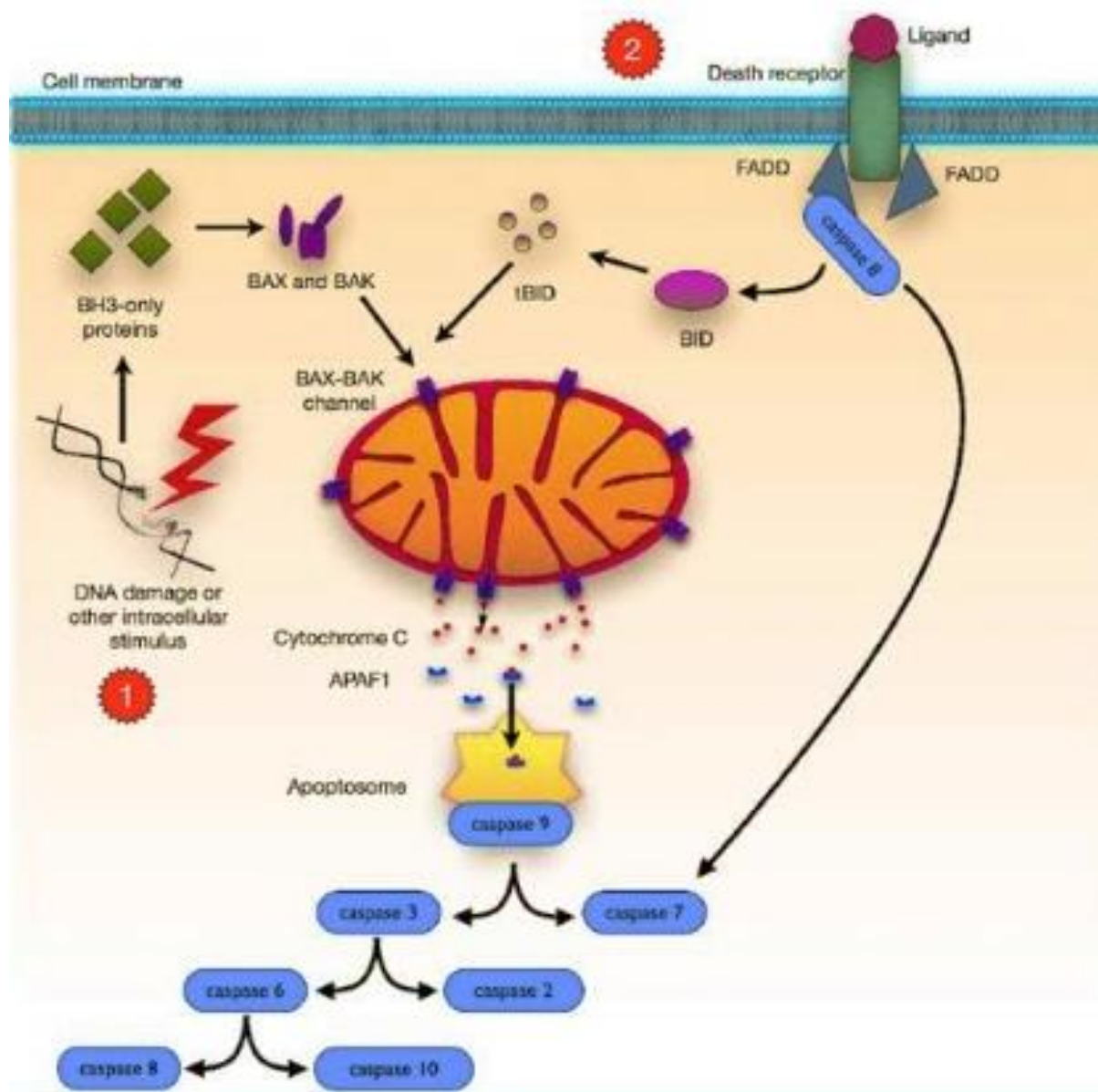


Figure 2.12: The extrinsic apoptotic pathway. Caspases are activated through the death receptor ligand. Binding of the Fas-ligand recruits the initiator caspases in their inactive forms, procaspase-8 and

procaspase-10 which are activated into their active forms. The DISC is formed which activates the downstream signal cascade (Glowacki *et al.*, 2013).

2.7.3 End-stage cell death

The main steps of apoptosis in chronologic order are shrinkage of the cell forming blebs, cell fragmentation, cytoskeleton collapses, disassembling of the nuclear envelope and then release of apoptotic bodies for phagocytosis (Figure 2.13). This distinguishes apoptosis from other modes of cell death, such as necrosis and pyroptosis (Figure 2.13). Caspase 3/7 are effector caspases responsible for cleaving downstream substrates such as poly (ADP-ribose) polymerase (PARP) and ADP-ribose, which contribute to cell death by depleting the cell of NAD and ATP (Boulares *et al.*, 1999). Cleavage of lamins by caspase 3 is essential for disintegrating the nuclear matrix during apoptosis (Kivinen *et al.*, 2005). Caspase 3/7 also activates the nuclease enzyme caspase activated DNase (Fortugno *et al.*) by degrading the nuclease inhibitor iCAD. Active nucleases degrade the nucleic acids in the nucleus and the cell starts to die. Activation of certain downstream signals such as caspase-3/7 results in enzymes like scramblases collapsing the polarized distribution of phosphatidylserine from the inner leaflet of the phospholipid bilayer to the outer layer. The external exposure of phosphatidylserine flags as an apoptotic signal attracting phagocytosis of the cell by macrophages (Figure 2.13) (Budhu *et al.*, 2021) (Gottlieb *et al.*).

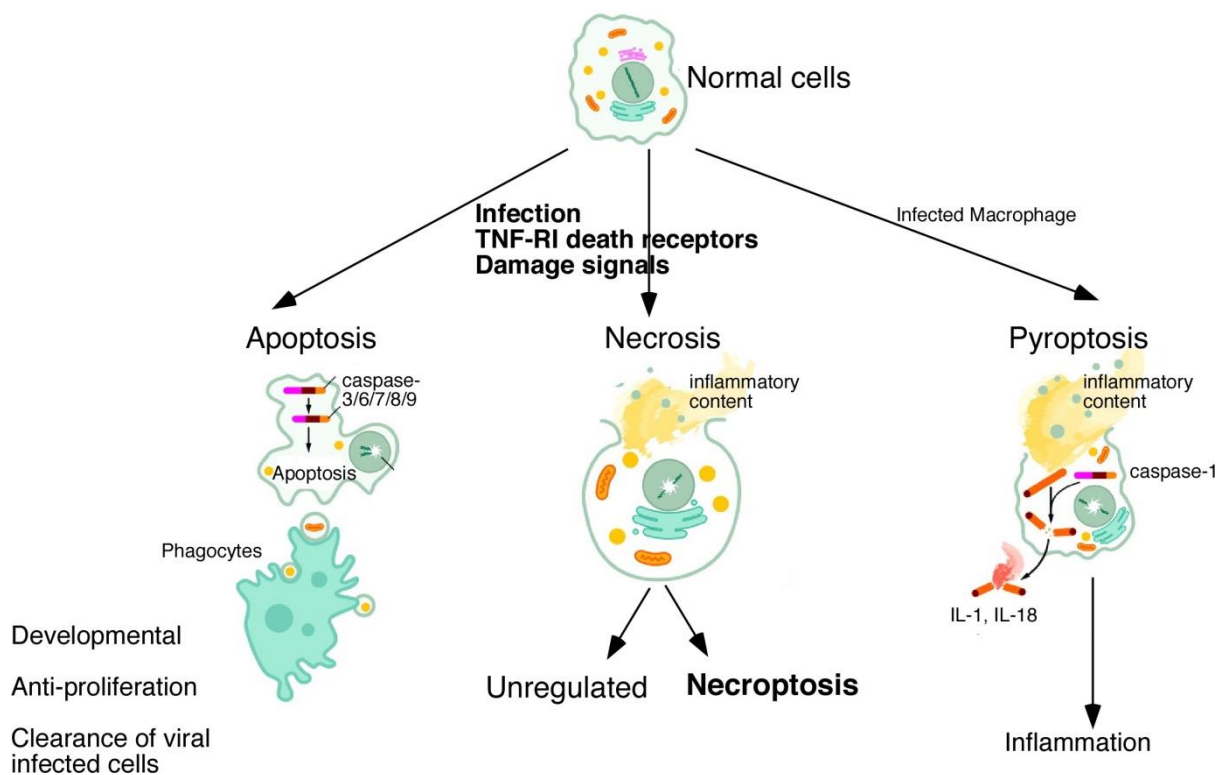


Figure 2.13: Characteristics of apoptosis (Adapted from Winoto lab). Apoptosis is chiefly regulated by caspases and the target cell shrinks forming blebs that later bud off as apoptotic bodies that are engulfed by phagocytes.

CHAPTER 3: MATERIALS AND METHODS

3.1 Materials

Cell culture vessels including flasks, plates, sterilin tubes and eppendorfs and reagents such as Eagle's Minimum Essential Medium (EMEM), penicillin-streptomycin-fungizone, L-glutamine and trypsin were purchased from Whitehead Scientific (Johannesburg, South Africa). Trypan blue, phosphate-buffered saline (PBS), 3-(4, 5-dimethyl-2-thiazolyl)-2, 5-diphenyl-2H-tetrazolium bromide, malondialdehyde (MDA), thiobarbituric acid (TBA) and β -actin were obtained from Sigma (Johannesburg, South Africa). Foetal calf serum, bovine serum albumin (BSA) and all primers were purchased from Inqaba Biotech (Johannesburg, South Africa). Western Blotting and PCR equipment and reagents were obtained from Bio-Rad (Hercules, CA, USA). Cell Signalling Technology antibodies and Promega luminometry kits were procured from Anatech (Johannesburg, South Africa). All other reagents were purchased from Merck (Darmstadt, Germany), unless stated otherwise. All tissue culture reagents and apparatus were obtained from Whitehead Scientific (Johannesburg, South Africa). The bicinchoninic acid (BCA) assay kit, β -actin and methylthiazol tetrazolium (MTT) salt were purchased from Sigma (Johannesburg, South Africa). Promega luminometry kits and Cell Signaling Technology (CST) antibodies were procured from Anatech (Johannesburg, South Africa), while protease and phosphatase inhibitors were obtained from Roche Diagnostics (Johannesburg, South Africa). Western blot reagents were purchased from Bio-Rad (Hercules, CA, USA) and all other reagents were obtained from Merck (Johannesburg, South Africa), unless specified otherwise.

3.2 Tissue culture

Vials of cryopreserved HepG2 cells were received from the Discipline of Medical Biochemistry, Howard College, University of KwaZulu-Natal, Durban. The vials were thawed at 37°C and reconstituted in 20 mL complete culture media (CCM; Eagle's Modified Eagle's Medium, 10% foetal calf serum, 1% L-glutamine and 1% penicillin-streptomycin-fungizone. The cells were incubated at 37°C with 5% carbon dioxide supply overnight. The CCM was changed to remove residual dimethyl sulfoxide (DMSO). Thereafter, the cells were maintained by changing the media as appropriate every 24-48 hours. Once confluence was reached the media was discarded, the cells were trypsinised, then resuspended in CCM and counted using the trypan blue method. The cell number was adjusted as required for various assays.

3.2.1 Trypsinisation

Cell media was decanted and cells were washed thrice using 5 mL of PBS each time, then 1 mL of trypsin was added to each flask for 1-3 minutes before discarding the trypsin. The flasks were gently banged to dislodge the cells before adding 10 mL of fresh CCM.

3.2.2 Cell counting

To an eppendorf, 150 µL of CCM, 50 µL of cell suspension and 50 µL of trypan blue were added. After mixing well, 10 µL of the mixture was pipetted to a haemacytometer and cells in all five quadrants were counted. The number of cells in suspension was determined using the formula below:

$$\text{cells/mL} = \frac{\text{total number of cells}}{5} \times 5 \times 10^4$$

3.3 Preparation of plant extracts

Terminalia phanerophlebia Engl. & Diels leaf extract was obtained from the Department of Medical Biochemistry, Howard College, University of KwaZulu-Natal, Durban (voucher specimen - 5544000 and accession No.18267). A 10 mg/mL aqueous stock solution of the extract was prepared and the solution was centrifuged at 400 rpm, 24°C for 10 minutes and used to prepare the concentrations of *T. phanerophlebia* crude extract required for the study (HepG2: IC₅₀ - 1396 µg/mL).

3.4 3-(4, 5-dimethylthiazol-2-yl)-2, 5-diphenyltetrazolium bromide (MTT) assay

3.4.1 Principle

The purpose of the MTT assay is to assess cell metabolic activity/viability/proliferation. The MTT (yellow salt) enters the cells and then the mitochondria where it is reduced by mitochondrial dehydrogenase to formazan (purple insoluble salt, Figure 3.1). The MTT salt is impermeable to synthetic lipid membranes, but passes the plasma membrane of living cells through active transport via endocytosis (van Meerloo *et al.*, 2011). Reduction can only be measured in metabolically active cells. The assay is a quantitative colorimetric method checking absorption at 570 nm and a reference wavelength of 690 nm. Reference wavelengths are used to correct or normalize changes that are not from the measuring wavelength of the analyte (Martin *et al.*, 2005). The assay determines effective concentration rather than lethal concentration. In cytotoxicity assays like the MTT assay, the concentration required to kill 50% of the cell population also referred to as IC₅₀/LD₅₀, should be measured (Adan *et al.*, 2016).

However, MTT cannot differentiate between cytostatic and cytocidal effects and is less effective when there is no cell proliferation. Assay conditions can alter metabolic activity and the tetrazolium dye reduction without affecting cell viability. Dimethyl sulfoxide (DMSO) is added to formazan to solubilise it before reading the absorbance (Bruggisser *et al.*, 2002). In this study, MTT assay will be used for cytotoxicity testing of *T. phanerophlebia* on HepG2 cells.

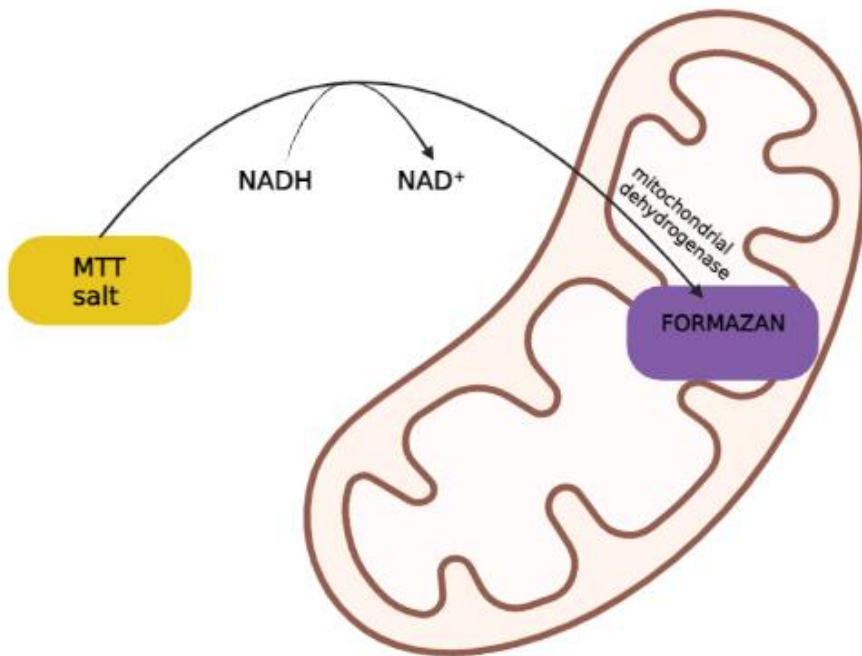


Figure 3.1: The MTT assay principle. The MTT salt (yellow) is reduced by the enzyme mitochondrial dehydrogenase to formazan (purple) in the mitochondria of active cells [Adapted from (Ali-Boucetta *et al.*, 2011)].

3.4.2 Protocol

The MTT assay was used to determine the half-maximum inhibitory concentration (IC_{50}). Confluent flasks of HepG2 cells were washed thrice using phosphate buffer solution (PBS) each time. The cells were dislodged by trypsinisation and resuspended in CCM. Cells were counted and 20000 cells (200 μ L) were seeded per well in triplicate for each treatment that was used in the MTT assay. Cells were allowed to adhere overnight, after which 300 μ L of the treatment medium (0 - 5 mg/mL) was added to the relevant wells. After 48 hours the treatment medium was removed and replaced with a solution containing 8 mg MTT salt, 1600 μ L PBS and 8000 μ L warm CCM. Following 4 hours of incubation, the solution was discarded and replaced with DMSO for 1 hour (to dissolve the purple formazan). The absorbance was then read at 570 nm with a reference wavelength of 690 nm using a Biotek μ Quant

spectrophotometer, USA. The absorbance values were used to calculate the cell viability according to the equation:

$$\frac{\text{Absorbance of treated cells}}{\text{Absorbance of control cells}} \times 100$$

The log concentration and cell viability were analysed using Graphpad Prism (V) to produce the regression curve (Figure 4.1) from which the half-maximum inhibitory concentration (IC_{50}) was determined.

Using the IC_{50} for HepG2 cells obtained from the MTT assay, cell viability of HEK293 cells was determined by the MTT assay in order to evaluate cytotoxicity to non-cancerous cells. For each subsequent assay, 25 cm² flasks with confluent HepG2 cells were treated with the IC_{50} of *T. phanerophlebia*. All subsequent assays were conducted in triplicate to obtain comparable results.

3.5 Thiobarbituric acid reactive substances (TBARS) assay

3.5.1 Principle

The thiobarbituric acid reactive substances (TBARS) assay is a colorimetric assay used to test for lipid peroxidation. Thiobarbituric acid reactive substances formed as a by-product of lipid peroxidation include malondialdehyde (MDA), which can react with thiobarbituric acid (TBA) to form a pink chromogenic adduct when exposed to low pH and high temperature (Figure 3.2). Butylated hydroxytoluene (BHT) is added to the reaction to prevent formation of oxidised products during the reaction. The absorbance of the reactive substances is measured at 532 nm/690 nm using a spectrophotometer (Antić *et al.*, 2020).

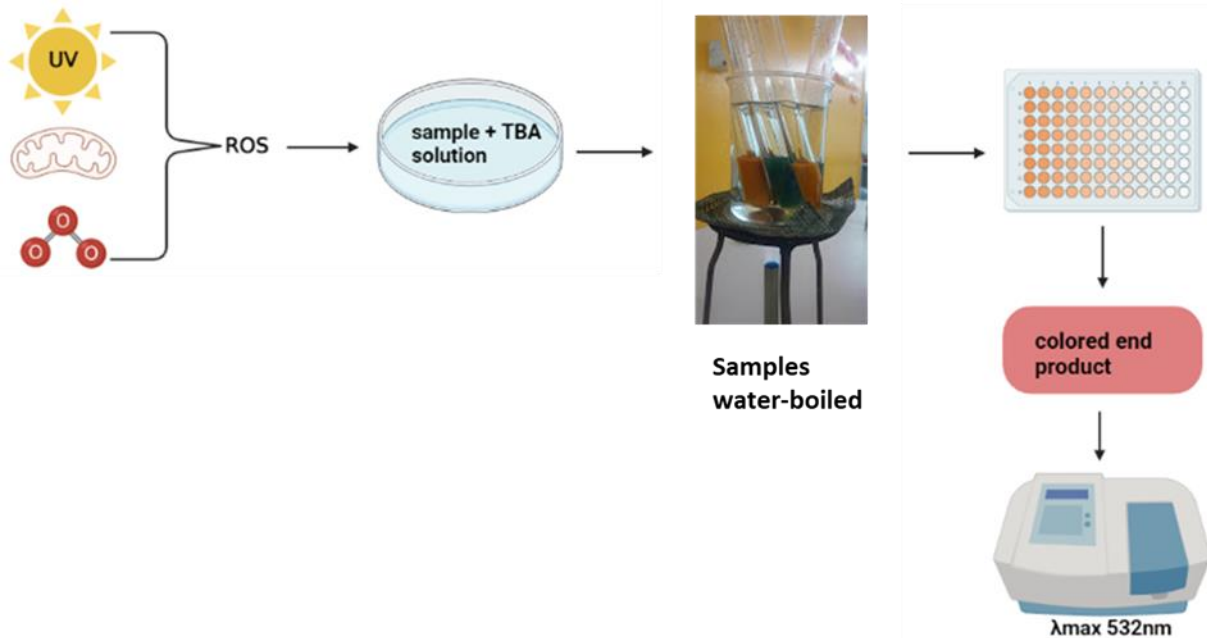


Figure 3.2: TBARS assay principle. The reactive substances which are by-products of lipid peroxidation e.g. MDA react with TBA/BHT producing a coloured compound [Adapted from R & D Systems].

3.5.2 Protocol

The TBARS assay was used to test for lipid peroxidation which results from oxidative stress. The treatment medium was used to determine the levels of lipid peroxidation. A positive control (containing 1 μL of MDA) and the negative control (a blank without MDA), samples (untreated control and IC₅₀) were also used. To each test tube representing each sample, 200 μL of 7% H₃PO₄ (4.1 mL in 45.9 mL distilled water) was added, after which 400 μL of TBA/BHT solution (0.1 g NaOH; 0.5 g TBA; 250 μL BHT from 20 mM stock (440.8 mg in 100 mL ethanol) all dissolved and made up to 50 mL using distilled water) was added to each test tube excluding the blank (negative control). To the blank 400 μL of 3 mM of HCl (30 μL from 1M stock in 9.97 mL distilled water) was added. To each sample 200 μL of 1M HCl (4.92 mL from 32% HCl topped to 50 mL) was added and all test tubes were vortexed before being placed in a water bath at 100°C for 15 minutes and then cooled to room temperature. Butanol was then added to each test tube (1500 μL each) and each test tube was vortexed. The samples were allowed to settle until two distinct phases were visible. To respective eppendorfs, the upper phase was pipetted and 100 μL of each sample was plated in triplicate into a 96-well microtitre plate. The absorbance at 532nm with a reference wavelength of 600nm was measured using a Biotek μQuant spectrophotometer (Winooski, Vermont, USA). The equation below was used to convert the absorbance values to MDA concentration (μM):

$$\left(\frac{\text{Absorbance of samples} - \text{Absorbance of blanks}}{156mM^{-1}} \times 1000 \right)$$

3.6 Nitric oxide (NO) assay

3.6.1 Principle

The NO assay is a colorimetric assay which quantifies the RNS. One such RNS is NO which is highly unstable and has a very short half-life therefore it is measured indirectly through nitrate and nitrite reactions. First vanadium chloride catalyses the reduction of nitrates to nitrites (Figure 3.3). The nitrites then react with sulphanilic acid to produce a diazonium salt which then reacts with N-(1naphthyl) ethylenediamine dihydrochloride (NEDD) to produce the pink azonium dye that is detectable at 540nm with a reference angle of 690nm (Tsikas, 2005).

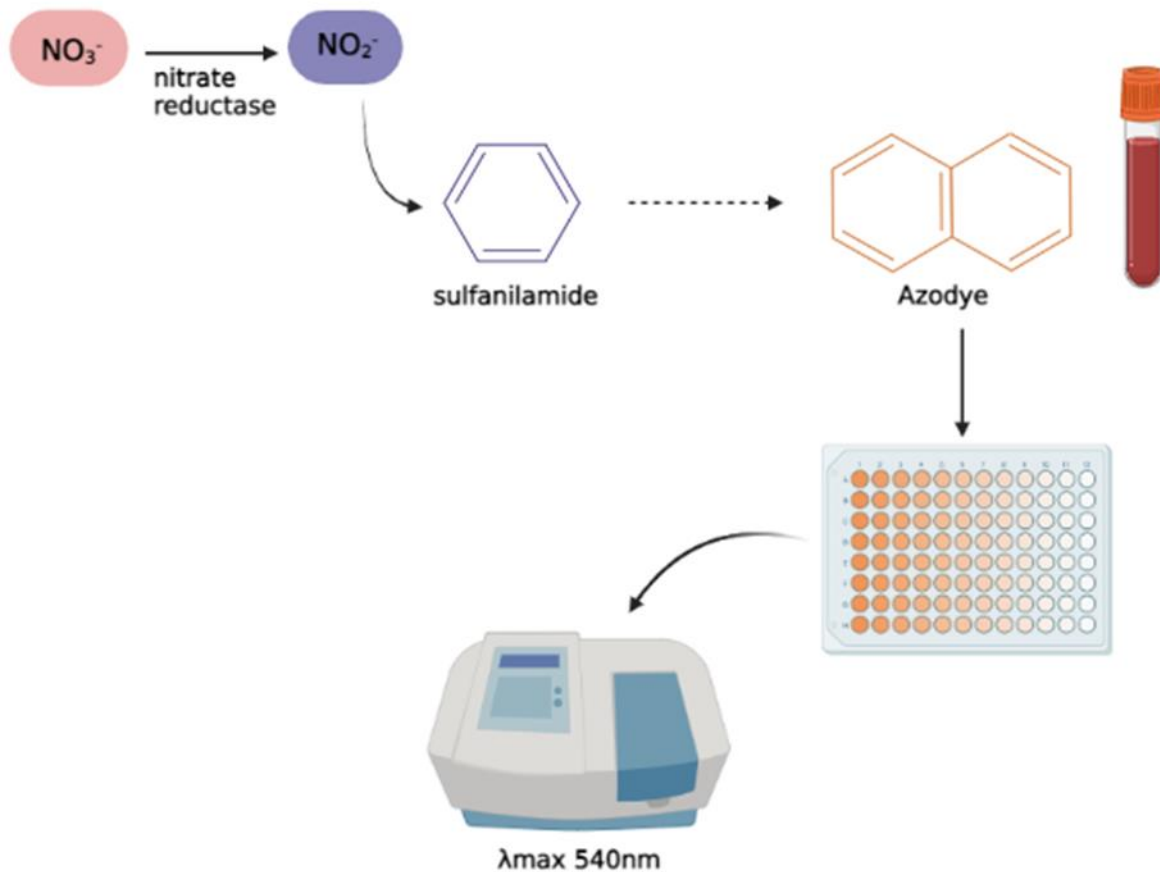


Figure 3.3: NO assay principle. Reactive nitrogen species (RNS) which lead to oxidative stress are tested using the azodye. A red coloured product indicates the presence of RNS [Adapted from (Lopes, 2014)].

3.6.2 Protocol

The NO assay was used to test and quantify the reactive nitrogen species. The treatment media (50 µL) was used to measure reactive nitrogen species present in the CCM. From a 1000 µM stock solution, 7 serial dilutions (0 - 200 µM) were prepared and 50 µL of each standard was added to a 96-well microtitre plate in triplicate. The sample (50 µL of control and IC₅₀ for both the medium and cells were plated in duplicate. To each well 50 µL of vanadium chloride, 25 µL of sulfanilimide and 50 µL of NEDD were added each well. The plate was incubated for 45 minutes in the dark at 37°C before reading the absorbance using a Biotek® µQuant (Winooski, Vermont, USA) spectrophotometer at a wavelength of 540 nm and a reference wavelength of 690 nm. A standard curve was prepared and sample NO concentrations were extrapolated from the standard curve. Data were represented as µM.

3.7 The lactic acid dehydrogenase (LDH) assay

3.7.1 Principle

The LDH assay tests for signs of tissue damage. Plasma membrane damage is a key feature of cells undergoing apoptosis, necrosis, and other forms of cellular damage. The enzyme LDH is a soluble cytosolic enzyme present in almost all eukaryotic cells and catalyses the reduction of NAD⁺ to NADH by oxidation of lactate to pyruvate (Figure 3.4). In the second step of the assay, diaphorase uses the newly formed NADH to catalyse the reduction of a tetrazolium salt (Chinta *et al.*) to formazan (red) and absorbance is measured at 450 nm (Figure 3.4). The NADH produced during the conversion of lactate to pyruvate is used to quantify LDH activity (Kumar *et al.*, 2018). The amount of formazan is directly proportional to the amount of LDH in the culture, which is also directly proportional to the number of dead or damaged cells. Detection of more LDH indicates severe cell damage due to cancer or another disease (Khan *et al.*, 2020).

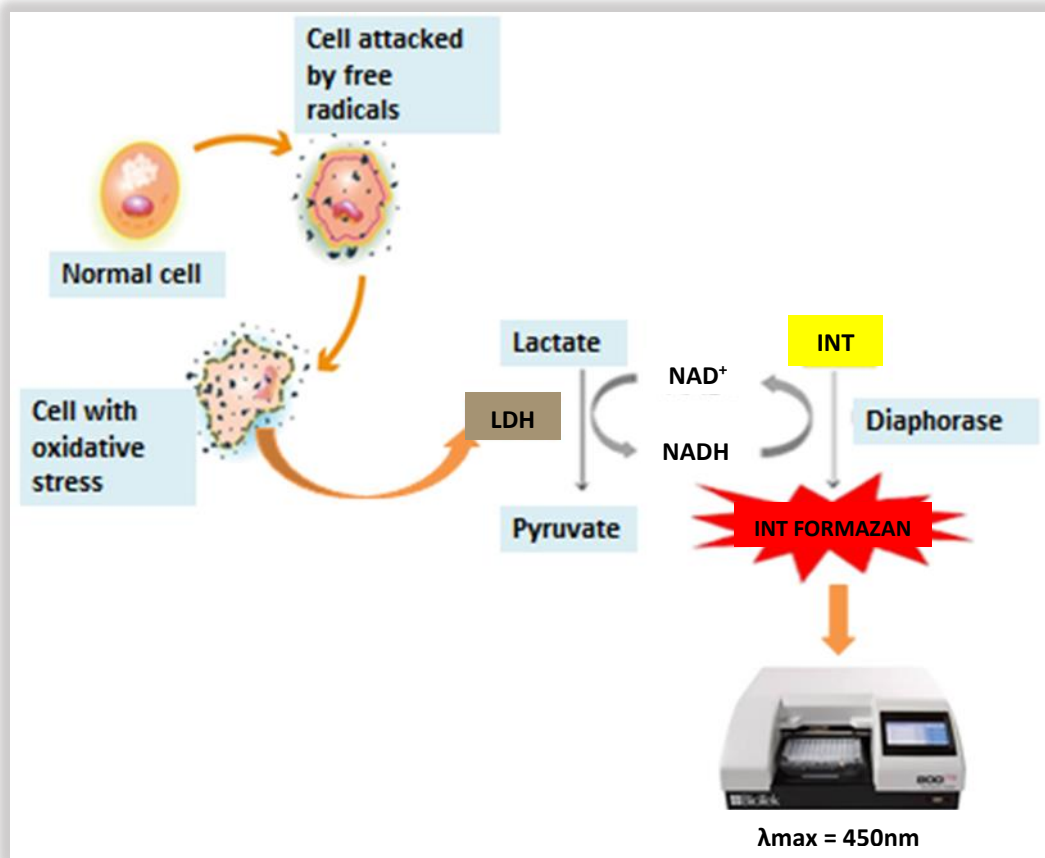


Figure 3.4: LDH assay principle. The LDH protein is rapidly released into the cell culture supernatant when the plasma membrane is damaged. The yellow tetrazolium salt, INT, is reduced by NADH into a red, water-soluble formazan-class dye detected by a spectrophotometer at an absorbance of 450 nm [Adapted from (Forest *et al.*, 2015)].

3.7.2 Protocol

The LDH cytotoxicity detection kit (04744926001) was used to quantify LDH levels in the treated cells. A 96-well micro-titer plate was used to plate 50 μL of the treatment media and blank (negative control with CCM) in triplicate followed by 25 μL of the LDH reagent. The plate was incubated in the dark at room temperature for 30 minutes before 12.5 μL of a stop solution was added after incubation. A spectrophotometer (Biotek® μQuant (Winooski, Vermont, USA)) was used to determine the absorbance (490/600 nm). Data obtained was presented as absorbance units.

3.8 Luminometry

Luminometry is a bioluminescent immunoassay that uses the enzyme luciferase to cleave luciferin; in the presence of oxygen the light produced can be measured by a luminometer. The

light is directly proportional to the amount of or activity of a molecule of interest therefore luminometry can be used to quantify the activity of various molecules. In this study, luminometry was used to detect mitochondrial stress using JC-10 assay, to quantify ATP, to measure the concentration of glutathione (GSH), determine Cytochrome P₄₅₀ 3A4 activity and assess apoptosis using Annexin-V and caspase activity.

3.8.1 ATP assay

3.8.1.1 Principle

The ATP assay quantifies ATP in order to determine the viability of cells in culture. The enzyme luciferase in the reagent catalyses the reaction of luciferin and ATP from viable cells to produce a bioluminescent light (Figure 3.5) that can be detected by a luminometer (Aslantürk, 2018). Viable cells indicate the presence of metabolically active cells and are directly proportional to the luminescence output (Kamiloglu *et al.*, 2020).

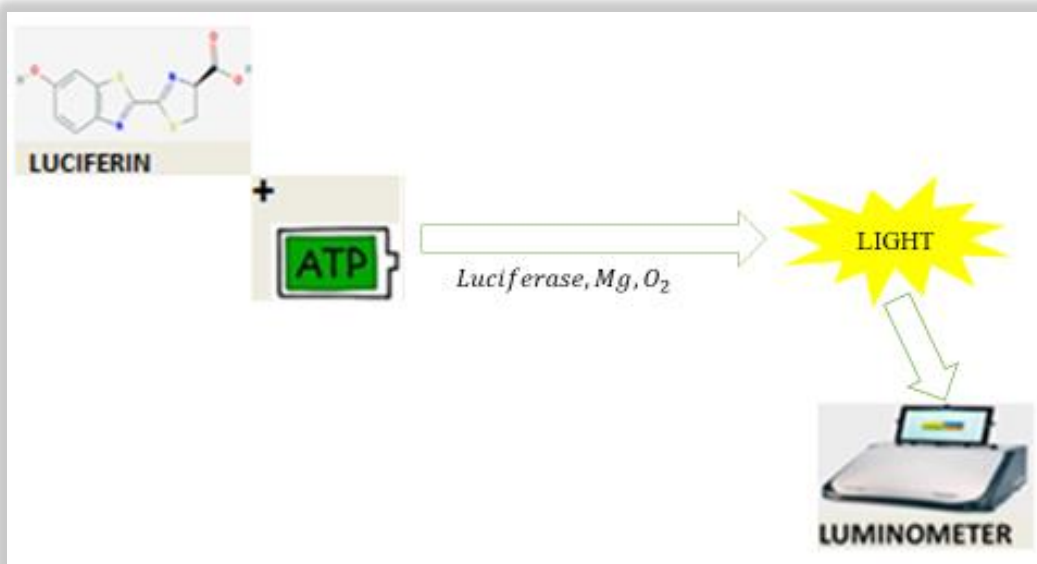


Figure 3.5: Luciferin reagent permeates the membranes of viable cells to interact with intracellular ATP. Intracellular ATPases are inactivated and the reaction produces bioluminescent light that is measured via luminometry to determine the intracellular ATP levels [Adapted from (Niles *et al.*, 2007)].

3.8.1.2 Protocol

To each well, 20000 HepG2 cells were plated in triplicate into an opaque 96-well white plate. After incubating the plate overnight at 37°C for cells to adhere, the culture medium was then removed and the treatment concentrations were added (control and IC₅₀) to respective wells for 48 hours. The CellTiter-Glo® reagent (Cat. #G7570) was prepared according to the

manufacturer's protocol. The treatment medium was removed and 25 µl of the ATP reagent was added to the respective wells. The ATP plate was mixed briefly on a shaker, incubated at room temperature for 30 minutes and then read using the Modulus™ microplate luminometer (Turner Biosystems, Sunnyvale, USA). Data was expressed in relative light units (RLU).

3.8.2 GSH assay

3.8.2.1 Principle

The GSH-Glo™ assay uses luminescence principles to detect and quantify reduced GSH in cells. The test is based on the conversion of the luciferin derivative to luciferin in a reaction catalyzed by Glutathione-S-transferase (GST) that uses intracellular GSH as a co-factor; GSH is oxidised to GSSG (Choromańska *et al.*, 2020). The reaction is coupled with luciferase to produce a glow-type luminescent signal that is proportional to the amount of GSH in the sample (Figure 3.6) (Stoleriu *et al.*, 2020). A change in GSH levels is important in the assessment of toxicological responses and is an indicator of oxidative stress which potentially leads to apoptosis or cell death. A decrease in GSH concentration indicates an increase in oxidative stress.

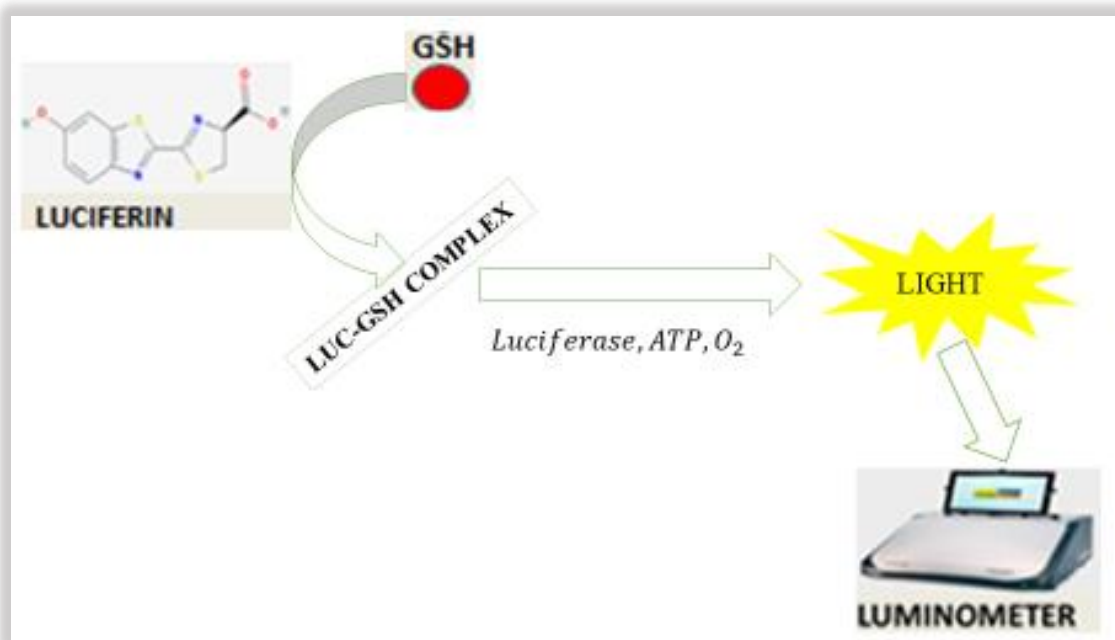


Figure 3.6: Cells are lysed in the presence of the luciferin substrate and glutathione S-transferase. Glutathione in the cells contributes to the formation of luciferin. Luciferin Detection Reagent is then added to produce light that is directly proportional to the amount of GSH in the reaction [Adapted from (Lou *et al.*, 2014)].

3.8.2.2 Protocol

To an opaque 96-well white plate, 20000 cells/ well were plated in triplicate. The plate was left overnight for cells to adhere. The culture medium was removed and the treatment concentrations were added (control and IC₅₀) to respective wells. After 48 hours, the treatment medium was removed and replaced with 50 µL PBS. The GSH assay reagents (Cat. #V6911) were prepared according to the manufacturer's protocol, then 50 µL of prepared 2X GSH-Glo™ reagent was added to each well. The plate was mixed briefly on a shaker and then incubated at room temperature for 30 minutes, after which it was reconstituted with luciferin detection reagent (50 µL) to each well. The plate was mixed briefly on a shaker before incubating it for 15 minutes and the luminescence was measured using the Modulus™ microplate luminometer (Turner Biosystems, Sunnyvale, USA). Data was expressed in RLU.

3.8.3 Caspase assay

3.8.3.1 Principle

Caspases are a family of cysteine proteases that specifically cleave substrates only after an aspartic acid residue. Caspases are synthesized as inactive precursors and a wide range of physiological and pathological stimuli such as oxidative stress result in their activation. Caspase activation can be measured through the catalytic activity of luciferase and the cleaved substrate which results in a bioluminescent light proportional to caspase activity (Niles *et al.*, 2008). The Caspase-Glo® reagent is comprised of a DEVD-aminoluciferin specific for a single caspase (8, 9 or 3/7) and a cell lysis reagent (Do *et al.*, 2020). When added to the sample, lysis will expose the luciferin substrate to the relevant caspase. Cleavage of the substrate by caspase releases aminoluciferin, which is subsequently cleaved in the luciferase reaction resulting in a light signal (Figure 3.7). The signal produced is proportional to the caspase activity present.

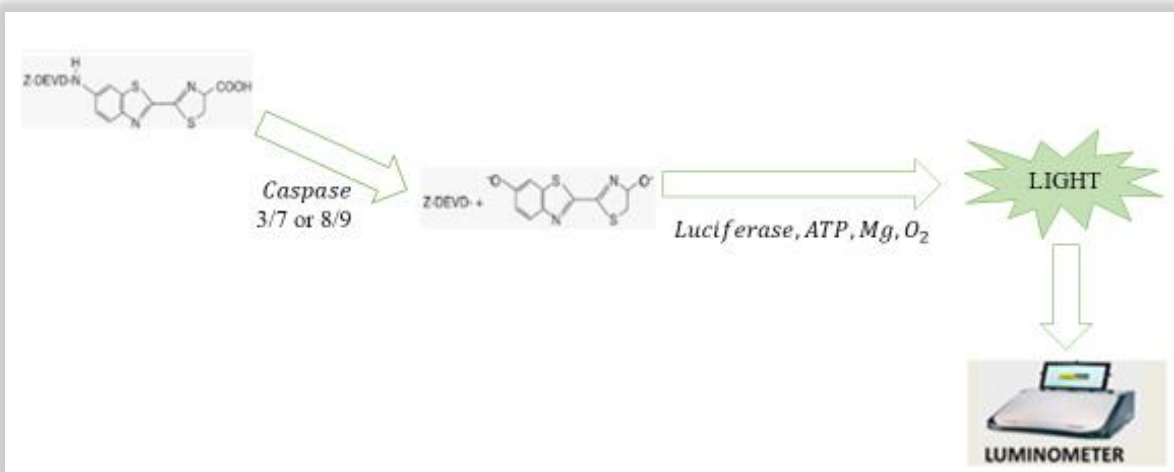


Figure 3.7: After the cleavage of Z-DEVD substrate, aminoluciferin is released, resulting in luciferase activity and generation of light by luciferase [Adapted from (Khalilzadeh *et al.*, 2018)].

3.8.3.2 Protocol

Promega Caspase-Glo®, South Africa was used to assess the caspase activities [caspase 8 (Cat. #G8200), caspase 9 (Cat. #G8210) and caspase 3/7 (Cat. #G8090)] according to the manufacturer's instructions. A luminometer plate was used to plate 200 µL of cell suspension (20000 cells/treatment) in triplicate. The plate was left overnight for cells to adhere. The culture medium was removed and the treatment concentrations were added (control and IC₅₀) to respective wells for 48 hours. The treatment was then removed and replaced with 50 µL of initiator caspases 8 before mixing on a plate shaker. The plate was then incubated for 30 minutes at room temperature in the dark after which samples were analysed using Modulus™ microplate luminometer (Turner Biosystems, Sunnyvale, USA). Results were expressed in RLU. This procedure was repeated for caspase 9 and caspase 3/7.

3.8.4 Annexin V and Necrosis assay

3.8.4.1 Principle

Apoptosis is often assessed by measuring phosphatidylserine exposure on the outer surface of the cell membrane, while necrotic cells can be differentiated from apoptotic cells using propidium iodide (PI) penetration into dead / non-viable cells, where it intercalates with DNA. The RealTime-Glo™ Annexin V Apoptosis and Necrosis Assay (Cat. #JA1011) employs a simple luminescence signal to detect Annexin V that binds to externalised PS, and a fluorescent signal generated after PI binding distinguishes necrotic cells (Figure 3.8). The kit comprises two Annexin V fusion proteins (annexin V-LgBiT and annexin V-SmByT) that contain

NanoBiT® luciferase complementary sub-units, a luciferase substrate and a pro-fluorescent DNA probe that detects necrosis (Kamiloglu et al., 2020).

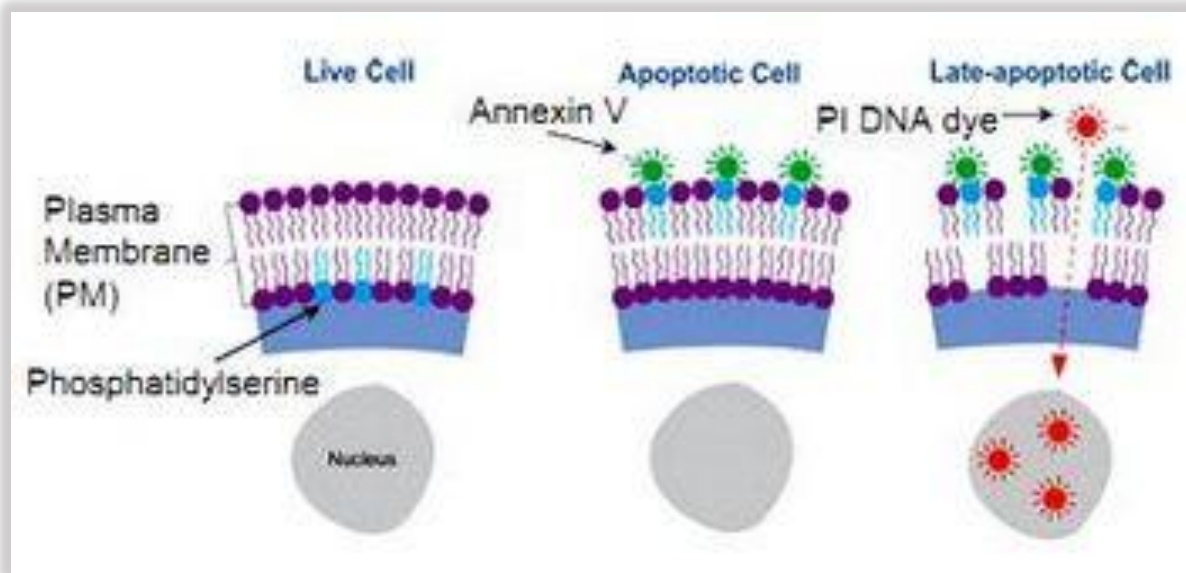


Figure 3.8: In a healthy viable cell, PS is confined in the inner phospholipid bilayer but translocates to be exposed externally in apoptotic cells. Propidium iodide (PI) permeates the membrane of necrotic cells to bind with DNA producing a fluorescent DNA dye and aids in distinguishing between apoptotic and necrotic cells [Adapted from SinoBiological].

3.8.4.2 Protocol

The HepG2 cells (20 000 cells, 200 μ l/well) were plated into a white multi-well plate in triplicate. The cells were treated with *T. phanerophlebia* for 48 hours which was removed before adding 50 μ l PBS to each well. The 2X detection reagent was prepared according to the manufacturer's instruction and 25 μ l of this mixture was added to each well. The contents were mixed briefly on an orbital shaker and the plate was incubated at room temperature for 30 min. Apoptosis and necrosis were quantified using the Modulus™ microplate luminometer (Turner Biosystems, Sunnyvale, USA) and measured in RLU for apoptosis and relative fluorescence units (RFU) for necrosis respectively.

3.8.5 Cytochrome P₄₅₀ 3A4, CYP3A4

3.8.5.1 Principle

Xenobiotics as well as endogenous hormones are mainly metabolized by the cytochromes P450 (CYPs) family of monooxidase enzymes. The most active drug-metabolizing CYP is CYP3A4, which carries out a prominent role in adverse drug-drug interactions and is highly expressed in

the liver and intestines (Cali *et al.*, 2009). Drugs that inhibit CYP3A4 enzyme activity lead to toxicity and those that induce CYP3A4 expression lead to reduced efficacy. *In vitro* testing of compounds assists in predicting the potential of the outcome early in drug discovery. Bioluminescent CYP assays are highly sensitive and produce highly predictive results. The assay monitors the conversion of inactive D-luciferin by CYPs to an active form that produces light when firefly luciferase is added to the reaction mixture (Figure 3.9). The light intensity is proportional to CYP activity.

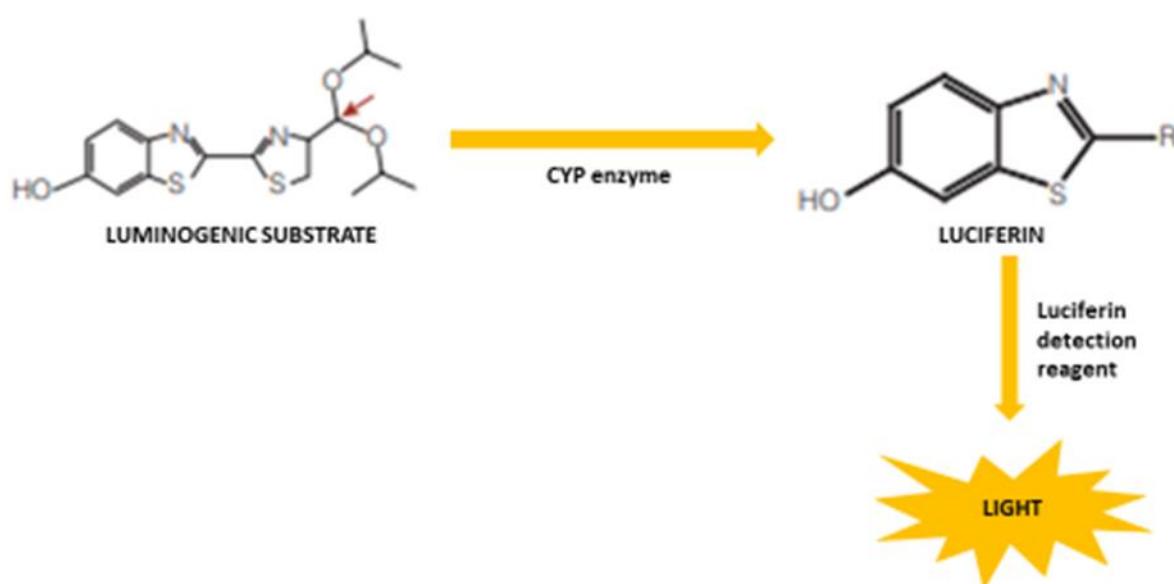


Figure 3.9: CYP enzymes selectively act on a luminogenic substrate depending on the structure of the proluciferin substrate resulting in a luminometric luciferin product. The Luciferin Detection Reagent is added after the CYP reaction has been completed [Adapted from Biovision].

3.8.5.2 Protocol

The CYP3A4 kit (Cat# V8801) was used to assess CYP3A4 activity according to the manufacturer's instructions. A luminometer plate was used to plate 200 µL of cell suspension (20000 cells/treatment) in triplicate. The plate was left overnight for cells to adhere. The culture medium was removed and the treatment concentrations were added (control and IC₅₀) to respective wells for 48 hours. The treatment was then removed and replaced with 50 µL of CYP3A4 reagent before mixing on a plate shaker. The plate was then incubated for 30 minutes at room temperature in the dark after which samples were analysed using Modulus™ microplate luminometer (Turner Biosystems, Sunnyvale, USA). Results were expressed in RLU.

3.8.6 Mitochondrial membrane potential ($\Delta\Psi_M$) - JC-10 Assay

3.8.6.1 Principle

Redox transformations occurring in the mitochondrial membrane during the Krebs cycle give rise to an electrochemical proton gradient referred to as the mitochondrial membrane potential ($\Delta\Psi_M$) which is used to produce ATP. During the intrinsic apoptotic pathway, the collapse of the $\Delta\Psi_M$ coincides with the opening of the mitochondrial permeability transition pores which release cytochrome c into the cytosol. Cytochrome c facilitates the formation of apoptosis protease activating factor 1 (APAF-1) resulting in a signaling cascade that activates the caspase-9 and formation of the apoptosome. The JC-10 is a cationic, lipophilic dye that is more water-soluble than JC-1 and forms reversible red-fluorescent JC-10 aggregates ($\lambda_{ex}=540/\lambda_{em}=590\text{nm}$) in the mitochondria of cells with polarized mitochondrial membrane (Figure 3.10). The $\Delta\Psi_M$ collapse in apoptotic cells results in failure to retain the JC-10 in the mitochondria, therefore the dye in its monomeric state exhibits green fluorescence ($\lambda_{ex} = 490/\lambda_{em}= 525\text{nm}$, Figure 3.10). The red/green fluorescence dye ratio indicates mitochondrial membrane polarization. The higher is the $\Delta\Psi_M$, the more elevated is the redshift of the dye (more J aggregates are formed) (Sivandzade *et al.*, 2019).

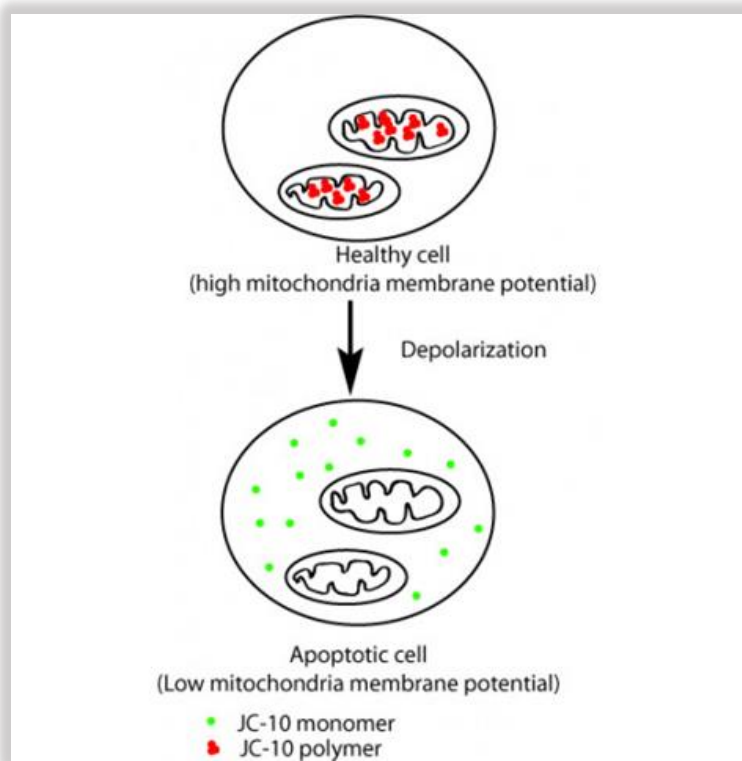


Figure 3.10: The JC-10 dye forms polymer aggregates exhibiting red fluorescence in an intact, polarised membrane and monomer aggregates exhibiting green fluorescence in an unpolarised membrane resulting from apoptosis [Adapted from G-Biosciences]

3.8.5.2 Protocol

The HepG2 cells (20 000 cells, 200 μ l/well) were plated into a white multi-well plate in triplicate. The cells were treated with *T. phanerophlebia* for 48 hours. The treatment medium was removed from the 96-well microplate, and 50 μ L PBS was added to each well, followed by the addition of 25 μ L JC-10 dye working solution (1:10 dye: buffer) to each well according to manufacturer's protocol. The plate was incubated at 37°C for 30 minutes protected from light before measuring the fluorescence at 490/525 nm and 540/590 nm in RFU with a Modulus™ microplate luminometer (Turner Biosystems, Sunnyvale, USA). The results are presented as red/green fluorescence.

3.9 Western Blot

3.9.1 Principle

Western blotting is also known as immunoblotting or protein blotting and is a quantitative technique used to identify specific proteins from cells. The first step is gel electrophoresis which separates protein types by size (Mahmood and Yang, 2012) before the proteins are transferred from sodium dodecyl sulfate (SDS) polyacrylamide gel to an adsorbent membrane (Figure 3.11), which is usually a nitrocellulose membrane through electric transfer (Ma and Shieh, 2006, Kurien and Scofield, 2006). Primary antibodies are used to bind to specific antigens and secondary antibodies are used as protein/antigen markers and only bind to proteins of interest forming bands whose thickness corresponds to the amount of protein available (Mahmood and Yang, 2012). The antibodies will bind to the available antigens which allow quantification of the antigen concentration. Western blotting does not use much transfer reagents and successive multiple analyses can be done on the same protein transfer. Immobilised proteins are accessible to different ligands and transferred patterns can be stored for long periods before use and high resolutions of immunogenic antigens within a sample are produced (Kurien and Scofield, 2006). The sample should be kept cool or on ice so that proteases do not degrade as that would cause the appearance of unexpected bands (Mahmood and Yang, 2012). In this study, western blotting will be used to quantify and determine the presence of proteins/ antioxidants produced due to oxidative stress, inflammation and apoptosis such as SOD2, Fas, p-p38, p-38, p-STAT3, STAT3 and HSP90.

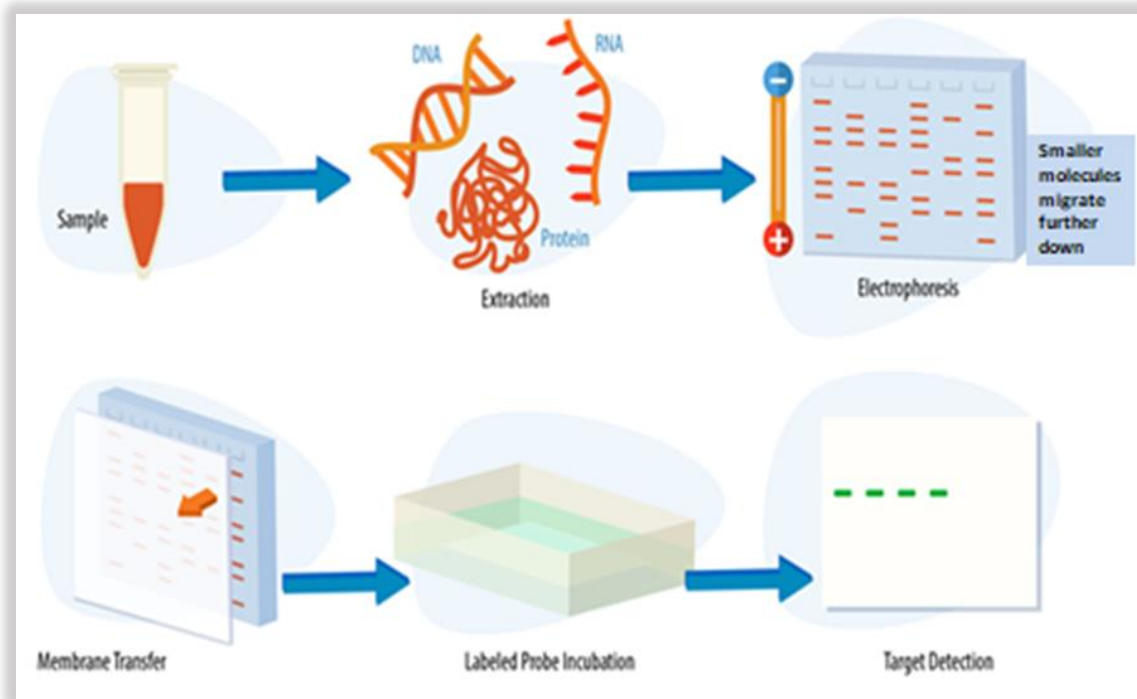


Figure 3.11: Western Blot assay principle. A sample containing proteins is loaded onto an SDS-PAGE gel and electrophoresis is used to separate the proteins depending on their molecular weight. The exact replica of SDS-PAGE gel is transferred to a membrane that is further suspended in a primary antibody which binds to a specific band on the blot. The secondary antibody conjugated to an enzyme (alkaline phosphatase or horseradish peroxidase) is then allowed to bind to the primary antibody. Chemiluminescence reagent is added to the membrane for color development of specific bands before viewing [Adapted from Labmanager].

3.9.2 Protocol

The western blot was used to quantify the proteins/antioxidants produced due to oxidative stress which are SOD2 (#13141), HSP90 (#4877), p-p38 (#4511), p38 (#8690), p-STAT3 (#9145), STAT3 (#4904) and Fas (#4232).

3.9.2.1 Protein isolation and standardisation

Flasks with confluent cells were treated with *T. phanerophlebia* (HepG2: control and IC₅₀ – 1396 mg/mL were incubated for 48 hours at 37°C with 5% CO₂ supply). The media was discarded and cells were washed twice with PBS. Cytobuster containing protease and phosphatase inhibitors (300 µL) was added to each flask. The cells were incubated on ice for 15 minutes. Cells were scraped, transferred to an eppendorf and centrifuged (2000 x g; 4°C, 5 minutes). The supernatant was collected and protein quantified using the BCA assay (25 µL

sample/standard solution + 200 µL BCA working solution) and incubated in the dark for 30 minutes at 37°C before reading the absorbance at 562 nm on a Biotek µQuant spectrophotometer, USA. The absorbance was used to extrapolate crude protein concentration, which was used to standardise the protein to 0.7 mg/mL. Sample/Laemmli buffer (5X dilution: 4 g SDS, 8 mL β-mercaptoethanol, 20 mL glycerol, 12 mL 1M Tris, 8 mg bromophenol blue) was prepared and used to dilute the standardised protein (4 parts crude protein: 1part buffer). Samples were boiled for 5 minutes to denature the proteins then cooled to room temperature.

3.9.2.2 Protein separation

The mini-PROTEAN 3 SDS-PAGE apparatus were assembled according to the manufacturer's instruction. A 10% resolving gel was prepared [dH₂O, acrylamide/Bis, 1.5M Tris (pH8.8), 10% w/v SDS, 10% APS and TEMED] and 4% stacking gel [dH₂O, 0.5M Tris (pH 6.8), 10% SDS, Bis/acrylamide, 10% APS and TEMED]. 1X electrode/running buffer [dH₂O, Tris, glycine, SDS pH (8.3)] was added to the tank and 25 µL of samples and 5 µL of molecular weight markers were loaded to respective wells. Electrophoresis was carried out (150 V for 90 minutes) using a Bio-Rad compact power supplier (Bio-Rad, Hercules, California, USA) until the tracker dye reached the bottom of the gel.

3.9.2.3 Protein transfer and immunoblotting

Transfer buffer [25 mM Tris (pH 7.4), 192 mM glycine, 20% v/v methanol; pH 8.3] was used to equilibrate the gel and nitrocellulose membrane for 10 minutes. A gel sandwich was prepared in a transblot plate (Bio-Rad, Hercules, California, USA) and a constant current of 2.5 mA (25 V) was applied for 30 minutes. When the transfer was completed, the membrane was placed in a blocking solution (5% BSA in TTBS for 2 hours. Thereafter primary antibodies: 5% BSA in TTBS (1:1000 dilution) were added. The membranes were placed on a shaker for 1 hour before being left overnight at 4°C. Membranes were then allowed to return to room temperature before being washed five times with Tris-buffered saline (TTBS) (10 mL) and probed with matched secondary antibodies (anti-mouse or anti-rabbit IgG) in 5% BSA in TTBS (1:2500) for 2 hours at room temperature on a shaker. Membranes were then washed with TTBS (10 mL) 5 times and rinsed with deionized water. The membrane was covered with Bio-Rad chemiluminescence reagent (mixed luminol/enhancer and peroxide buffer in 1:1 ratio, each 500 µL). The proteins of interest were viewed using Molecular Image® Chemidoc™ XRS and Bio-Rad imaging system (Bio-Rad, Hercules, California, USA). The bands were then analysed by Bio-Rad Image Lab software (6.0.1) (Bio-Rad, Hercules, California, USA).

The membranes were then prepared for probing for the housekeeping protein (β -actin). The membrane was washed with 10 mL water for 1 minute. The water was discarded and, 5 mL of H₂O₂ was added and incubated at 37°C for 30 minutes. The H₂O₂ was then discarded after incubation and the membrane was washed with 10 mL of water, then 10 mL of TTBS for 1 minute each. Thereafter, the buffer was discarded and the membrane was blocked with 5% BSA for 2 hours. HRP-conjugated housekeeping antibody β -actin (A5441) (1:5000 dilution in 5% BSA/TTBS 1 hour) was then added. After successive washes in TTBS, the membrane was viewed as described previously. The band intensity was measured for the respective proteins and β -actin, and data was expressed as relative band intensity (RBI).

3.10 Quantitative polymerase chain reaction (qPCR)

Quantitative PCR monitors the amplification of a targeted DNA molecule during PCR in real-time.

3.10.1 Principle

The workflow for a complete qPCR is shown in Figure 3.12. The mRNA is isolated from cells, quantified and used to synthesise complementary DNA (cDNA). Cell lysis reagents are necessary to release cell components whilst maintaining mRNA integrity. Spectrophotometry is used to assess the purity of the isolated mRNA by using UV spectrophotometry. Since RNA absorbs well at A260nm and proteins at A280nm, the ratio of A260nm/A280nm indicates its purity; a ratio of ~2 indicates pure RNA (Nagar and Schwessinger, 2018). The template mRNA is used to synthesise cDNA through a process of reverse transcription in a reaction that requires primers, dNTPs and reverse transcriptase. The cDNA formed is single-stranded and can be used as a template for real-time qPCR to amplify the cDNA (Kuang *et al.*, 2018).

SYBR green is a fluorescent dye that can be used in qPCR. The dye binds to a double-stranded DNA and emits a fluorescent signal. The amount of double-stranded DNA available and bound to the dye is directly proportional to the intensity of the signal (Thornton and Basu, 2011). Housekeeping genes are genes that are expressed in normal cells and maintain their cellular properties despite the treatment or experimental conditions and thus produce predictable results. The use of housekeeping genes in gene expression is important because they are used as controls to determine the integrity of the experimental results. Examples of housekeeping

genes are 18S rRNA (ribosomal RNA), beta-actin (β -actin) and glyceraldehyde 3-phosphate dehydrogenase (GAPDH) (Xia *et al.*, 2017).

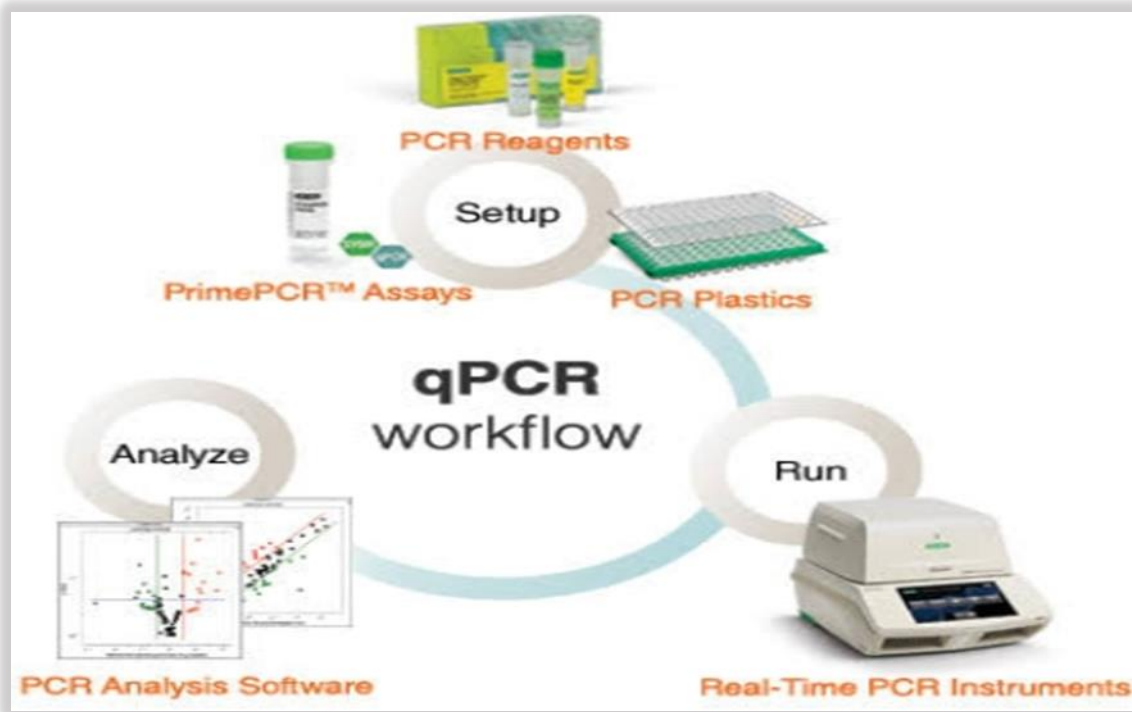


Figure 3.12: qPCR workflow. Custom primers and PCR reagents are used for amplification reactions. Reactions are run in pre-set real-time PCR instruments and the data collected is analysed using specialized software (Adapted from Bio-Rad).

3.10.2 Protocol

3.10.2.1 RNA extraction

Trizol was used to isolate RNA according to the manufacturer's protocol. To each flask, 500 μ L of Trizol reagent was added and the flasks were incubated at 4°C for 10 min after which cells transferred to an eppendorf and stored in Trizol at -80°C overnight. After thawing the samples to RT, chloroform (100 μ L) was added and eppendorfs were incubated at RT for 3 min. Cell suspensions were then centrifuged (12000g, 4°C, 15 min) and the aqueous phase was removed. Isopropanol (250 μ L) was added and samples were left overnight at -80°C. Samples were thawed, centrifuged (12 000 g, 4°C, 20 min) and the pellet was retained and washed with 75% cold ethanol (500 μ L). The sample was centrifuged again (7400 g, 4°C, 15 min) before removing the ethanol and air-drying the pellet. Nuclease-free water (15 μ L) was used to resuspend the pellet before incubation (RT, 3 min). The RNA was quantified using the Nanodrop2000 spectrometer and the A260/A280 ratio was used to assess the RNA integrity. The ratio of absorbance at 260nm and 280nm is used to assess the purity of DNA and RNA. A

ratio of ~1.8 is generally accepted as pure for DNA and a ratio of ~2.0 is generally accepted as pure for RNA. The RNA concentration was standardised to 1000 ng/ μ L and used to prepare cDNA.

3.10.2.2 cDNA synthesis

The iScript cDNA synthesis Kit (Bio-Rad, Hercules, California, USA Catalogue # 1708891) was used as per the manufacturer's protocol to synthesise cDNA from the standardised RNA. Tubes representing each sample and a reaction mix containing 4 μ L 5x iScript reaction mix, 1 μ L iScript reverse transcriptase, 11 μ L nuclease-free water and 4 μ L of each RNA sample were prepared. The tubes were then incubated in a thermocycler (GeneAmp®PCR System 9700, Applied Biosciences) for 35 min (5 min at 25 °C, 25 min at 42 °C and 5 min at 85 °C). Thereafter, 80 μ l nuclease-free water was added to each sample, and samples were stored at -80°C.

3.10.2.3 qPCR

iScript SYBR Green PCR kit (Bio-Rad, Hercules, California, USA Catalogue #1725121) was used to analyse gene expression according to the manufacturer's protocol. Each reaction volume totaled 13 μ L (SYBR Green, forward primer, reverse primer, nuclease-free water and cDNA sample). The house-keeping genes used were β -Actin and GAPDH. The initial denaturation, 37 denaturation cycles and annealing were at 95°C (4 min), (95°C, 15 sec) and 40 secs respectively. The annealing temperatures were specific for each protein. Extension was at 72°C for 30 secs and the plate was read using CFX96 Touch™Real-Time PCR detection System.

3.10.2.4 Analysis

The Cq values obtained were normalised against the housekeeping gene (GAPDH) and mRNA expression ($2^{-\Delta\Delta CT}$) relative to the control was calculated using the Livak method (Livak and Schmittgen, 2001). Data were represented as relative fold change (RFC) in mRNA expression.

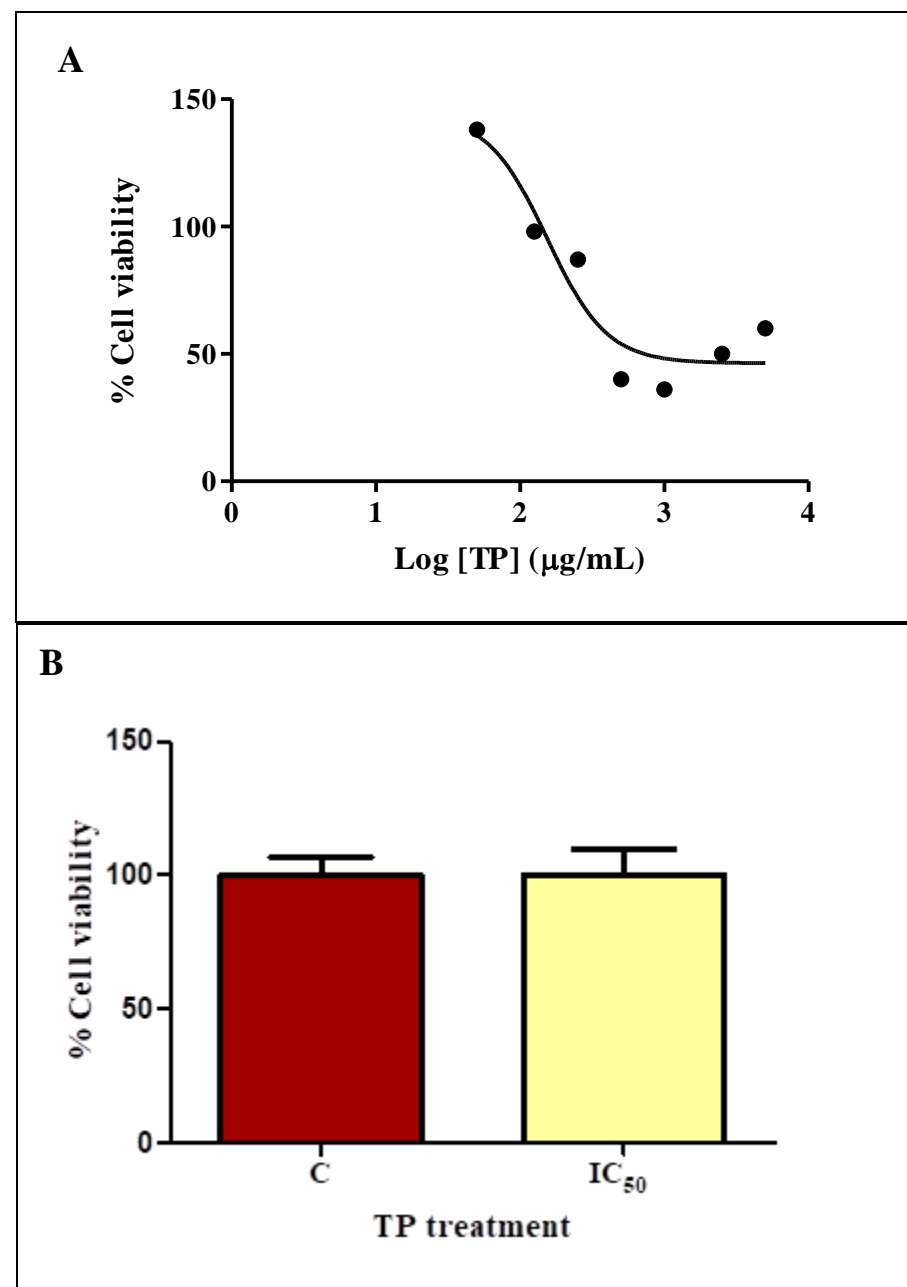
3.11 Statistical analysis

Statistical analysis was carried out using Graph Pad Prism software version 5.0. Bars in the graphs are mean \pm standard deviation of 3 replicates. Significant difference was determined using the student's *t*-test with Welch's correction. The 95% confidence interval was set at $p < 0.05$.

CHAPTER 4: RESULTS

4.1 MTT Assay

The MTT assay is centered on the transformation of MTT salt into formazan crystals by viable cells, which determines mitochondrial activity (Buranaamnuay, 2021). The cytotoxicity of *T. phanerophlebia* on HepG2 cells was measured using the MTT assay. Cell viability was increased to 138% for the 50 µg/mL *T. phanerophlebia* treatment compared to the control (100%), then decreased back to control levels for the 125.9 µg/mL treatment (Figure 4.1A, C). The cell viability decreased to 87%, 40% and 36% at subsequent concentrations, with the lowest cell viability of 36% recorded for the 1000 µg/mL treatment (Figure 4.1A, C). Further increases in concentration to 2511 µg/mL and 5011.9 µg/mL caused increased cell viability to 50% and 60% respectively. The potency of *T. phanerophlebia* in inhibiting 50% of the HepG2 cells was determined to be 1396 µg/mL from the analysis of the dose-response curve (Figure 4.1A, C). The HEK293 cell line was used as a control and the cell viability for HEK293 (Figure 4.1B) was similar in both the control and treated IC₅₀ giving a clear illustration of the effect of *T. phanerophlebia* in the HepG2 cell line.



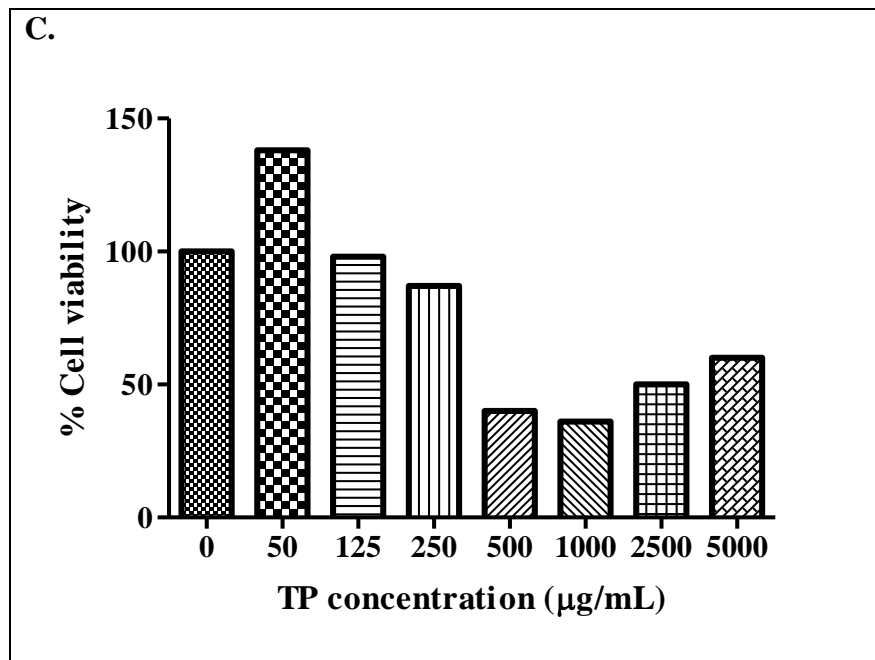


Figure 4.1: (A) Cell viability of HepG2 cells following 48 hours treatment with *T. phanerophlebia*. A dose-dependent decline was observed relative to the untreated control therefore *T. phanerophlebia* has anti-proliferative effects on the HCC cell line. (B) Cell viability of Hek293 cells remained the same for both the treated cells and the untreated control. (C) A dose-dependent decrease in cell viability observed post a 48 hours exposure of HepG2 cells to *T. phanerophlebia*.

4.2 ATP Assay

The ATP assay is an indicator of cellular metabolic activity since the luciferase reaction requires ATP (Kamiloglu et al., 2020). The luminescence produced is proportional to the amount of ATP present. The ATP concentration in the control produced a luminescence of 9779000 ± 984800 RLU, with a decrease in ATP to 182800 ± 43050 RLU for IC₅₀-treated HepG2 cells ($p = 0.0104$) (Figure 4.2).

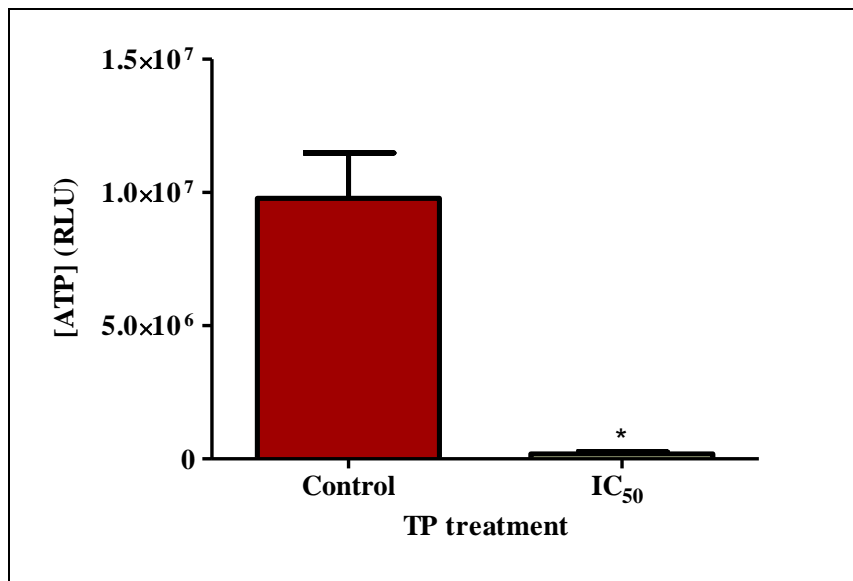


Figure 4.2: ATP concentration. There was significant decrease in the IC₅₀ (* $p = 0.0104$) [* Unpaired *t*-test with Welch's correction].

4.3 JC-10 Assay

The cationic, lipophilic JC-10 dye was used to assist in monitoring the $\Delta\Psi_M$ necessary to produce ATP. There was a significant decrease in the $\Delta\Psi_M$ of the treated cells relative to the control ($p = 0.0024$). The $\Delta\Psi_M$ decreased from 53.91 ± 1.543 in the control to 22.13 ± 0.2609 for the IC₅₀, a notable 2.5-fold decrease (Figure 4.3).

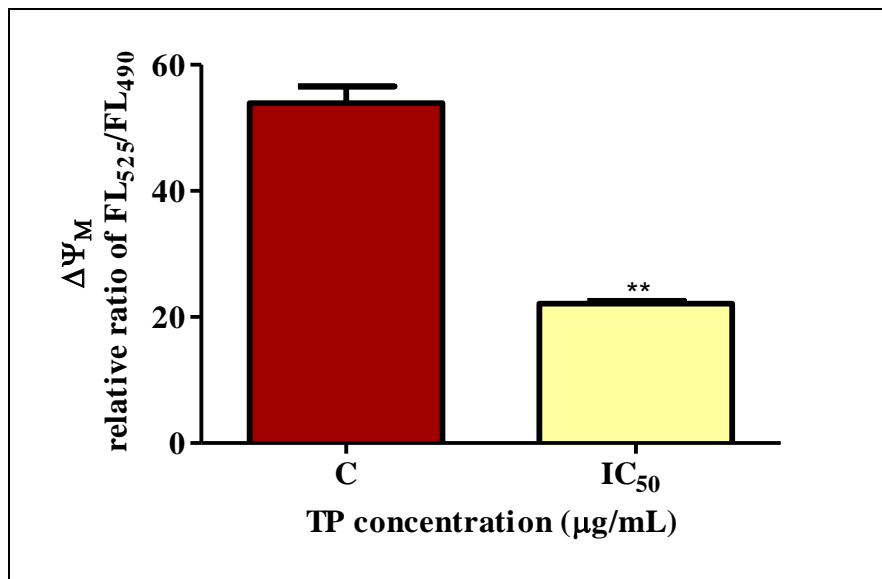


Figure 4.3: A significant 2-fold decrease in membrane potential ($p = 0.0024$) was displayed relative to the control. [** Unpaired t – test with Welch`s correction]

4.4 TBARS Assay

The TBARS assay was used to detect oxidative stress by measuring lipid peroxidation as a consequence of increased ROS (Figure 4.4). The MDA concentration in untreated HepG2 cells was $0.1122 \pm 0.003205 \mu\text{M}$, and was significantly decreased 8-fold in IC_{50} -treated cells to $0.01560 \pm 0.004209 \mu\text{M}$ ($p = 0.0030$) (Figure 4.4).

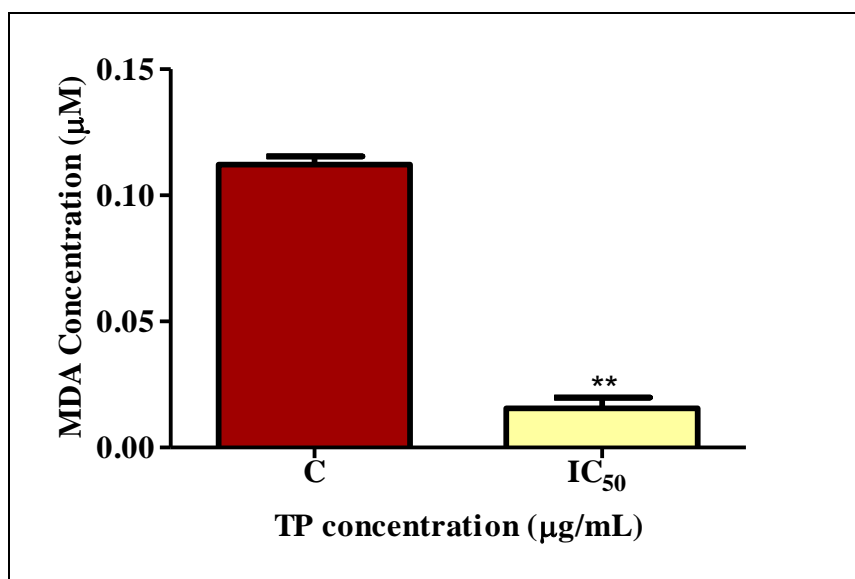


Figure 4.4: An 8-fold decrease in MDA concentration was noted in the IC_{50} -treated HepG2 cells compared to the control (** $p = 0.0030$; Unpaired t -test with Welch's correction).

4.5 NO Assay

Nitric oxide is a reactive nitrogen species (RNS) that is produced by nitric oxide synthase (NOS) and contributes to an oxidative stress environment (Tsikas, 2005). The RNS were indirectly determined using the cell culture medium to detect NO concentration. However, there are limitations to NO accurate detection and quantification using culture medium due to the extremely short physiological half-life of this gaseous free radical. Nitric oxide (NO) is a diatomic free radical that is extremely short lived (less than 1 second in circulating blood) in biological systems (Bryan and Grisham, 2007). The NO concentration for the control was $0.0575 \pm 0.002500 \mu\text{M}$. There was a non-significant decrease in the IC₅₀-treatment to NO concentrations of $0.05533 \pm 0.002404 \mu\text{M}$ (Figure 4.5).

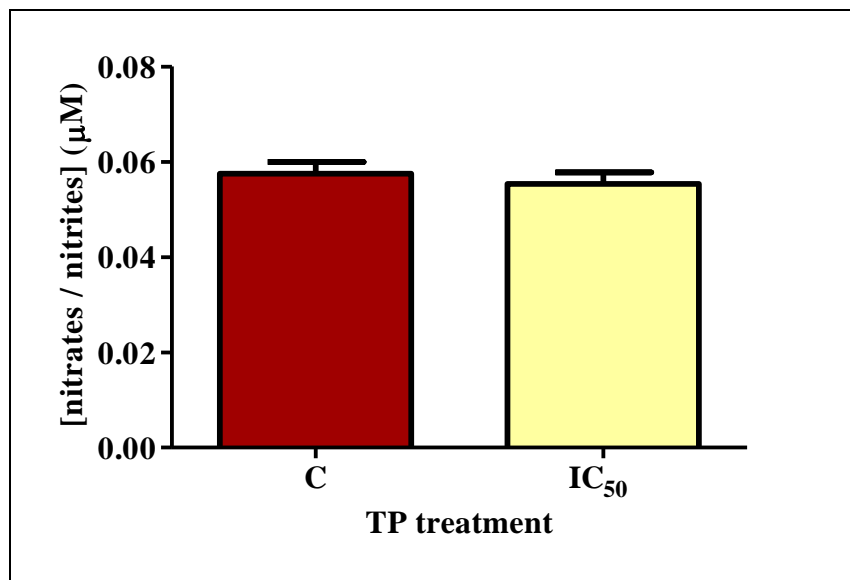


Figure 4.5: Nitrates and nitrites concentration for the IC₅₀ displayed a slight decrease of 1.039-fold relative to the control.

4.6 GSH assay

Glutathione (GSH) is a three amino-acid peptide antioxidant and a cofactor to GPx-1 whose main biological role is to protect the organism from oxidative damage by free radicals and is a key indicator of oxidative stress (Hausladen and Alscher, 2017). A decrease in GSH was noted in the IC₅₀ displaying a significant drop to 64930 ± 1564 RLU ($p = 0.0430$) relative to 1862000 ± 385100 RLU in the control (Figure 4.6).

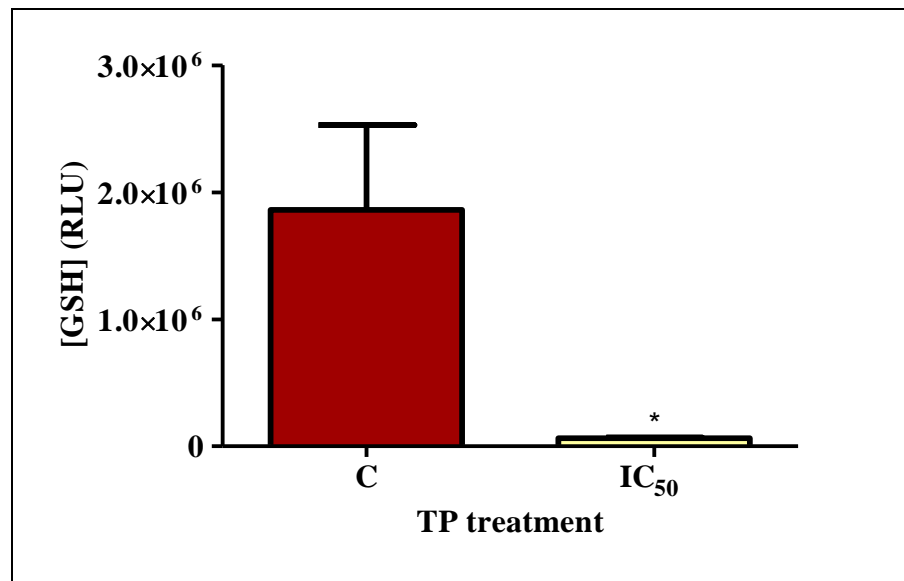


Figure 4.6: A decrease in the GSH concentration was observed for IC₅₀ ($p = 0.0430$) treatments [*Unpaired t-test with Welch's correction].

4.7 LDH Assay

The LDH assay is an indicator of cytotoxicity because intracellular LDH is lost and released into the culture medium due to cell membrane damage that is associated with lipid peroxidation or irreversible cell death (Kamiloglu et al., 2020). The extracellular LDH in the control was 0.2460 ± 0.0410 absorbance units, which was similar LDH measured for the IC₅₀ (0.2265 ± 0.0765 absorbance units) (Figure 4.7).

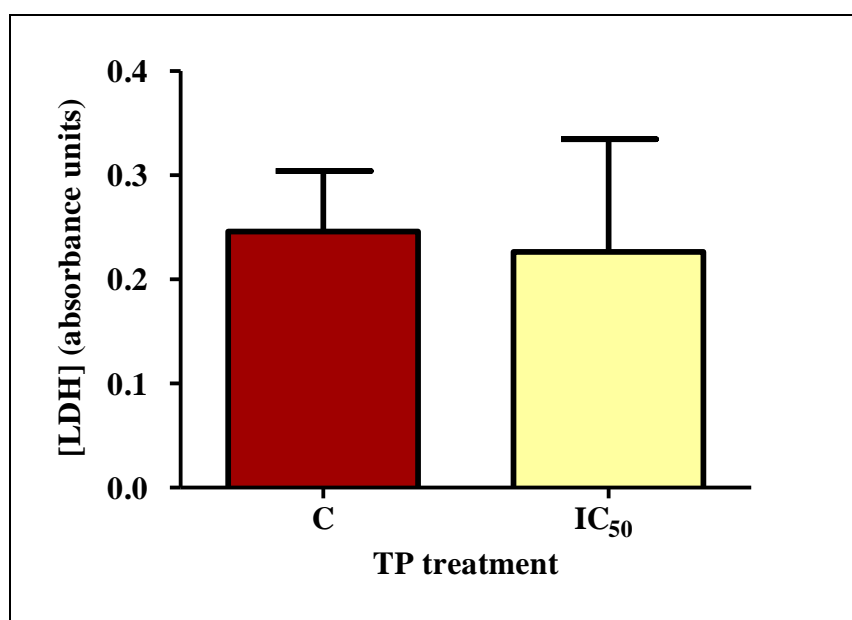


Figure 4.7: The extracellular LDH released from IC₅₀-treated cells was similar to the control.

4.8 qPCR

qPCR is a technique that allows exponential amplification of DNA sequences using a DNA polymerase to extend a pair of primers that are complementary to the gene sequence of interest. There was an increase in *Nrf2* gene expression for the IC₅₀ treatment (Figure 4.8A). There was a significant decrease in *GPx-1* ($p = 0.0151$) (Figure 4.8B). *T. phanerophlebia* increased the gene expression of *SOD2* (Figure 4.8C), while a significant decrease in *NF-κB* ($p = 0.0078$) was noted (Figure 4.8D).

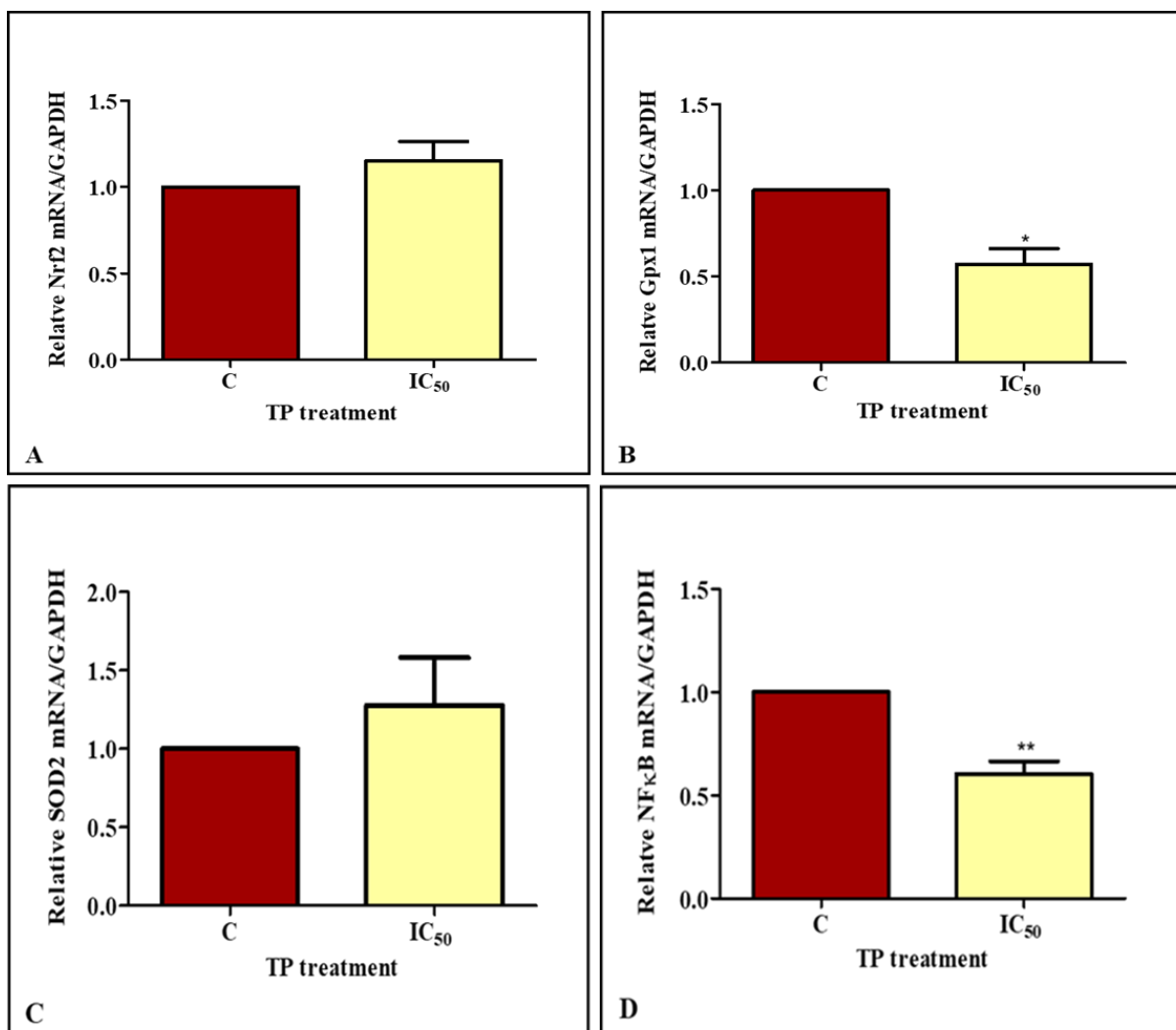


Figure 4.8: Gene expression following treatment with *T. phanerophlebia*. **(A)** *Nrf2* gene expression had a 1.152-fold increase. **(B)** The mRNA for *GPx-1* in the IC₅₀-treated HepG2 cells had 1.755-fold decrease compared to the control (* $p = 0.0151$). **(C)** *T. phanerophlebia* increased *SOD2* gene expression for the IC₅₀ treatment by 1.279-fold. **(D)** A significant decrease (1.654-fold) in *NFκB* mRNA expression was observed for the *T. phanerophlebia* treated cells (** $p = 0.0078$).

4.9 Western blotting

Western blotting was used to detect and quantify specific proteins and antioxidants produced due to oxidative stress and apoptosis. There was significant decrease of Fas protein expression (RBI: C - 2 917 565 IC₅₀ – 1 731543) ($p < 0.0001$, Figure 4.9A). The STAT3 protein expression was similar to the control for the IC₅₀ treatment (RBI: C - 10 022 233 IC₅₀ - 8 427 381) (Figure 4.9B). *T. phanerophlebia* crude aqueous leaf extract decreased the protein expression of HSP90 (RBI: C - 15 114 438 IC₅₀ - 11 210 403) ($p < 0.0001$, Figure 4.9C). There was significant increase in SOD2 (RBI: C – 2 631 564 IC₅₀ – 11 819 176) (Figure 4.9D) for the *T. phanerophlebia* treatment ($p < 0.0001$). For p38 (Figure 4.9E), the *T. phanerophlebia* treatment increased protein expression (RBI: C - 14 543 828 IC₅₀ – 18 881 254) ($p = 0.0114$).

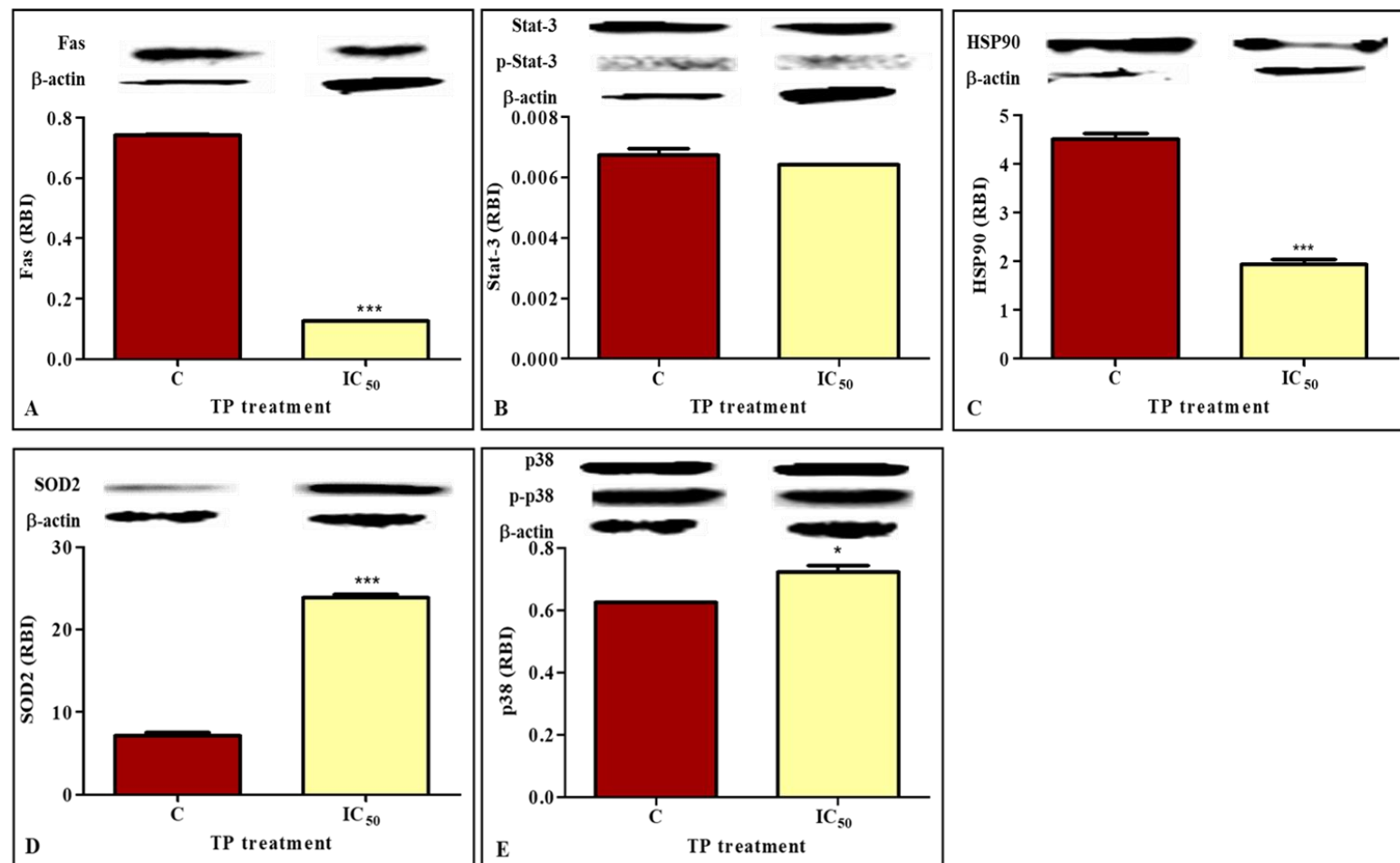


Figure 4.9: Protein expression following treatment with TP. (A) Fas protein expression was significantly decreased following TP treatment of HepG2 cells ($***p < 0.0001$). (B) The IC_{50} remained similar to the control for STAT3 protein expression. (C) TP decreased HSP90 protein expression for the IC_{50} treatment ($***p < 0.0001$). (D) Significant increase in SOD2 protein expression was observed for the TP treated cells ($***p < 0.0001$). (E) The protein expression of p38 was increased by the IC_{50} treatment ($*p = 0.0114$). [*Unpaired t-test with Welch's correction].

4.10 Caspase activity

The cysteine aspartic acid-specific protease (caspase) family has differentiated members to carry out either the initiator or effector roles in apoptosis. Following 48-hour treatment of HepG2 cells with *T. phanerophlebia*, the initiator caspases 8 and 9, and the effector caspase 3 all displayed significant decrease in caspase activity (Figure 4.10). Caspase 8 control luminescence was recorded as 1899000 ± 37770 RLU (Figure 4.10A). There was significant decrease ($p = 0.0004$) in the IC₅₀ to 12190 ± 1485 RLU (Figure 4.10A). Caspase 9 control recorded 2520000 ± 120900 RLU, and there was a 25-fold significant decrease ($p = 0.0004$) in the IC₅₀ to 99940 ± 72700 RLU (Figure 4.10B). Caspase 3/7 displayed a significant decrease ($p = 0.0003$) in the IC₅₀ (5238 ± 571.3 RLU) (Figure 4.10 C) compared to the control (233100 ± 3955 RLU).

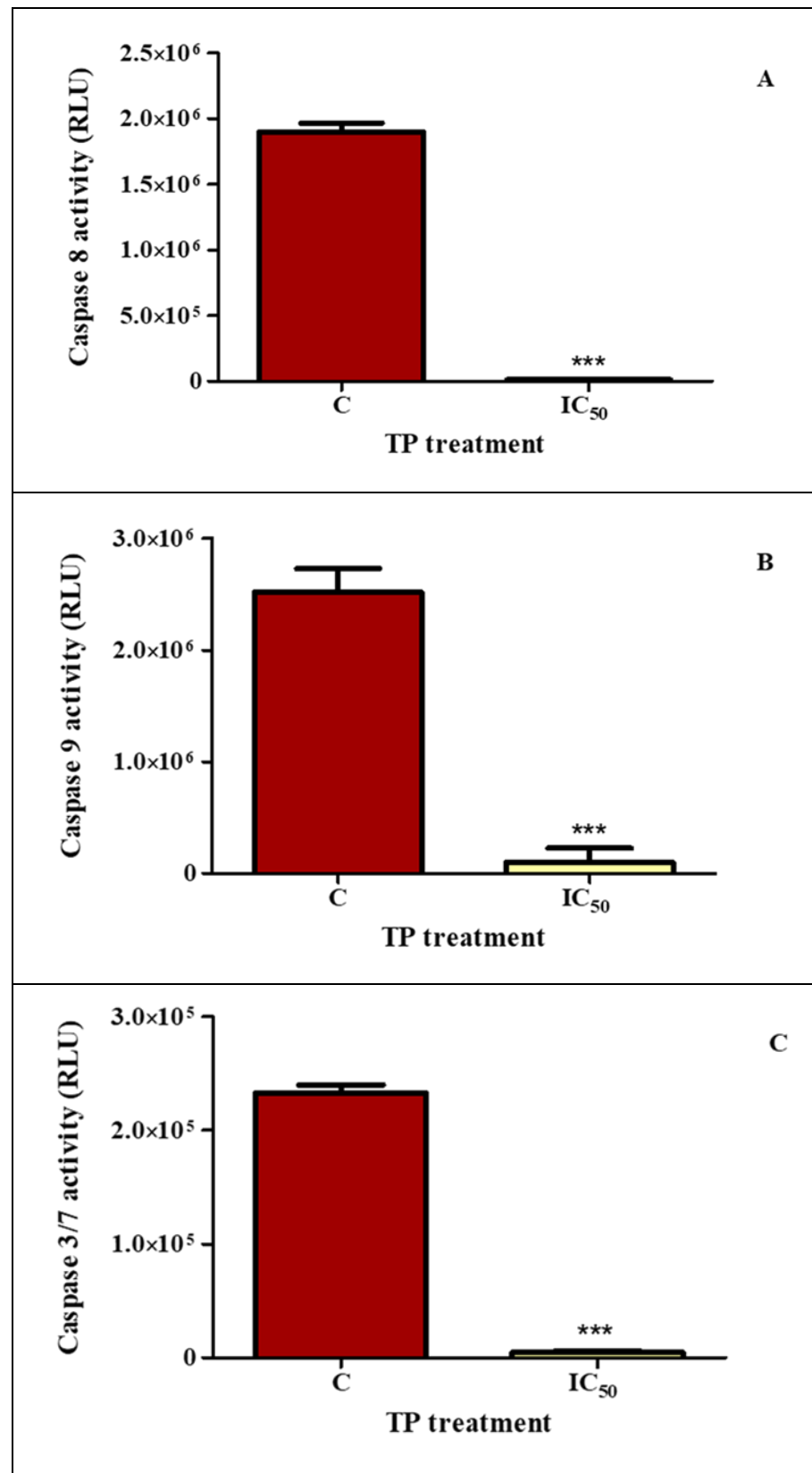


Figure 4.10: Significant decrease in initiator caspase 8 ($***p = 0.0004$) and caspase 9 ($***p = 0.0004$), as well as effector caspase 3/7 ($***p = 0.0003$) luminescence was observed in *T. phanerophlebia* treated HepG2 cells. [*Unpaired t-test with Welch's correction].

4.11 Markers of apoptosis and necrosis

Annexin V detects cells that express PS on the cell surface, a marker of early apoptosis, while PI fluorescence indicates necrotic cells. There was a decrease in apoptotic cells (Figure 4.11A; 82760 ± 2729 RLU compared to the control 111300 ± 17360 RLU). There was also a significant decrease in the necrotic cells for IC₅₀ treatment (Figure 4.11 B; 78470 ± 4395 RFU ($p = 0.0263$) compared to the control (152600 ± 11430 RFU).

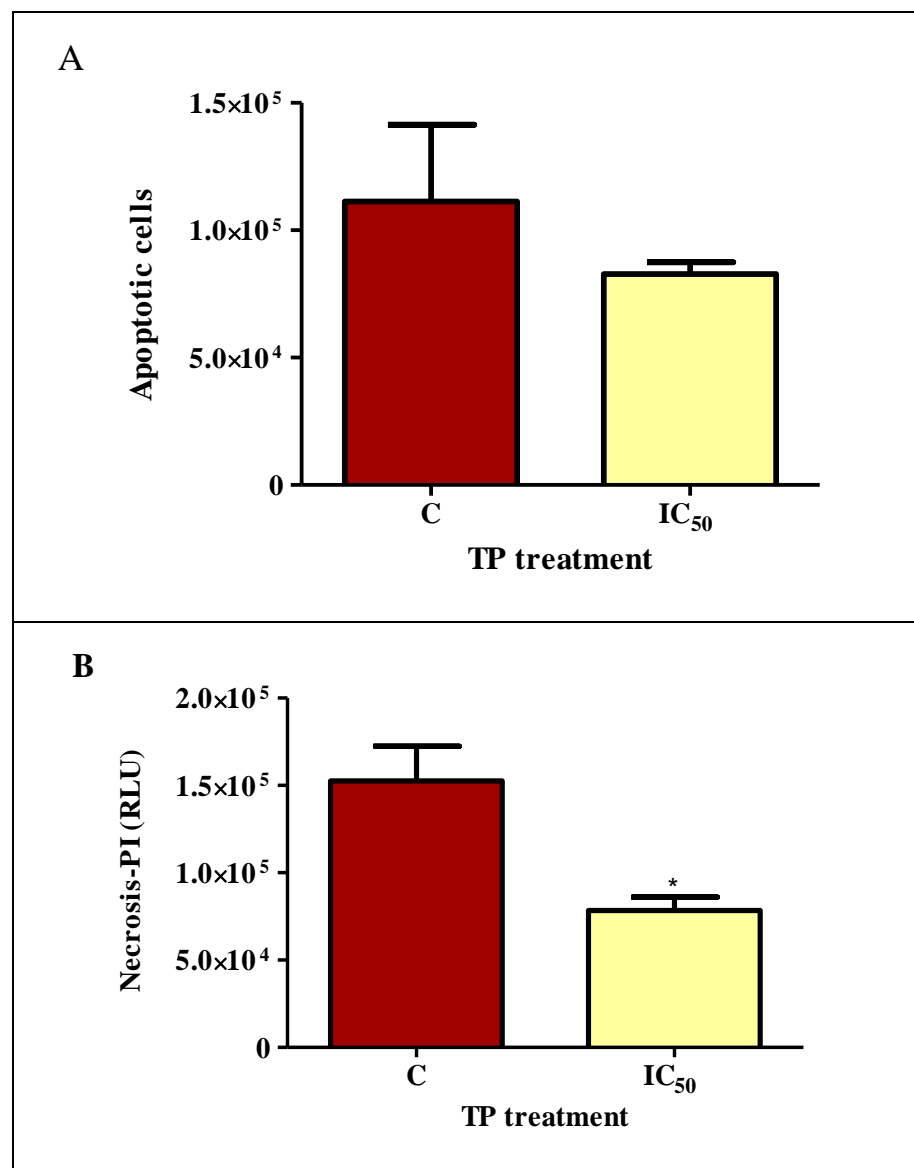


Figure 4.11: There was significant decrease in apoptotic and necrotic cells ($p = 0.0263$). [*Unpaired *t*-test with Welch's correction]

4.12 Cytochrome P₄₅₀ 3A4 activity

Cytochrome P₄₅₀ enzymes are ubiquitously expressed in the liver and play pivotal roles in the exposure and effects of drugs, by catabolizing drugs to inactive metabolites or by bio-activating pro-drugs to their active forms (Cali et al., 2009). Figure 4.12 below shows a non-significant decrease in cytochrome P₄₅₀ 3A4 activity from 2757 ± 94.13 RLU in the control to 1973 ± 188.8 RLU for the IC₅₀ treatment.

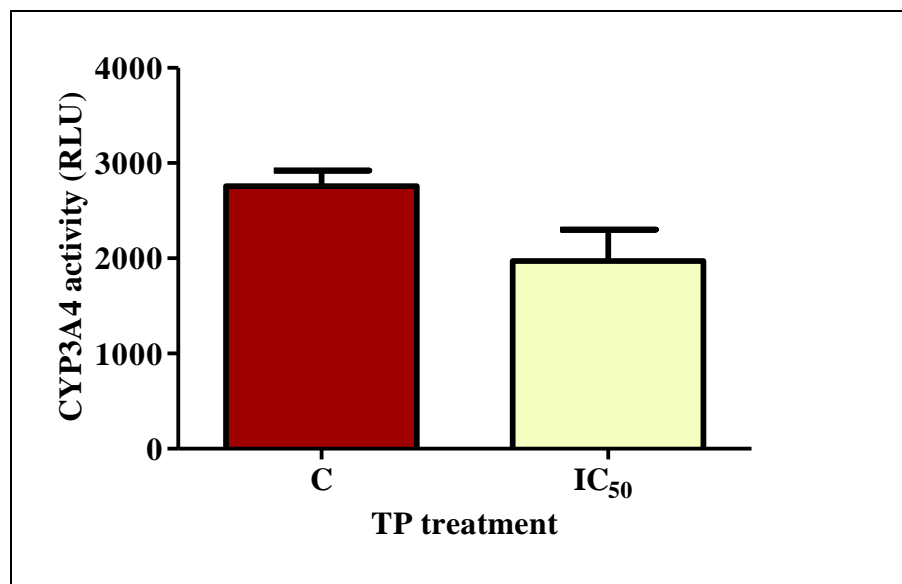


Figure 4.12: A non-significant 0.28-fold decrease in CYP3A4 activity was observed for the IC₅₀ treatment.

CHAPTER 5: DISCUSSION

Cancer currently contributes significantly to deaths attributed to non-communicable diseases (NCDs) and is the second leading cause of death globally following cardiovascular diseases (Bray *et al.*, 2021). The swift rise in cancer incidence and mortality in Sub-Saharan Africa due to high prevalence of risk factors and limited medical facilities is alarming because this is a region previously dominated by infectious diseases (Gouda *et al.*, 2019, Sung *et al.*, 2021). The lack of distinct symptoms causes poor prognosis and it is the main reason for high mortality rates and short survival time of cancer patients (Ozakyol, 2017). This presents a serious worldwide health burden as liver cancer remains a major public health concern globally (Liu *et al.*, 2019). Current liver cancer therapies include trans-arterial chemoembolization (TACE), chemotherapy and oral dosing with sorafenib, radiation therapy and ablation therapy. However, these therapies are not valuably effective in improving outcomes of cancer because they result in drug toxicity, inefficacy and resistance (Anwanwan *et al.*, 2020). Therefore, a need for novel plant-derived anticancer agents which have less invasive effects compared to synthetic medicine arises and this has increased the use of medicinal plants therapeutically (Roy *et al.*, 2017). The genus *Terminalia* possesses polyphenolic compounds such as flavonoids, tannins, and phenolic acids and has been used since ancient times in the formulation of ayurvedic medicines for antimalarial, antimicrobial, antioxidant, antiplasmodial and anti-inflammatory therapy (Patra *et al.*, 2020). *T. phanerophlebia* is a species from the genus *Terminalia* with limited information on its mechanism of action. In this study, it was hypothesized that *T. phanerophlebia* crude leaf extract would induce cytotoxic effects on hepatocellular carcinoma (HepG2) cell line.

Cytochrome P450 3A4 is the largest subfamily of cytochromes and a crucial P450 enzyme found in the liver and gastrointestinal tract. It plays pivotal roles in the metabolism of endogenous steroids and exogenous compounds such as plant phytochemicals making them water-soluble for excretion (Gallo *et al.*, 2019). Upregulation of CYP3A4 decreases the efficacy of a drug as it is rapidly metabolised and excreted whilst inhibition of CYP3A4 increases bioavailability of active components in a drug (Le Corvaisier *et al.*, 2021, Chen *et al.*, 2021). In this study, *T. phanerophlebia* inhibited CYP3A4 activity (Figure 4.12). This finding suggests that HepG2 cells are highly susceptible and sensitive to the cytotoxicity of *T. phanerophlebia*, this may be due to their reduced capacity to metabolise *T. phanerophlebia*. It

is possible that the inhibition of CYP3A4 in our study could have been due to flavonoids or other phytochemicals in *T. phanerophlebia*. Indeed, the flavonoids and furanocoumarins found in grapefruit such as quercetin and bergapten had a dose-dependent inhibitory effect on CYP3A4 activity in human liver microsomes (Ho *et al.*, 2001). In addition, the *in vitro* inhibition of cytochrome P450 by *Terminalia chebula* hydroalcoholic fruit pulp extract in rat liver microsomes could have been due to chebulagic acid, chebulinic acid, ellagic acid or gallic acid found in the extract (Ponnusankar *et al.*, 2011). *T. phanerophlebia*, amongst other *Terminalia* species, was found to contain phenolics, flavonoids, triterpenoids and tannins (Adebayo *et al.*, 2015).

The structure and organization of the mitochondria are pivotal to maintaining mitochondrial homeostasis and an emerging biological target in aging, inflammation, neurodegeneration and cancer (Mertens *et al.*, 2021). The mitochondria are not only the powerhouse of the cell as they generate most of the ATP via the Krebs cycle, but they also have a significant role in cell signaling and cell viability (Jain *et al.*, 2016). As observed in Figure 4.1, treatment with *T. phanerophlebia* resulted in a dose–response decrease in cell viability. Loss of mitochondrial integrity results in decreased enzymatic activity of various complexes for the electron transport chain, including mitochondrial succinate dehydrogenase as well as the reducing equivalents such as co-enzyme NADH, which causes reduced mitochondrial MTT conversion and decreased cell viability (Stockert *et al.*, 2018). The antiproliferative effects displayed by *T. phanerophlebia* (Figure 4.1) may thus be mediated at complex II of the ETC, resulting in a decrease of MTT conversion to formazan. In this study, the IC₅₀ for *T. phanerophlebia* was 1396 µg/mL, which was slightly higher than the IC₅₀ of 1360 µg/mL obtained in a recent study on *T. phanerophlebia* (Nyahada *et al.*, 2021).

The significant decrease in ATP production (Figure 4.2) and dissipation of the ΔΨ_M observed in this study (Figure 4.3) attests to a disruption of mitochondrial integrity. Complexes I, III and IV of the ETC generate the ΔΨ_M through the redox transformations in the Krebs cycle (Zorova *et al.*, 2018). The ΔΨ_M drives inward transport of cations and outward transport of anions creating an electrochemical proton gradient across the mitochondrial membrane that is used to produce ATP (Sivandzade *et al.*, 2019). Limited fluctuations of both ΔΨ_M and ATP levels do occur under normal physiological activity, but an elongated shift from ΔΨ_M threshold induces inevitable loss of cell viability (Figure 4.1) and contributes to various pathologies (Zorova *et al.*, 2018). It is presumed that exposure of HepG2 cells to *T. phanerophlebia* for 48 hours

caused uncoupling of oxidative phosphorylation, which resulted in inhibition of ATP synthesis as well as disruption of the $\Delta\Psi_M$. In a study by Maués (2019) on murine glioma cells, flavonoids resulted in the loss of mitochondrial integrity (Maués *et al.*, 2019). Thus, flavonoids in *T. phanerophlebia* may be implicated for the decrease in ATP production and $\Delta\Psi_M$.

The mitochondria are also the major source of ROS production. The results in Figure 4.8C, strongly suggest that the uncoupling of oxidative phosphorylation may have facilitated the accumulation of O_2^- , which then triggered the upregulation of mitochondrial SOD2 (Figure 4.9D) in order to prevent the oxidation of macromolecules, such as lipids by catalyzing the dismutation of O_2^- to H_2O_2 and O_2 . Furthermore, the SOD2 (Figure 4.8C and 4.9D) dismutation of the O_2^- to H_2O_2 effectively inhibited the production of RNS such as $ONOO^-$ (Figure 4.5). Similarly in a study by Gu (2006) there was increase in O_2^- generation and a decrease in endothelial NO synthase protein expression following inhibition of HSP90 by geldanamycin which binds to the ATP binding site of HSP90 inhibiting the ATP/ADP cycle (Gu *et al.*, 2006). In this study, the significant decrease in HSP90 protein expression (Figure 4.9C) may be attributed to inhibition by flavonoids found in *T. phanerophlebia* because epigallocatechin gallate, the primary flavonoid in green tea has been reported to inhibit HSP90 by binding at or near to a C-terminal ATP-binding site of HSP90 thereby preventing dimerization (Yin *et al.*, 2009, Steinmann *et al.*, 2013, M. Hugel and Jackson, 2012, Huo *et al.*, 2008). The HSP inhibition disrupts H_2O_2 balance by increasing H_2O_2 and O_2^- leading to generation of oxidative stress (Sable *et al.*, 2018). Complex II of the ETC is also a major site of H_2O_2 production when there are increased concentrations of succinate (Kamarauskaitė *et al.*, 2020, Jardim-Messeder *et al.*, 2015).

The fate of H_2O_2 would be $\cdot OH$ which through Fenton-type reactions is an initiator of lipid peroxidation. However, the decrease in MDA (Figure 4.4) and extracellular LDH (Figure 4.7) suggests that the phytochemicals in *T. phanerophlebia* could have inhibited lipid oxidation. According to Matsui and co-researchers (2001), ellagitannins and anthocyanins possibly contribute to modulating the oxidative stress environment; these phytochemicals are present in *T. phanerophlebia* (Bedekar *et al.*, 2010, Matsui *et al.*, 2001, Yi *et al.*, 2020, Brown and Kelly, 2007). Furthermore, methyl gallate found in *Terminalia* species has protective properties against H_2O_2 injury (Acharyya *et al.*, 2015, Crispo *et al.*, 2010). The presence of methyl gallate

in *T. phanerophlebia* could have protected the HepG2 cells from lipid peroxidation and contributed to the maintenance of the cell membrane integrity observed in this study.

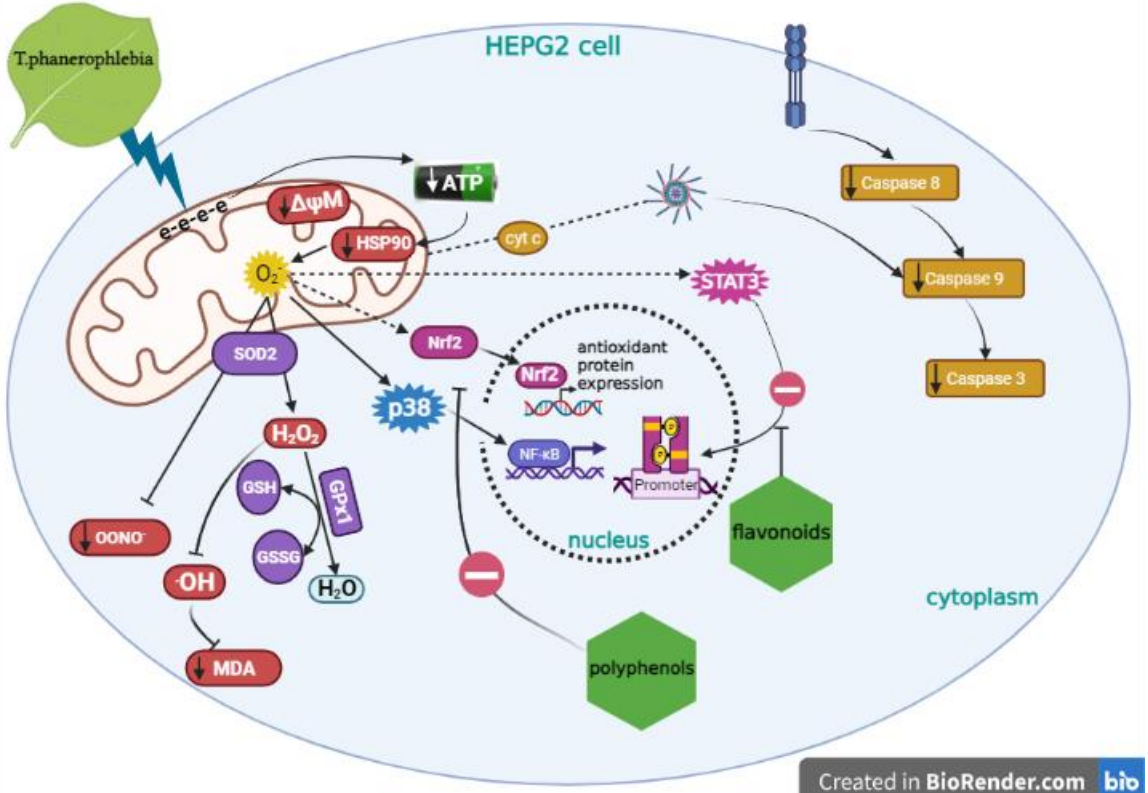
The protective effect of *T. phanerophlebia* on oxidative stress was associated with elevated *Nrf2* mRNA expression (Figure 4.8A), and associated increase in the transcription of the antioxidant genes such as *SOD2* (Figure 4.9D). The transcription factor Nrf2 is a modulator of oxidative stress that regulates components of the glutathione and thioredoxin antioxidant systems by regulating gene expression of antioxidant response elements (ARE) and phase II detoxifying enzymes such as GSH, SOD2, NADPH, NAD(P)H quinone oxidoreductase 1, heme oxygenase 1 (HO-1), GPx-1 and ferritin resulting in inhibition of inflammation (Ahmed *et al.*, 2017, Reuland *et al.*, 2013, Ma, 2013, Tonelli *et al.*, 2018). However, GSH (Figure 4.6) and *GPx-1* (Figure 4.8B) were decreased in this study. The decrease in GSH concentration (Figure 4.6) suggests that GSH may have been employed to neutralise H₂O₂ and lipid radicals because at lower concentrations H₂O₂ can be decomposed to water by GPx-1, using GSH as an electron donor (Mahesh *et al.*, 2009, Sharma *et al.*, 2018). The significant decrease of GSH levels and the activities of antioxidant enzymes SOD2 (Figure 4.9D) and *GPx-1* (Figure 4.8B) was similar to a study on rat erythrocytes conducted by Hebbani and co-investigators (2021), whereby activities of GSH and GPx-1 were decreased and SOD2 increased in response to *T. arjuna* (Hebbani *et al.*, 2021).

Transcription factor STAT3 is a cytoprotective transcription factor in cells exposed to oxidative stress and deletion of STAT3 sensitizes and increases the susceptibility of cells to the effects of oxidative stress (Barry *et al.*, 2009). In this study, the protein expression of STAT3 (Figure 4.9B) was similar to the control following exposure to *T. phanerophlebia* suggesting that HepG2 cell death was not in response to oxidative stress as the STAT3 protein expression was unchanged. The activity of STAT3 is highly dependent on the electron transport chain, on the activities of ATP synthase and adenine nucleotide translocase (Suchalatha *et al.*, 2007). A study by Xie and co-researchers (2018) revealed that the chemical and genetic inhibition of STAT3 sensitized HCC cells thereby inducing downstream events that led to cell death (Xie *et al.*, 2018).

Apoptosis is programmed cell death that occurs in multicellular organisms and can either be executed through the intrinsic or extrinsic pathway (Kaczanowski, 2020). In this study, *T. phanerophlebia* caused a down-regulation of both Fas protein (Figure 4.9A) and the activity of

caspase 8 (Figure 4.10A) in treated cells, relative to the control implying that the extrinsic pathway leading to cell death was not activated. Caspase 9 (Figure 4.10B) and caspase 3/7 (Figure 4.10C) activities were also downregulated. Figure 4.11 supports these findings since there was no externalisation of PS and cell death was neither through apoptosis or necrosis and suggesting that apoptosis was not executed. The p38 MAPK is activated by stressful stimuli especially ROS and is linked to the oxidative stress response and inflammation as it further activates NF- κ B and COX2 (Yong *et al.*, 2009, Nys *et al.*, 2010, Zhao *et al.*, 2019, Yang *et al.*, 2014). In this study, there was up-regulation of p38 (Figure 4.9E) in response to *T. phanerophlebia* suggesting cellular response to the oxidative stress environment. However, NF- κ B was down regulated (Figure 4.8D) despite upregulation of pro-inflammatory and stressful stimuli, NF- κ B was potentially inhibited by some polyphenols in *T. phanerophlebia*, thus inhibiting both the extrinsic and intrinsic apoptosis. Some phytochemicals such as gallic acid have been found to inhibit the translocation and transcriptional activity of NF- κ B in the nucleus by inhibiting its binding to target DNA (Seo *et al.*, 2018). In cultured Human Umbilical Vein Endothelial Cells (HUVEC), gallic acid was found to inhibit TNF- α that plays a role in the induction of translocation of NF- κ B (Bustami *et al.*, 2018). A study on osthole by Yang and co-authors (2014) yielded similar results to the present study whereby Nrf2 was upregulated, but NF- κ B and apoptosis were inhibited in a mouse model of accelerated focal and segmental glomerulosclerosis (FSGS). (Yang *et al.*, 2014). In another study by Wen (2010), *Terminalia catappa* L. hydrophilic extract attenuated the expression of MMP-1, -3, and -9 by inhibiting the phosphorylation of ERK, JNK, and p38 (Wen *et al.*, 2010).

Thus *T. phanerophlebia* activated the Nrf2-mediated antioxidant defence in order to combat oxidative stress in the HepG2 cells (Figure 5.1).



Created in BioRender.com

Figure 5.1: The collective biochemical effects of *T. phanerophlebia* crude aqueous leaf extracts on HepG2 cells. There was a decrease in both $\Delta\Psi_M$ and ATP resulting in HSP90 activity which increased O_2^- and H_2O_2 . The increase in O_2^- triggered the upregulation of Nrf2 and SOD2 which neutralised the free radicals to H_2O by GSH. Even though p38 was upregulated, apoptotic cell death was prevented through downregulation of NF- κ B and STAT3 (prepared by author).

CHAPTER 6: CONCLUSION

The study investigated the safety of the *T.phanerophlebia* aqueous extract as well as its potential anticancer activity. Discovery of natural plant extracts or plant-derived compounds that are safe and capable of selectively inhibiting the proliferation of cancer or inducing cancer cell apoptosis would benefit research and cancer therapy.

In summary (Figure 5.1), *T. phanerophlebia* caused a decrease in $\Delta\Psi_M$ accompanied by a decrease in ATP resulting in HSP90 activity which increased O_2^- and H_2O_2 . The increase in O_2^- was supported by the increase in *SOD2*. However, oxidative stress was prevented by upregulation of *Nrf2*, which facilitated neutralisation of free radicals to H_2O by GSH and the decrease in MDA. Despite p38 upregulation, apoptotic cell death was prevented through downregulation of *NF-κB* and *STAT3*. *T. phanerophlebia* therefore activates *Nrf2* to prevent oxidative stress, but induces cell death through a signaling pathway other than apoptosis or necrosis.

Future studies should involve a positive control in order to have more comparable results of the effects of *T. phanerophlebia*. There were also limitations in this study in measuring NO concentration from the cell culture medium due to its very short half-life. There is need for future studies measuring cellular nitrate/nitrite from cell lysates. Future studies are also required to determine the mode of cell death initiated by *T. phanerophlebia* in HepG2 cells as well as possible effects of *T. phanerophlebia* *in vivo*.

REFERENCES

- ACHARYYA, S., SARKAR, P., SAHA, D. R., PATRA, A., RAMAMURTHY, T. & BAG, P. K. 2015. Intracellular and membrane-damaging activities of methyl gallate isolated from Terminalia chebula against multidrug-resistant *Shigella* spp. *J Med Microbiol*, 64, 901-909.
- ADAN, A., KIRAZ, Y. & BARAN, Y. 2016. Cell proliferation and cytotoxicity assays. *Current pharmaceutical biotechnology*, 17, 1213-1221.
- ADEBAYO, S. A., DZOYEM, J. P., SHAI, L. J. & ELOFF, J. N. 2015. The anti-inflammatory and antioxidant activity of 25 plant species used traditionally to treat pain in southern African. *BMC complementary alternative medicine*, 15, 1-10.
- AHMED, S. M. U., LUO, L., NAMANI, A., WANG, X. J. & TANG, X. 2017. Nrf2 signaling pathway: Pivotal roles in inflammation. *Biochimica et Biophysica Acta -Molecular Basis of Disease*, 1863, 585-597.
- AKHTAR, M. F., SALEEM, A., RASUL, A., BAIG, M. M. F. A., BIN-JUMAH, M. & DAIM, M. M. A. 2020. Anticancer natural medicines: An overview of cell signaling and other targets of anticancer phytochemicals. *European Journal of Pharmacology*, 888, 173488.
- ALI-BOUCETTA, H., AL-JAMAL, K. T. & KOSTARELOS, K. 2011. Cytotoxic assessment of carbon nanotube interaction with cell cultures. *Biomedical Nanotechnology*. Springer.
- ALKHOURI, N., KHEIRANDISH-GOZAL, L., MATLOOB, A., ALONSO-ÁLVAREZ, M. L., KHALYFA, A., TERÁN-SANTOS, J., OKWU, V., LOPEZ, R., GILELES-HILLEL, A. & DWEIK, R. 2015. Evaluation of circulating markers of hepatic apoptosis and inflammation in obese children with and without obstructive sleep apnea. *Sleep medicine*, 16, 1031-1035.
- ALTEKRUSE, S. F., HENLEY, S. J., CUCINELLI, J. E. & MCGLYNN, K. A. 2014. Changing hepatocellular carcinoma incidence and liver cancer mortality rates in the United States. *The American journal of gastroenterology*, 109, 542.
- AN, Y., ZHANG, H., WANG, C., JIAO, F., XU, H., WANG, X., LUAN, W., MA, F., NI, L. & TANG, X. 2019. Activation of ROS/MAPKs/NF-κB/NLRP3 and inhibition of efferocytosis in osteoclast-mediated diabetic osteoporosis. *The FASEB Journal*, 33, 12515-12527.
- ANTIĆ, S., DRAGINIĆ, N., PILČEVIĆ, D., ŽIVKOVIĆ, V., SREJOVIĆ, I., JEREMIĆ, N., PETROVIĆ, D. & JAKOVLJEVIĆ, V. 2020. The influence of vitamin E coated dialysis membrane on oxidative stress during the single session of on-line hemodiafiltration. *Vojnosanitetski pregled*, 97-97.
- ANWANWAN, D., SINGH, S. K., SINGH, S., SAIKAM, V. & SINGH, R. 2020. Challenges in liver cancer and possible treatment approaches. *Biochimica et Biophysica Acta -Reviews on Cancer*, 1873, 188314.
- ARUMUGAM, J., JEDDY, N., RAMAMURTHY, A. & THANGAVELU, R. 2017. The expression of Bcl-2 in oral squamous cell carcinoma—A review. *Journal of Orofacial Sciences*, 9, 71.
- ARZUMANOV, A., REIS, H. M. & FEITELSON, M. A. 2013. Pathogenic mechanisms in HBV-and HCV-associated hepatocellular carcinoma. *Nature Reviews Cancer*, 13, 123-135.
- ASHRAF, M. A. 2020. Phytochemicals as potential anticancer drugs: time to ponder nature's bounty. *BioMed research international*, 2020.
- ASLANTÜRK, Ö. S. 2018. In vitro cytotoxicity and cell viability assays: principles, advantages, and disadvantages. *Genotoxicity-A predictable risk to our actual world*, 2, 64-80.
- BAGAEV, A. V., GARAЕVA, A. Y., LEBEDEVA, E. S., PICHUGIN, A. V., ATAULLAKHANOV, R. I. & ATAULLAKHANOV, F. I. 2019. Elevated pre-activation basal level of nuclear NF-κB in native macrophages accelerates LPS-induced translocation of cytosolic NF-κB into the cell nucleus. *Scientific reports*, 9, 1-16.
- BANERJEE, A. & ROYCHOUDHURY, A. 2018. Abiotic stress, generation of reactive oxygen species, and their consequences: an overview. *Plant Physiology*, 23-50.

- BARRY, S. P., TOWNSEND, P. A., MCCORMICK, J., KNIGHT, R. A., SCARABELLI, T. M., LATCHMAN, D. S. & STEPHANOU, A. 2009. STAT3 deletion sensitizes cells to oxidative stress. *Biochemical and biophysical research communications*, 385, 324-329.
- BEDEKAR, A., SHAH, K. & KOFFAS, M. 2010. Natural products for type II diabetes treatment. *Advances in applied microbiology*, 71, 21-73.
- BEIGI, M., HAGHANI, E., ALIZADEH, A. & SAMANI, Z. N. 2018. THE PHARMACOLOGICAL PROPERTIES OF SEVERAL SPECIES OF TERMINALIA IN THE WORLD. *INTERNATIONAL JOURNAL OF PHARMACEUTICAL SCIENCES AND RESEARCH*, 9, 4079-4088.
- BISHAYEE, A., AHMED, S., BRANKOV, N. & PERLOFF, M. 2011. Triterpenoids as potential agents for the chemoprevention and therapy of breast cancer. *Frontiers in bioscience: a journal and virtual library*, 16, 980.
- BISWAS, M., BISWAS, K., KARAN, T. K., BHATTACHARYA, S., GHOSH, A. K. & HALDAR, P. K. 2011. Evaluation of analgesic and anti-inflammatory activities of Terminalia arjuna leaf. *Journal of Phytotherapy*.
- BLASKOVICH, M. A., SUN, J., CANTOR, A., TURKSON, J., JOVE, R. & SEBTI, S. M. 2003. Discovery of JSI-124 (cucurbitacin I), a selective Janus kinase/signal transducer and activator of transcription 3 signaling pathway inhibitor with potent antitumor activity against human and murine cancer cells in mice. *Cancer research*, 63, 1270-1279.
- BOULARES, A. H., YAKOVLEV, A. G., IVANOVA, V., STOICA, B. A., WANG, G., IYER, S. & SMULSON, M. 1999. Role of poly (ADP-ribose) polymerase (PARP) cleavage in apoptosis: caspase 3-resistant PARP mutant increases rates of apoptosis in transfected cells. *Journal of Biological Chemistry*, 274, 22932-22940.
- BOYLE, M., MASSON, S. & ANSTEE, Q. M. 2018. The bidirectional impacts of alcohol consumption and the metabolic syndrome: cofactors for progressive fatty liver disease. *Journal of hepatology*, 68, 251-267.
- BRAY, F., FERLAY, J., SOERJOMATARAM, I., SIEGEL, R. L., TORRE, L. A. & JEMAL, A. 2018. Global cancer statistics 2018: GLOBOCAN estimates of incidence and mortality worldwide for 36 cancers in 185 countries. *CA: a cancer journal for clinicians*, 68, 394-424.
- BRAY, F., LAVERSANNE, M., WEIDERPASS, E. & SOERJOMATARAM, I. 2021. The ever-increasing importance of cancer as a leading cause of premature death worldwide. *Cancer*.
- BRÉCHOT, C. 2004. Pathogenesis of hepatitis B virus—related hepatocellular carcinoma: old and new paradigms. *Gastroenterology*, 127, S56-S61.
- BROWN, J. E. & KELLY, M. F. 2007. Inhibition of lipid peroxidation by anthocyanins, anthocyanidins and their phenolic degradation products. *European Journal of Lipid Science Technology*, 109, 66-71.
- BRUGGISSER, R., VON DAENIKEN, K., JUNDT, G., SCHAFFNER, W. & TULLBERG-REINERT, H. 2002. Interference of plant extracts, phytoestrogens and antioxidants with the MTT tetrazolium assay. *Planta medica*, 68, 445-448.
- BRYAN, N. S. & GRISHAM, M. B. 2007. Methods to detect nitric oxide and its metabolites in biological samples. *Free radical biology and medicine*, 43, 645-657.
- BUDHU, S., GIESE, R., GUPTA, A., FITZGERALD, K., ZAPPASODI, R., SCHAD, S., HIRSCHHORN, D., CAMPESATO, L. F., DE HENAU, O. & GIGOUX, M. 2021. Targeting phosphatidylserine enhances the anti-tumor response to tumor-directed radiation therapy in a preclinical model of melanoma. *Cell reports*, 34, 108620.
- BURANAAMNUAY, K. 2021. The MTT assay application to measure the viability of spermatozoa: A variety of the assay protocols. *Open Veterinary Journal*, 11, 251-269.
- BUSTAMI, A., SOPIAH, P., MUHARAM, R. & WIBOWO, H. 2018. Effects of gallic acid and its derivatives on inflammatory regulation of endometriotic primary cultures: study on NF- κ B mRNA expression and IL-6 secretion. *Biomedical*

Pharmacology Journal, 11, 1479-1484.

- CALI, J. J., SOBOL, M., MA, D., UYEDA, H. T. & MEISENHEIMER, P. 2009. CYP3A4 P450-Glo® Assays with Luciferin-IPA: The Most Sensitive and Selective Bioluminescent CYP3A4 Assay. *Promega Corporation*. Available online at: <http://www.promega.com/resources/pubhub/cellnotes/cyp3a4-p450-glo-assays-with-luciferin-ipa-the-most-sensitive-and-selective-bioluminescent-cyp3a4/Updated>.
- CAO, W., CHEN, H., YU, Y., LI, N. & CHEN, W. 2021. Changing profiles of cancer burden worldwide and in China: a secondary analysis of the global cancer statistics 2020. *Chinese Medical Journal*, 134, 783.
- CARNEIRO, B. A. & EL-DEIRY, W. S. 2020. Targeting apoptosis in cancer therapy. *Nature reviews Clinical oncology*, 17, 395-417.
- CHEN, J., LIU, J., HUANG, Y., LI, R., MA, C., ZHANG, B., WU, F., YU, W., ZUO, X. & LIANG, Y. 2021. Insights into oral bioavailability enhancement of therapeutic herbal constituents by cytochrome P450 3A inhibition. *Drug Metabolism Reviews*, 1-17.
- CHEN, M. & WONG, C. 2020. The emerging roles of N6-methyladenosine (m6A) deregulation in liver carcinogenesis. *Molecular cancer*, 19, 1-12.
- CHINTA, S. J., RANE, A., YADAVA, N., ANDERSEN, J. K., NICHOLLS, D. G., POLSTER, B. M. & MEDICINE 2009. Reactive oxygen species regulation by AIF-and complex I-depleted brain mitochondria. *Free Radical Biology*, 46, 939-947.
- CHO, H., KIM, S., KYAW, Y., WIN, A., KOO, S., KIM, H. & CHEONG, J. 2015. HBx induces the proliferation of hepatocellular carcinoma cells via AP1 over-expressed as a result of ER stress. *Biochemical Journal*, 466, 115-121.
- CHOROMAŃSKA, B., MYŚLIWIEC, P., ŁUBA, M., WOJSKOWICZ, P., MYŚLIWIEC, H., CHOROMAŃSKA, K., DADAN, J., ZALEWSKA, A. & MACIEJCZYK, M. 2020. The impact of hypertension and metabolic syndrome on nitrosative stress and glutathione metabolism in patients with morbid obesity. *Oxidative medicine and cellular longevity*, 2020.
- COCK, I. 2015. The medicinal properties and phytochemistry of plants of the genus Terminalia (Combretaceae). *Inflammopharmacology*, 23, 203-229.
- COCKRAM, P. E., KIST, M., PRAKASH, S., CHEN, S., WERTZ, I. E. & VUCIC, D. 2021. Ubiquitination in the regulation of inflammatory cell death and cancer. *Cell Death and Differentiation*, 28, 591-605.
- COSTILLA, M., MACRI DELBONO, R., KLECHA, A., CREMASCHI, G. A. & BARREIRO ARCOS, M. L. 2019. Oxidative stress produced by hyperthyroidism status induces the antioxidant enzyme transcription through the activation of the Nrf-2 factor in lymphoid tissues of Balb/c mice. *Oxidative medicine and cellular longevity*, 2019.
- CRISPO, J. A., PICHÉ, M., ANSELL, D. R., EIBL, J. K., TAI, I., KUMAR, A., ROSS, G. M. & TAI, T. 2010. Protective effects of methyl gallate on H2O2-induced apoptosis in PC12 cells. *Biochemical and Biophysical Research Communications*, 393, 773-778.
- DINESH, M., SUBBARAYAN, R., RALLAPALLI, S., KANSRAJH, C. & KALAIVANI, R. 2014. Terminalia bellerica leaf extracts induce apoptosis in Hep G2 cells and regulates cell cycle progression by inducing G2/M cell cycle arrest. *Indian Journal of Research in Pharmacy and Biotechnology*, 2, 1044.
- DO, B. H., NGUYEN, T. P. T., HO, N. Q. C., LE, T. L., HOANG, N. S. & DOAN, C. C. 2020. Mitochondria-mediated Caspase-dependent and Caspase-independent apoptosis induced by aqueous extract from Moringa oleifera leaves in human melanoma cells. *Molecular biology reports*, 47, 3675-3689.

- DONATO, M. T., TOLOSA, L. & GÓMEZ-LECHÓN, M. J. 2015. Culture and functional characterization of human hepatoma HepG2 cells. *Protocols in In Vitro Hepatocyte Research*. Springer.
- EL-SERAG, H. B. 2020. Epidemiology of hepatocellular carcinoma. *The Liver: Biology and Pathobiology*, 758-772.
- FAHMY, N., AL-SAYED, E. & SINGAB, A. 2015. Genus Terminalia: A phytochemical and biological review. *Medicinal & Aromat Plants*, 4, 218.
- FATHI, N., RASHIDI, G., KHODADADI, A., SHAHI, S. & SHARIFI, S. 2018. STAT3 and apoptosis challenges in cancer. *International journal of biological macromolecules*, 117, 993-1001.
- FERENCI, P., FRIED, M., LABRECQUE, D., BRUIX, J., SHERMAN, M., OMATA, M., HEATHCOTE, J., PIRATSIVUTH, T., KEW, M. & OTEGBAYO, J. A. 2010. World gastroenterology organisation global guideline. hepatocellular carcinoma (hcc): a global perspective. *gastrointestin liver dis*, 19, 311-317.
- FERLAY, J., COLOMBET, M., SOERJOMATARAM, I., PARKIN, D. M., PIÑEROS, M., ZNAOR, A. & BRAY, F. 2021. Cancer statistics for the year 2020: An overview. *International Journal of Cancer*.
- FOREST, V., FIGAROL, A., BOUDARD, D., COTTIER, M., GROSSEAU, P. & POURCHEZ, J. 2015. Adsorption of lactate dehydrogenase enzyme on carbon nanotubes: How to get accurate results for the cytotoxicity of these nanomaterials. *Langmuir*, 31, 3635-3643.
- FORTUGNO, P., BELTRAMI, E., PLESCIA, J., FONTANA, J., PRADHAN, D., MARCHISIO, P. C., SESSA, W. C. & ALTIERI, D. C. 2003. Regulation of survivin function by Hsp90. *Proceedings of the National Academy of Sciences*, 100, 13791-13796.
- GALLO, P., DE VINCENTIS, A., PEDONE, C., NOBILI, A., TETTAMANTI, M., GENTILUCCI, U. V., PICARDI, A., MANNUCCI, P. M., INCALZI, R. A. & INVESTIGATORS, R. 2019. Drug–drug interactions involving CYP3A4 and p-glycoprotein in hospitalized elderly patients. *European journal of internal medicine*, 65, 51-57.
- GÀO, X. & SCHÖTTKER, B. 2017. Reduction–oxidation pathways involved in cancer development: a systematic review of literature reviews. *Oncotarget*, 8, 51888.
- GIRVAN, H. M. & MUNRO, A. W. 2016. Applications of microbial cytochrome P450 enzymes in biotechnology and synthetic biology. *Current opinion in chemical biology*, 31, 136-145.
- GLOWACKI, S., SYNOWIEC, E. & BLASIAK, J. 2013. The role of mitochondrial DNA damage and repair in the resistance of BCR/ABL-expressing cells to tyrosine kinase inhibitors. *International journal of molecular sciences*, 14, 16348-16364.
- GOMEZ-LECHON, M., DONATO, M., CASTELL, J. & JOVER, R. 2003. Human hepatocytes as a tool for studying toxicity and drug metabolism. *Current drug metabolism*, 4, 292-312.
- GOTTLIEB, E., ARMOUR, S., HARRIS, M. & THOMPSON, C. 2003. Mitochondrial membrane potential regulates matrix configuration and cytochrome c release during apoptosis. *Cell Death Differentiation*, 10, 709-717.
- GOUDA, H. N., CHARLSON, F., SORSDAHL, K., AHMADZADA, S., FERRARI, A. J., ERSKINE, H., LEUNG, J., SANTAMAURO, D., LUND, C. & AMINDE, L. N. 2019. Burden of non-communicable diseases in sub-Saharan Africa, 1990–2017: results from the Global Burden of Disease Study 2017. *The Lancet Global Health*, 7, e1375-e1387.
- GRITSKO, T., WILLIAMS, A., TURKSON, J., KANEKO, S., BOWMAN, T., HUANG, M., NAM, S., EWEIS, I., DIAZ, N. & SULLIVAN, D. 2006. Persistent activation of stat3 signaling induces survivin gene expression and confers resistance to apoptosis in human breast cancer cells. *Clinical cancer research*, 12, 11-19.
- GU, Y., LEWIS, D. F., ZHANG, Y., GROOME, L. J. & WANG, Y. 2006. Increased superoxide generation and decreased stress protein Hsp90 expression in human umbilical cord vein endothelial cells (HUEVCs) from pregnancies complicated by preeclampsia. *Hypertension in pregnancy*, 25, 169-182.
- GUENGERICH, F. P., WATERMAN, M. R. & EGLI, M. 2016. Recent structural insights into cytochrome P450 function. *Trends in pharmacological sciences*, 37, 625-640.

- GUPTA, P. C. 2012. Biological and pharmacological properties of Terminalia chebula Retz.(Haritaki)-An overview. *Int J pharm pharm Sci*, 4, 62-68.
- HAUSLADEN, A. & ALSCHER, R. G. 2017. Glutathione. *Antioxidants in higher plants*. CRC Press.
- HEBBANI, A. V., VADDI, D. R., DD, P. P. & NCH, V. 2021. Protective effect of Terminalia arjuna against alcohol induced oxidative damage of rat erythrocyte membranes. *Journal of Ayurveda Integrative Medicine*, 12, 330-339.
- HO, P., SAVILLE, D. J. & WANWIMOLRUK, S. 2001. Inhibition of human CYP3A4 activity by grapefruit flavonoids, furanocoumarins and related compounds. *J Pharm Pharm Sci*, 4, 217-27.
- HUO, C., WAN, S., LAM, W., LI, L., WANG, Z., LANDIS-PIWOWAR, K., CHEN, D., DOU, Q. & CHAN, T. 2008. The challenge of developing green tea polyphenols as therapeutic agents. *Inflammopharmacology*, 16, 248-252.
- IJOMONE, O. M., IROEGBU, J. D., ASCHNER, M. & BORNHORST, J. 2021. Impact of environmental toxicants on p38-and ERK-MAPK signaling pathways in the central nervous system. *Neurotoxicology*, 86, 166-171.
- JAIN, S., DWIVEDI, J., JAIN, P. K., SATPATHY, S. & PATRA, A. 2016. Medicinal plants for treatment of cancer: A brief review. *Pharmacognosy Journal*, 8.
- JALMI, S. K. & SINHA, A. K. 2015. ROS mediated MAPK signaling in abiotic and biotic stress-striking similarities and differences. *Frontiers in plant science*, 6, 769.
- JARDIM-MESSEDER, D., CAVERZAN, A., RAUBER, R., DE SOUZA FERREIRA, E., MARGIS-PINHEIRO, M. & GALINA, A. 2015. Succinate dehydrogenase (mitochondrial complex II) is a source of reactive oxygen species in plants and regulates development and stress responses. *New Phytologist*, 208, 776-789.
- JAYACHANDRAN, A., SHRESTHA, R., BRIDLE, K. R. & CRAWFORD, D. H. 2020. Association between hereditary hemochromatosis and hepatocellular carcinoma: a comprehensive review. *Hepatoma Research*, 6.
- JAYAPRAKASAM, B., SEERAM, N. P. & NAIR, M. G. 2003. Anticancer and antiinflammatory activities of cucurbitacins from Cucurbita andreana. *Cancer letters*, 189, 11-16.
- JEMAL, A., BRAY, F., CENTER, M. M., FERLAY, J., WARD, E. & FORMAN, D. 2011. Global cancer statistics. *CA: a cancer journal for clinicians*, 61, 69-90.
- JUAN, C. A., PÉREZ DE LA LASTRA, J. M., PLOU, F. J. & PÉREZ-LEBEÑA, E. 2021. The Chemistry of Reactive Oxygen Species (ROS) Revisited: Outlining Their Role in Biological Macromolecules (DNA, Lipids and Proteins) and Induced Pathologies. *International Journal of Molecular Sciences*, 22, 4642.
- KACZANOWSKI, S. 2020. Symbiotic Origin of Apoptosis. *Symbiosis: Cellular, Molecular, Medical and Evolutionary Aspects*. Springer.
- KAMARAUSKAITE, J., BANIENE, R., TRUMBECKAS, D., STRAZDAUSKAS, A. & TRUMBECKAITE, S. 2020. Increased Succinate Accumulation Induces ROS Generation in In Vivo Ischemia/Reperfusion-Affected Rat Kidney Mitochondria. *BioMed Research International*, 2020, 8855585.
- KAMILOGLU, S., SARI, G., OZDAL, T. & CAPANOGLU, E. 2020. Guidelines for cell viability assays. *Food Frontiers*, 1, 332-349.
- KAUR, K., JAIN, M., KAUR, T. & JAIN, R. 2009. Antimalarials from nature. *Bioorganic & medicinal chemistry*, 17, 3229-3256.
- KHALAF, M. M. 2019. *The role of CFTR in normal human lung microvascular endothelial cells*. University of Portsmouth.
- KHALILZADEH, B., SHADJOU, N., KANBEROGLU, G. S., AFSHARAN, H., DE LA GUARDIA, M., CHAROUDEH, H. J., OSTADRAHIMI, A. & RASHIDI, M. 2018. Advances in nanomaterial based optical biosensing and bioimaging of apoptosis via caspase-3 activity: a review. *Microchimica Acta*, 185, 1-19.
- KHAN, A. A., ALLEMAILEM, K. S., ALHUMAYDHI, F. A., GOWDER, S. J. & RAHMANI, A. H. 2020. The biochemical and clinical perspectives of lactate dehydrogenase: an enzyme of active metabolism. *Endocrine, Metabolic*

- Immune Disorders-Drug Targets*, 20, 855-868.
- KHONSARY, S. A. 2017. Guyton and Hall: textbook of medical physiology. *Surgical neurology international*, 8.
- KIVINEN, K., KALLAJOKI, M. & TAIMEN, P. 2005. Caspase-3 is required in the apoptotic disintegration of the nuclear matrix. *Experimental cell research*, 311, 62-73.
- KUANG, J., YAN, X., GENDERS, A. J., GRANATA, C. & BISHOP, D. J. 2018. An overview of technical considerations when using quantitative real-time PCR analysis of gene expression in human exercise research. *PloS one*, 13, e0196438.
- KUMAR, P., NAGARAJAN, A. & UCHIL, P. D. 2018. Analysis of cell viability by the lactate dehydrogenase assay. *Cold Spring Harbor Protocols*, 2018, pdb. prot095497.
- KURIEN, B. T. & SCOFIELD, R. H. 2006. Western blotting. *Methods*, 38, 283-293.
- LE CORVAISIER, C., CAPELLE, A., FRANCE, M., BOURGUIGNON, L., TOD, M. & GOUTELLE, S. 2021. Drug interactions between emergency contraceptive drugs and cytochrome inducers: literature review and quantitative prediction. *Fundamental clinical pharmacology*, 35, 208-216.
- LEE, D., KEO, S., CHENG, S., OH, H. & KIM, Y. 2017. Protective effects of Cambodian medicinal plants on tert-butyl hydroperoxide-induced hepatotoxicity via Nrf2-mediated heme oxygenase-1. *Molecular medicine reports*, 15, 451-459.
- LENAZ, G. 2001. The mitochondrial production of reactive oxygen species: mechanisms and implications in human pathology. *IUBMB life*, 52, 159-164.
- LEVY, D. E. & LEE, C. 2002. What does Stat3 do? *The Journal of clinical investigation*, 109, 1143-1148.
- LIAO, J., BROSSE, N., PIZZI, A. & HOPPE, S. 2019. Dynamically cross-linked tannin as a reinforcement of polypropylene and UV protection properties. *Polymers*, 11, 102.
- LIM, K., CHOI, H. S., PARK, Y. K., PARK, E., SHIN, G. C., KIM, D. H., AHN, S. H. & KIM, K. 2013. HBx-induced NF-κB signaling in liver cells is potentially mediated by the ternary complex of HBx with p22-FLIP and NEMO. *PLoS One*, 8, e57331.
- LIU, J.-J., NILSSON, Å., OREDSSON, S., BADMAEV, V., ZHAO, W.-Z. & DUAN, R.-D. 2002. Boswellic acids trigger apoptosis via a pathway dependent on caspase-8 activation but independent on Fas/Fas ligand interaction in colon cancer HT-29 cells. *Carcinogenesis*, 23, 2087-2093.
- LIU, Z., JIANG, Y., YUAN, H., FANG, Q., CAI, N., SUO, C., JIN, L., ZHANG, T. & CHEN, X. 2019. The trends in incidence of primary liver cancer caused by specific etiologies: results from the Global Burden of Disease Study 2016 and implications for liver cancer prevention. *Journal of hepatology*, 70, 674-683.
- LIVAK, K. J. & SCHMITTGEN, T. D. 2001. Analysis of relative gene expression data using real-time quantitative PCR and the 2^{-ΔΔCT} method. *methods*, 25, 402-408.
- LIVER, E. A. F. T. S. O. T. 2018. EASL clinical practice guidelines: management of hepatocellular carcinoma. *Journal of hepatology*, 69, 182-236.
- LOPES, G. L. L. 2014. *Seaweeds from the Portuguese Coast: Chemistry, antimicrobial and anti-inflammatory capacity*. Universidade do Porto (Portugal).
- LOU, X., HONG, Y., CHEN, S., LEUNG, C. W. T., ZHAO, N., SITU, B., LAM, J. W. Y. & TANG, B. Z. 2014. A selective glutathione probe based on AIE fluorogen and its application in enzymatic activity assay. *Scientific reports*, 4, 1-6.
- M. HUGEL, H. & JACKSON, N. 2012. Redox chemistry of green tea polyphenols: therapeutic benefits in neurodegenerative diseases. *Mini reviews in medicinal chemistry*, 12, 380.
- MA, H. & SHIEH, K. 2006. Western blotting method. *J Am Sci*, 2, 23-27.
- MA, Q. 2013. Role of nrf2 in oxidative stress and toxicity. *Annual review of pharmacology toxicology*, 53, 401-426.
- MADIKIZELA, B. 2014. Isolation and characterization of antimicrobial compounds. *Journal of ethnopharmacology*.

MAHESH, R., BHUVANA, S., HAZEENA, B. & VAVA, M. 2009. Effect of Terminalia chebula aqueous extract on oxidative stress and antioxidant status in the liver and kidney of young and aged rats. *Cell Biochemistry Function*, 27, 358-363.

MAHMOOD, T. & YANG, P.-C. 2012. Western blot: technique, theory, and trouble shooting. *North American journal of medical sciences*, 4, 429.

MAN, S., GAO, W., ZHANG, Y., HUANG, L. & LIU, C. 2010. Chemical study and medical application of saponins as anti-cancer agents. *Fitoterapia*, 81, 703-714.

MARTIN, F., LINDEN, T., KATSCHINSKI, D. M., OEHME, F., FLAMME, I., MUKHOPADHYAY, C. K., ECKHARDT, K., TRÖGER, J., BARTH, S. & CAMENISCH, G. 2005. Copper-dependent activation of hypoxia-inducible factor (HIF)-1: implications for ceruloplasmin regulation. *Blood*, 105, 4613-4619.

MARTINEZ-RUIZ, G., MALDONADO, V., CEBALLOS-CANCINO, G., GRAJEDA, J. P. R. & MELENDEZ-ZAJGLA, J. 2008. Role of Smac/DIABLO in cancer progression. *Journal of experimental clinical cancer research*, 27, 1-7.

MATSUI, T., UEDA, K., OKI, T., SUGITA, K., TERAHARA, N. & MATSUMOTO, K. 2001. α -Glucosidase inhibitory action of natural acylated anthocyanins. 1. Survey of natural pigments with potent inhibitory activity. *Journal of Agricultural Food Chemistry*, 49, 1948-1951.

MAUÉS, L., ALVES, G., COUTO, N., DA SILVA, B., ARRUDA, M., MACCHI, B., SENA, C., PRADO, A., CRESPO-LOPEZ, M. & SILVA, E. 2019. Flavonoids from the Amazon plant Brosimum acutifolium induce C6 glioma cell line apoptosis by disrupting mitochondrial membrane potential and reducing AKT phosphorylation. *Biomedicine Pharmacotherapy*, 113, 108728.

MAURIN, O. 2009. A phylogenetic study of the family Combretaceae with emphasis on the genus Combretum in Africa. University of Johannesburg.

MELI, M. A. A., SHAFIE, N. H., LOH, S. P. & RAHMAT, A. 2019. Anti-proliferative and Apoptosis-Inducing Effects of Morinda citrifolia L. Shoot on Breast, Liver, and Colorectal Cancer Cell Lines. *Mal J Med Health Sci*, 15, 129-35.

MERTENS, R. T., JENNINGS, W. C., OFORI, S., KIM, J. H., PARKIN, S., KWAKYE, G. F. & AWUAH, S. G. 2021. Synthetic Control of Mitochondrial Dynamics: Developing Three-Coordinate Au (I) Probes for Perturbation of Mitochondria Structure and Function. *JACS Au*, 1, 439-449.

MITRA, V. & METCALF, J. 2012. Metabolic functions of the liver. *Anaesthesia Intensive Care Medicine*, 13, 54-55.

NAGAR, R. & SCHWESSINGER, B. 2018. Multi-Step High Purity High Molecular Weight DNA Extraction Protocol from Challenging Fungal Tissues. *Protocols. Io*, 10.

NAIR, J., AREMU, A. & VAN STADEN, J. 2012. Anti-inflammatory effects of Terminalia phanerophlebia (Combretaceae) and identification of the active constituent principles. *South African Journal of Botany*, 81, 79-80.

NAYAK, S. K., KHATIK, G. L., NARANG, R., MONGA, V. & CHOPRA, H. K. 2018. p53-Mdm2 interaction inhibitors as novel nongenotoxic anticancer agents. *Current cancer drug targets*, 18, 749-772.

NEUMANN, C., BAIN, P. & SHAW, G. 2007. Studies of the comparative in vitro toxicology of the cyanobacterial metabolite deoxycyclindrospermopsin. *Journal of Toxicology Environmental Health, Part A*, 70, 1679-1686.

NIKOLETOPOULOU, V., MARKAKI, M., PALIKARAS, K. & TAVERNARAKIS, N. 2013. Crosstalk between apoptosis, necrosis and autophagy. *Biochimica et Biophysica Acta (BBA)-Molecular Cell Research*, 1833, 3448-3459.

- NILES, A. L., MORAVEC, R. A., HESSELBERTH, P. E., SCURRIA, M. A., DAILY, W. J. & RISS, T. L. 2007. A homogeneous assay to measure live and dead cells in the same sample by detecting different protease markers. *Analytical biochemistry*, 366, 197-206.
- NILES, A. L., MORAVEC, R. A. & RISS, T. L. 2008. Caspase activity assays. *Apoptosis Cancer*, 137-150.
- NONYANE, F. 2014. Terminalia Phanerophlebia. *South African National Herbarium*.
- NOWAK, A., GIGER, R. S. & KRAYENBUEHL, P. 2018. Higher age at diagnosis of hemochromatosis is the strongest predictor of the occurrence of hepatocellular carcinoma in the Swiss hemochromatosis cohort: A prospective longitudinal observational study. *Medicine*, 97.
- NYAHADA, M. R., AMOAKO, D. G., SOMBORO, A. M., ARHIN, I., KHUMALO, H. M. & KHAN, R. B. 2021. The toxicogenic effect of Terminalia phanerophlebia Engl. & Diels leaf extract on oxidative stress parameters in an in vitro Hek293 model. *Journal of Pharmacy Pharmacognosy Research*, 9, 261-271.
- NYS, K., VAN LAETHEM, A., MICHELS, C., RUBIO, N., PIETTE, J. G., GARMYN, M. & AGOSTINIS, P. 2010. A p38MAPK/HIF-1 pathway initiated by UVB irradiation is required to induce noxa and apoptosis of human keratinocytes. *Journal of investigative dermatology*, 130, 2269-2276.
- OZAKYOL, A. 2017. Global epidemiology of hepatocellular carcinoma (HCC epidemiology). *Journal of gastrointestinal cancer*, 48, 238-240.
- OZOUGWU, J. C. 2017. Physiology of the liver. *International Journal of Research in Pharmacy and Biosciences*, 4, 13-24.
- PALMER, E. & PITMAN, N. 1972. Trees of Southern Africa: covering all known indigenous species in the Republic of South Africa, South-West Africa, Botswana, Lesotho & Swaziland. Volumes 1 & 2. *Trees of Southern Africa: covering all known indigenous species in the Republic of South Africa, South-West Africa, Botswana, Lesotho & Swaziland. Volumes 1 & 2*.
- PATRA, S., PANDA, P. K., NAIK, P. P., PANIGRAHI, D. P., PRAHARAJ, P. P., BHOL, C. S., MAHAPATRA, K. K., PADHI, P., JENA, M. & PATIL, S. 2020. Terminalia bellirica extract induces anticancer activity through modulation of apoptosis and autophagy in oral squamous cell carcinoma. *Food Chemical Toxicology*, 136, 111073.
- PEÑA-BLANCO, A. & GARCÍA-SÁEZ, A. J. 2018. Bax, Bak and beyond—mitochondrial performance in apoptosis. *The FEBS journal*, 285, 416-431.
- PFEFFER, C. M. & SINGH, A. T. 2018a. Apoptosis: a target for anticancer therapy. *International journal of molecular sciences*, 19, 448.
- PFEFFER, C. M. & SINGH, A. T. K. 2018b. Apoptosis: a target for anticancer therapy. *International journal of molecular sciences*, 19, 448.
- PINNA, A. D., YANG, T., MAZZAFERRO, V., DE CARLIS, L., ZHOU, J., ROAYAIE, S., SHEN, F., SPOSITO, C., CESCON, M. & DI SANDRO, S. 2018. Liver transplantation and hepatic resection can achieve cure for hepatocellular carcinoma. *Annals of surgery*, 268, 868-875.
- POLSTER, B. M. 2013. AIF, reactive oxygen species, and neurodegeneration: a “complex” problem. *Neurochemistry international*, 62, 695-702.
- PONNUSANKAR, S., PANDIT, S., VENKATESH, M., BANDYOPADHYAY, A. & MUKHERJEE, P. K. 2011. Cytochrome P450 inhibition assay for standardized extract of Terminalia chebula Retz. *Phytotherapy Research: An International Journal Devoted to Pharmacological*, 25, 151-154.
- PORRAS, G., CHASSAGNE, F., LYLES, J. T., MARQUEZ, L., DETTWEILER, M., SALAM, A. M., SAMARAKOON, T., SHABIH, S., FARROKH, D. R. & QUAVE, C. L. 2020. Ethnobotany and the role of plant natural products in antibiotic drug discovery. *Chemical Reviews*, 121, 3495-3560.
- PUSHPANGADAN, P., GEORGE, V., IJINU, T. & CHITHRA, M. 2018. Ethnomedicine. *Health Food Nutraceuticals-Traditional Wisdom of Maternal Child Health in India*, 113-117.

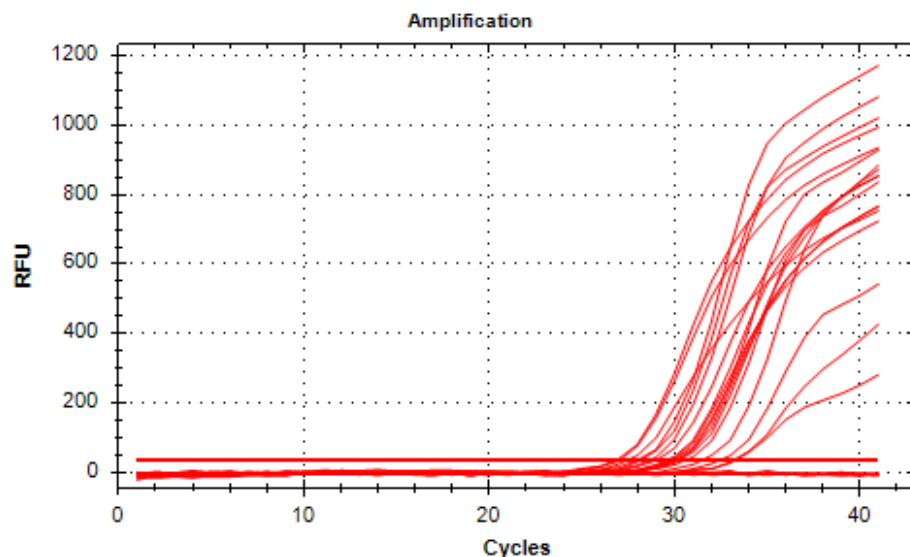
- RAAVÉ, R., VAN KUPPEVELT, T. H. & DAAMEN, W. F. 2018. Chemotherapeutic drug delivery by tumoral extracellular matrix targeting. *Journal of Controlled Release*, 274, 1-8.
- RABBANI, M., KANEVSKY, J., KAFI, K., CHANDELIER, F. & GILES, F. J. 2018. Role of artificial intelligence in the care of patients with nonsmall cell lung cancer. *European journal of clinical investigation*, 48, e12901.
- REDZA-DUTORDOIR, M. & AVERILL-BATES, D. A. 2016a. Activation of apoptosis signalling pathways by reactive oxygen species. *Biochimica et Biophysica Acta (BBA)-Molecular Cell Research*, 1863, 2977-2992.
- REDZA-DUTORDOIR, M. & AVERILL-BATES, D. A. 2016b. Activation of apoptosis signalling pathways by reactive oxygen species. *Biochimica et Biophysica Acta -Molecular Cell Research*, 1863, 2977-2992.
- REULAND, D. J., KHADEMI, S., CASTLE, C. J., IRWIN, D. C., MCCORD, J. M., MILLER, B. F. & HAMILTON, K. L. 2013. Upregulation of phase II enzymes through phytochemical activation of Nrf2 protects cardiomyocytes against oxidant stress. *Free Radical Biology Medicine*, 56, 102-111.
- ROBLEDINOS-ANTÓN, N., FERNÁNDEZ-GINÉS, R., MANDA, G. & CUADRADO, A. 2019. Activators and inhibitors of NRF2: a review of their potential for clinical development. *Oxidative medicine cellular longevity*, 2019.
- RODRÍGUEZ-GARCÍA, A., GARCÍA-VICENTE, R., MORALES, M. L., ORTIZ-RUIZ, A., MARTÍNEZ-LÓPEZ, J. & LINARES, M. 2020. Protein Carbonylation and Lipid Peroxidation in Hematological Malignancies. *Antioxidants*, 9, 1212.
- ROY, A., AHUJA, S. & BHARADVAJA, N. 2017. A review on medicinal plants against cancer. *Plant. Sci. Agric. Res*, 2, 1008.
- SABLE, A., RAI, K. M., CHOUDHARY, A., YADAV, V. K., AGARWAL, S. K. & SAWANT, S. V. 2018. Inhibition of heat shock proteins HSP90 and HSP70 induce oxidative stress, suppressing cotton fiber development. *Scientific reports*, 8, 1-17.
- SÁEZ, G. & ESTÁN-CAPELL, N. 2014. Antioxidant Enzymes. . Encyclopedia of Cancer: Springer-Verlag Berlin Heidelberg.
- SALMON, A. 2015. The anti-inflammatory and antioxidant activity of 25 medicinal plants in South Africa. *open access*.
- SEN, T. & SAMANTA, S. K. 2014. Medicinal plants, human health and biodiversity: a broad review. *Biotechnological applications of biodiversity*, 59-110.
- SEO, E., FISCHER, N. & EFFERTH, T. 2018. Phytochemicals as inhibitors of NF-κB for treatment of Alzheimer's disease. *Pharmacological research*, 129, 262-273.
- SHAI, L., MCGAW, L., MASOKO, P. & ELOFF, J. 2008. Antifungal and antibacterial activity of seven traditionally used South African plant species active against *Candida albicans*. *South African Journal of Botany*, 74, 677-684.
- SHAKERI, R., KHEIROLLAHI, A. & DAVOODI, J. 2017. Apaf-1: Regulation and function in cell death. *Biochimie*, 135, 111-125.
- SHALOM, J. & COCK, I. E. 2018. Terminalia ferdinandiana Exell. fruit and leaf extracts inhibit proliferation and induce apoptosis in selected human cancer cell lines. *Nutrition Cancer*, 70, 579-593.
- SHARMA, G. N., GUPTA, G. & SHARMA, P. 2018. A comprehensive review of free radicals, antioxidants, and their relationship with human ailments. *Critical Reviews™ in Eukaryotic Gene Expression*, 28.
- SHEIKH, M., ESHRAGHI, H., KHOSHNA, M., MAZANDARANI, M. & MORADI, A. 2017. Cytotoxicity effect of *Capparis spinosa* L. on the HepG2 human hepatocellular carcinoma cell line. *Indian Journal of Traditional Knowledge*.

- SHUNMUGAM, L. 2016. *Moringa oleifera* crude aqueous leaf extract induces apoptosis in human hepatocellular carcinoma cells via the upregulation of NF- κ B and IL-6/STAT3 pathway. University of KwaZulu Natal.
- SIBANDZE, G. & VAN ZYL, R. 2009. The antimalarial and toxicity studies of Swazi medicinal plants. *African Journal of Traditional, Complementary and Alternative Medicines*, 457-457.
- SINGAL, A. G., LAMPERTICO, P. & NAHON, P. 2020. Epidemiology and surveillance for hepatocellular carcinoma: new trends. *Journal of hepatology*, 72, 250-261.
- SITI, H. N., KAMISAH, Y. & KAMSIAH, J. 2015. The role of oxidative stress, antioxidants and vascular inflammation in cardiovascular disease (a review). *Vascular pharmacology*, 71, 40-56.
- SIVANDZADE, F., BHALERAO, A. & CUCULLO, L. 2019. Analysis of the mitochondrial membrane potential using the cationic JC-1 dye as a sensitive fluorescent probe. *Bio-protocol*, 9.
- SON, Y., CHEONG, Y., KIM, N., CHUNG, H., KANG, D. G. & PAE, H. 2011. Mitogen-activated protein kinases and reactive oxygen species: how can ROS activate MAPK pathways? *Journal of signal transduction*, 2011.
- SRINIVAS, U. S., TAN, B. W. Q., VELLAYAPPAN, B. A. & JEYASEKHARAN, A. D. 2019. ROS and the DNA damage response in cancer. *Redox biology*, 25, 101084.
- STEINMANN, J., BUER, J., PIETSCHMANN, T. & STEINMANN, E. 2013. Anti-infective properties of epigallocatechin-3-gallate (EGCG), a component of green tea. *British journal of pharmacology*, 168, 1059-1073.
- STOCKERT, J. C., HOROBIN, R. W., COLOMBO, L. L. & BLÁZQUEZ-CASTRO, A. 2018. Tetrazolium salts and formazan products in Cell Biology: Viability assessment, fluorescence imaging, and labeling perspectives. *Acta histochemica*, 120, 159-167.
- STOLERIU, S., LUNGU, C., GHITULICA, C. D., SURDU, A., VOICU, G., CUCURUZ, A., TURCULET, C. S. & CIOCAN, L. T. 2020. Influence of dopant nature on biological properties of ZnO thin-film coatings on Ti alloy substrate. *Nanomaterials*, 10, 129.
- STÖß, C., LASCHINGER, M., WANG, B., LU, M., ALTMAYR, F., HARTMANN, D., HÜSER, N. & HOLZMANN, B. 2020. TLR3 promotes hepatocyte proliferation after partial hepatectomy by stimulating uPA expression and the release of tissue-bound HGF. *The FASEB Journal*, 34, 10387-10397.
- SUCHALATHA, S., SRINIVASAN, P. & DEVI, C. S. S. 2007. Effect of *T. chebula* on mitochondrial alterations in experimental myocardial injury. *Chemico-biological interactions*, 169, 145-153.
- SUNG, H., FERLAY, J., SIEGEL, R. L., LAVERSANNE, M., SOERJOMATARAM, I., JEMAL, A. & BRAY, F. 2021. Global cancer statistics 2020: GLOBOCAN estimates of incidence and mortality worldwide for 36 cancers in 185 countries. *CA: a cancer journal for clinicians*, 71, 209-249.
- TAIT, S. W. & GREEN, D. R. 2010. Mitochondria and cell death: outer membrane permeabilization and beyond. *Nature reviews Molecular cell biology*, 11, 621-632.
- TANASH, H. A. & PIITULAINEN, E. 2019. Liver disease in adults with severe alpha-1-antitrypsin deficiency. *Journal of gastroenterology*, 54, 541-548.
- THORNTON, B. & BASU, C. 2011. Real-time PCR (qPCR) primer design using free online software. *Biochemistry*
- Molecular Biology Education*, 39, 145-154.
- TONELLI, C., CHIO, I. & TUVESEN, D. A. 2018. Transcriptional regulation by Nrf2. *Antioxidants redox signaling*, 29, 1727-1745.
- TSIKAS, D. 2005. Review Methods of quantitative analysis of the nitric oxide metabolites nitrite and nitrate in human biological fluids. *Free radical research*, 39, 797-815.
- UCHIDA, K. 2008. Activation of Stress Signaling Pathways by the end products of lipid peroxidation. *The journal of Biological Chemistry*.
- VAN MEERLOO, J., KASPERS, G. J. & CLOOS, J. 2011. Cell sensitivity assays: the MTT assay. *Cancer cell culture*. Springer.
- WEN, K., SHIH, I., HU, J., LIAO, S., SU, T. & CHIANG, H. 2010. Inhibitory effects of Terminalia catappa on UVB-induced photodamage in fibroblast cell line. *Evidence-Based Complementary*

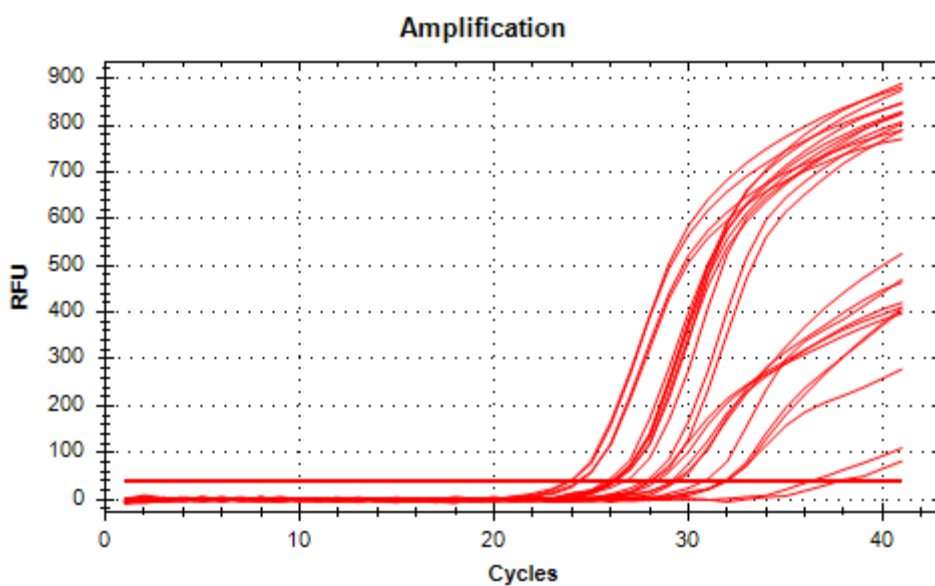
- Alternative Medicine*, 2011, 904532.
- XIA, X., HUO, W., WAN, R., XIA, X., DU, Q. & CHANG, Z. 2017. Identification of housekeeping genes as references for quantitative real-time RT-PCR analysis in *Misgurnus anguillicaudatus*. *Journal of genetics*, 96, 895-904.
- XIE, L., ZENG, Y., DAI, Z., HE, W., KE, H., LIN, Q., CHEN, Y., BU, J., LIN, D. & ZHENG, M. 2018. Chemical and genetic inhibition of STAT3 sensitizes hepatocellular carcinoma cells to sorafenib induced cell death. *International journal of biological sciences*, 14, 577.
- XIE, Y., TIAN, H., XIANG, B., ZHANG, Y., LIU, J., CAI, Z. & XIANG, H. 2021. Transarterial chemoembolization plus sorafenib versus sorafenib for intermediate–advanced hepatocellular carcinoma: A meta-analysis comparing clinical outcomes. *Medicine*, 100.
- XU, Q., TU, J., DOU, C., ZHANG, J., YANG, L., LIU, X., LEI, K., LIU, Z., WANG, Y. & LI, L. 2017. HSP90 promotes cell glycolysis, proliferation and inhibits apoptosis by regulating PKM2 abundance via Thr-328 phosphorylation in hepatocellular carcinoma. *Molecular cancer*, 16, 1-16.
- YADAV, V. R., PRASAD, S., SUNG, B., KANNAPPAN, R. & AGGARWAL, B. B. 2010. Targeting inflammatory pathways by triterpenoids for prevention and treatment of cancer. *Toxins*, 2, 2428-2466.
- YANG, L., WU, S., ZHANG, Q., LIU, F. & WU, P. 2007. 23, 24-Dihydrocucurbitacin B induces G2/M cell-cycle arrest and mitochondria-dependent apoptosis in human breast cancer cells (Bcap37). *Cancer letters*, 256, 267-278.
- YANG, S., CHAN, Y., HUA, K., CHANG, J., CHEN, H., TSAI, Y., HSU, Y., CHAO, L. K., FENG-LING, Y. & TSAI, Y. 2014. Osthole improves an accelerated focal segmental glomerulosclerosis model in the early stage by activating the Nrf2 antioxidant pathway and subsequently inhibiting NF-κB-mediated COX-2 expression and apoptosis. *Free Radical Biology Medicine*, 73, 260-269.
- YI, J., QIU, M., LIU, N., TIAN, L., ZHU, X., DECKER, E. A. & MCCLEMENTS, D. J. 2020. Inhibition of lipid and protein oxidation in whey-protein-stabilized emulsions using a natural antioxidant: black rice anthocyanins. *Journal of Agricultural Food Chemistry*, 68, 10149-10156.
- YIN, Z., HENRY, E. C. & GASIEWICZ, T. A. 2009. (-)-Epigallocatechin-3-gallate is a novel Hsp90 inhibitor. *Biochemistry*, 48, 336-345.
- YONG, H., KOH, M. & MOON, A. 2009. The p38 MAPK inhibitors for the treatment of inflammatory diseases and cancer. *Expert opinion on investigational drugs*, 18, 1893-1905.
- YOUNG, S., CRAIG, P. & GOLZARIAN, J. 2019. Current trends in the treatment of hepatocellular carcinoma with transarterial embolization: a cross-sectional survey of techniques. *European radiology*, 29, 3287-3295.
- ZHANG, X., KAUNDA, J. S., ZHU, H., WANG, D., YANG, C. & ZHANG, Y. 2019. The genus Terminalia (Combretaceae): An ethnopharmacological, phytochemical and pharmacological review. *Natural products bioprospecting*, 9, 357-392.
- ZHAO, Y., LIU, X., QU, Y., WANG, L., GENG, D., CHEN, W., LI, L., TIAN, Y., CHANG, S. & ZHAO, C. 2019. The roles of p38 MAPK→COX2 and NF-κB→COX2 signal pathways in age-related testosterone reduction. *Scientific reports*, 9, 1-11.
- ZOROVA, L. D., POPKOV, V. A., PLOTNIKOV, E. Y., SILACHEV, D. N., PEVZNER, I. B., JANKAUSKAS, S. S., BABENKO, V. A., ZOROV, S. D., BALAKIREVA, A. V. & JUHASZLOVA, M. 2018. Mitochondrial membrane potential. *Analytical biochemistry*, 552, 50-59.
- ZWEIER, J. L. & TALUKDER, M. H. 2006. The role of oxidants and free radicals in reperfusion injury. *Cardiovascular research*, 70, 181-190.

APPENDIX

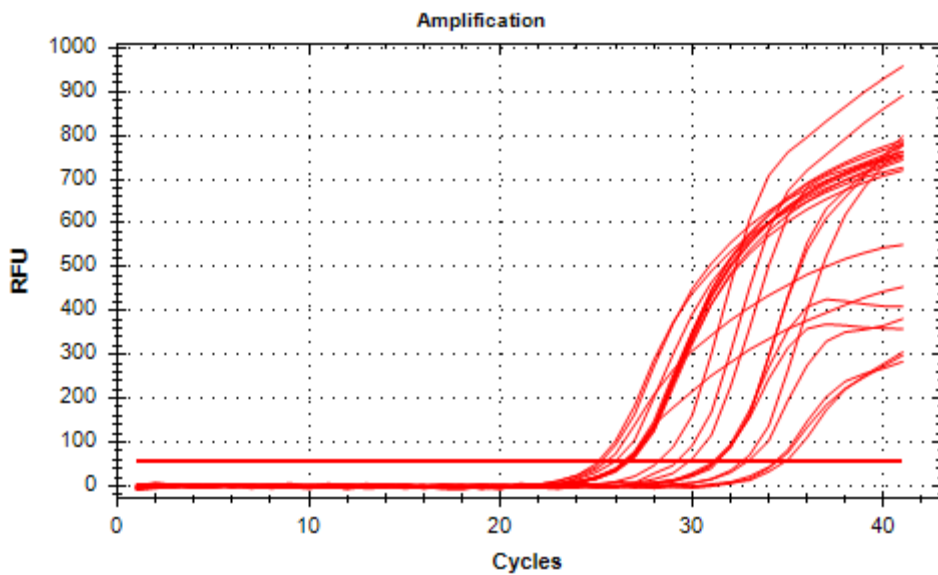
1. Nrf2 gene amplification



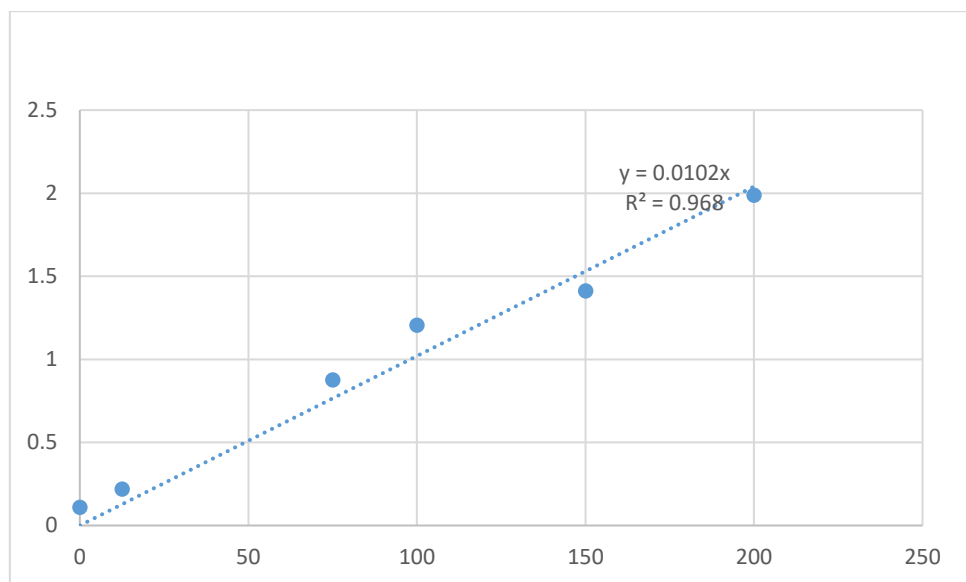
2. GPx-1 and NF-κB gene amplification



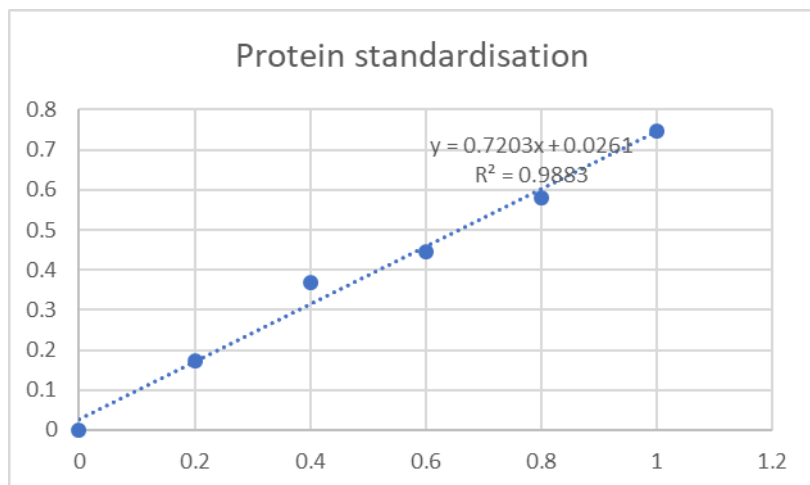
3. SOD2 gene amplification



4. Nitrates standard curve



5. Protein standardisation



6. Turnitin plagiarism report

Similarity: 15%

Masters thesis

ORIGINALITY REPORT

15%
SIMILARITY INDEX

9%
INTERNET SOURCES

4%
PUBLICATIONS

13%
STUDENT PAPERS

PRIMARY SOURCES

1 Submitted to University of KwaZulu-Natal **11%**
Student Paper

2 "Encyclopedia of Cancer", Springer Science
and Business Media LLC, 2017 **4%**
Publication